FAA-76-16

REPORT NO. FAA-RD-76-216

ILS GLIDE SLOPE PERFORMANCE PREDICTION MULTIPATH SCATTERING

S. Morin
D. Newsom
M. Scotto

U.S. Department of Transportation
Transportation Systems Center
Kendall Square
Cambridge MA 02142

DECEMBER 1976

FINAL REPORT

DOCUMENT IS AVAILABLE TO THE U.S. PUBLIC THROUGH THE NATIONAL TECHNICAL INFORMATION SERVICE, SPRINGFIELD, VIRGINIA 22161

Prepared for

U.S. DEPARTMENT OF TRANSPORTATION
FEDERAL AVIATION ADMINISTRATION
Systems Research and Development Service
Washington DC 20591

Technical Report Documentation Page

1. Report No.	2. Government Accession No.	3. Recipient's Catalog No.
FAA-RD-76-216		

4. Title and Subtitle	5. Report Date
ILS GLIDE SLOPE PERFORMANCE PREDICTION MULTIPATH SCATTERING	December 1976
	6. Performing Organization Code
7. Author(s)	8. Performing Organization Report No.
S. Morin, D. Newsom, M. Scotto	DOT-TSC-FAA-76-16
9. Performing Organization Name and Address U.S. Department of Transportation Transportation Systems Center Kendall Square Cambridge MA 02142	10. Work Unit No. (TRAIS) FA607/R7143
	11. Contract or Grant No.
12. Sponsoring Agency Name and Address U.S. Department of Transportation Federal Aviation Administration Systems Research & Development Service Washington DC 20591	13. Type of Report and Period Covered Final Report July 1975-March 1976
	14. Sponsoring Agency Code ARD-741

15. Supplementary Notes

16. Abstract

A mathematical model has been developed which predicts the performance of ILS glide slope systems subject to multipath scattering and the effects of irregular terrain contours. The model is discussed in detail and then applied to a test case for purposes of illustration. A complete listing of all computer programs has been appended to the report. A users' manual has been prepared under separate cover.

17. Key Words	18. Distribution Statement
ILS Derogation CDI Glide Slope	DOCUMENT IS AVAILABLE TO THE U.S. PUBLIC THROUGH THE NATIONAL TECHNICAL INFORMATION SERVICE, SPRINGFIELD, VIRGINIA 22161

19. Security Classif. (of this report)	20. Security Classif. (of this page)	21. No. of Pages	22. Price
Unclassified	Unclassified	82	

Form DOT F 1700.7 (8-72) Reproduction of completed page authorized

PREFACE

The work presented in this report has been sponsored by the Federal Aviation Administration as part of a program to provide navigational aids for the safe landing of aircraft. The program has been concerned with the application of instrument landing aids, and in particular the development of models to predict the performance of localizer and glide slope antenna systems. The present report is concerned with the glide slope portion of instrument landing system, and the effects of airport topography on its performance.

METRIC CONVERSION FACTORS

Approximate Conversions to Metric Measures

Symbol	When You Know	Multiply by	To Find	Symbol
	LENGTH			
in	inches	2.5	centimeters	cm
ft	feet	30	centimeters	cm
yd	yards	0.9	meters	m
mi	miles	1.6	kilometers	km
	AREA			
in^2	square inches	6.5	square centimeters	cm^2
ft^2	square feet	0.09	square meters	m^2
yd^2	square yards	0.8	square meters	m^2
mi^2	square miles	2.6	square kilometers	km^2
	acres	0.4	hectares	ha
	MASS (weight)			
oz	ounces	28	grams	g
lb	pounds	0.45	kilograms	kg
	short tons (2000 lb)	0.9	tonnes	t
	VOLUME			
tsp	teaspoons	5	milliliters	ml
Tbsp	tablespoons	15	milliliters	ml
fl oz	fluid ounces	30	milliliters	ml
c	cups	0.24	liters	l
pt	pints	0.47	liters	l
qt	quarts	0.95	liters	l
gal	gallons	3.8	liters	l
ft^3	cubic feet	0.03	cubic meters	m^3
yd^3	cubic yards	0.76	cubic meters	m^3
	TEMPERATURE (exact)			
°F	Fahrenheit temperature	5/9 (after subtracting 32)	Celsius temperature	°C

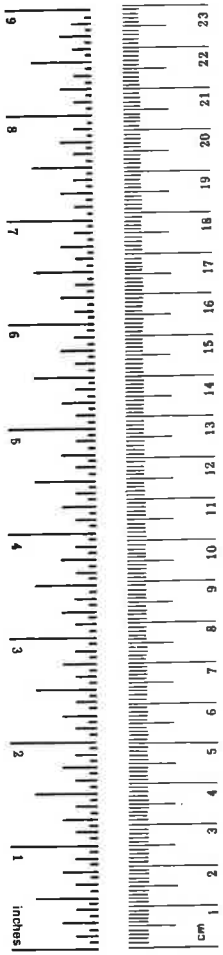

Approximate Conversions from Metric Measures

Symbol	When You Know	Multiply by	To Find	Symbol
	LENGTH			
mm	millimeters	0.04	inches	in
cm	centimeters	0.4	inches	in
m	meters	3.3	feet	ft
m	meters	1.1	yards	yd
km	kilometers	0.6	miles	mi
	AREA			
cm^2	square centimeters	0.16	square inches	in^2
m^2	square meters	1.2	square yards	yd^2
km^2	square kilometers	0.4	square miles	mi^2
ha	hectares (10,000 m^2)	2.5	acres	
	MASS (weight)			
g	grams	0.035	ounces	oz
kg	kilograms	2.2	pounds	lb
t	tonnes (1000 kg)	1.1	short tons	
	VOLUME			
ml	milliliters	0.03	fluid ounces	fl oz
l	liters	2.1	pints	pt
l	liters	1.06	quarts	qt
l	liters	0.26	gallons	gal
m^3	cubic meters	35	cubic feet	ft^3
m^3	cubic meters	1.3	cubic yards	yd^3
	TEMPERATURE (exact)			
°C	Celsius temperature	9/5 (then add 32)	Fahrenheit temperature	°F

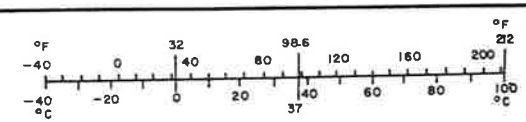

CONTENTS

ILLUSTRATIONS

1. INTRODUCTION

A mathematical model has been developed for predicting the performance of image-type glide slope arrays. The basic theory is developed in the following section of this report. In Part A of that section a model of the glide slope multipath problem is developed while in Part B the techniques for dealing with irregular terrain profiles are outlined. In the final section of the report some illustrative numerical results are presented.

2. BASIC THEORY

PART A

The presence in the airport environment of such large man-made structures as aircraft hangars as well as such natural terrain features as hillsides can lead to glide slope course derogation through multipath scattering. We begin our treatment of glide slope siting problems by developing a model for predicting the amount of such multipath derogation. A typical situation is depicted in Figure 1.

The touchdown point on the centerline of the runway opposite the glide slope array is chosen as the origin of coordinates 0. The z-axis is chosen to be the vertical axis passing through the origin 0, while the x-and y-axes are parallel to and perpendicular to the centerline, respectively. The positive z-axis points out of the page (Figure 1). The ground plane is assumed to be perfectly conducting. Consequently, any deviations from nominal glide slope performance are attributable to the multipath scattering produced by the various structures (both natural and man-made). For simplicity, we will assume that all such structures are perfectly conducting.

In the situation depicted in Figure 1, the scatterer (perhaps a small hill) is illuminated by the glide slope array and scatters

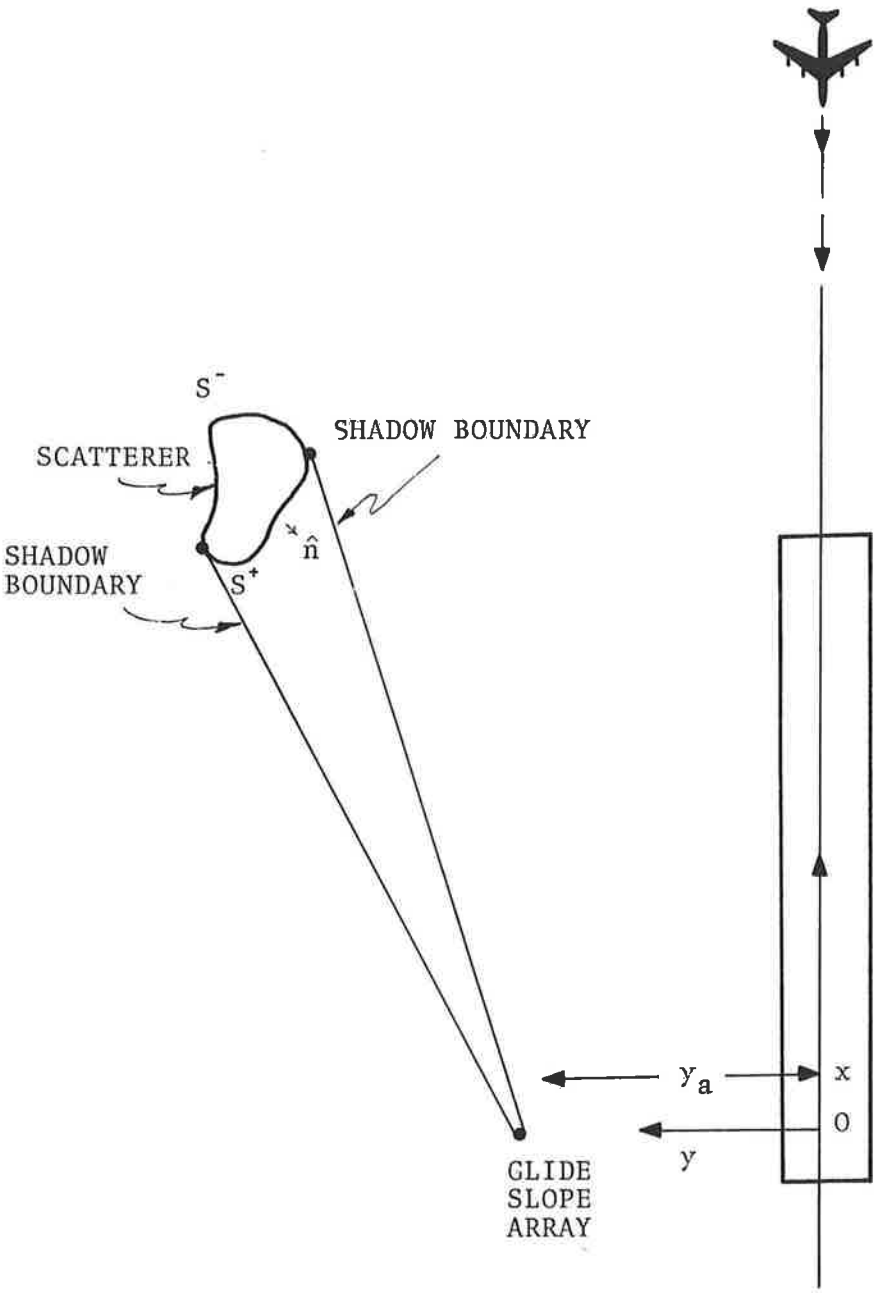

FIGURE 1. TYPICAL GEOMETRY FOR MULTIPATH SCATTERING

some of this signal back into the path of the approaching aircraft. We now proceed to calculate mathematical expressions for these scattered fields at the receiver. For convenience, we will work with magnetic field intensities.

For a perfect conductor, the surface current density K is given by:

$$\vec{K} = \hat{n} \times \vec{H} \quad , \tag{1}$$

where n is the local unit normal vector pointing out of the scattering surface and H is the total magnetic field,

$$\vec{H} = \vec{H}_i + \vec{H}_s, \tag{2}$$

where $\vec{H}_i$ is the incident and $\vec{H}_s$ the scattered field on the surface of the scattering structure. In terms of the surface current density $\vec{K}$, the scattered field $\vec{H}_s$ at the receiver is given by the following surface integral:

$$\vec{H}_s(\vec{r}_1) = \frac{1}{4\pi} \int_S \left[\vec{K}(\vec{r}) \times \vec{\nabla} G(\vec{r}_1, \vec{r}) \right] ds \tag{3}$$

In Equation (3), the vectors $\vec{r}_1$ and $\vec{r}$ denote, respectively, the position vector of the receiver and the position vector of some arbitrary source point on the surface of the scatterer relative to the origin of coordinates 0. The two-point Green's function $G(\vec{r}_1, \vec{r})$ is given by:

$$G(\vec{r}_1, \vec{r}) = \frac{e^{ik|\vec{r}_1 - \vec{r}|}}{|\vec{r}_1 - \vec{r}|} \tag{4}$$

where $k = 2\pi/\lambda$ and λ is the wavelength of the incident radiation. The integral is taken over the surface S of the scatterer.

We will adopt here the single scattering, physical optics approximation for the current density K. Specifically, we will assume that on those portions of the scattering surface not directly illuminated by the glide slope array, K is identically zero and

that on the directly illuminated portions of the scattering surface, K is proportional to twice the tangential component of the incident magnetic field:

$$\vec{K} \equiv 0 \quad \text{on } S_- \tag{5}$$

$$\vec{K} = 2\,(\hat{n} \times \vec{H}_i) \quad \text{on } S_+ \tag{6}$$

where S_+ and S_- denote, respectively, the illuminated and unilluminated portions of the scattering surface S (see Figure 1). For the current distribution defined by Equations (5) and (6), Equation (3) becomes

$$\vec{H}_s(r_1) = \frac{1}{2\pi} \int_{S_+} \left[\hat{n}(\vec{r}) \times \vec{H}_i(\vec{r})\right] \times \vec{\nabla} G(\vec{r}_1, \vec{r})\, ds. \tag{7}$$

The physical optics scattering model represented by equation (7) is based upon the existence of a sharp shadow boundary on the surface of the scattering structure. This assumption ignores such phenomena multiple reflections, surface waves, and diffraction but should provide reasonably accurate results as long as the surface features of the scattering structure do not vary greatly over dimensions which are small compared to the wavelength λ (about 3 feet at glide slope frequencies).

In principle, the solution to the problem at hand requires only that the magnet field H_i be determined. For simplicity, we will assume that the glide slope array is made up of electrically short dipoles. With this assumption, we in effect approximate by a cosine distribution the actual azimuthal pattern of the half-wave dipoles which make up glide slope arrays. This approximation should not be too restrictive and it does considerably expedite our calculations. Let $(0, y_a, h)$ denote the x, y, and z coordinates respectively of a typical dipole in the array and let (x, y, z) denote the coordinates of a point $\vec{r}$ at which we wish to know the magnetic field intensity H_a produced by the dipole at $(0, y_a, h)$. In our earlier

glide slope performance prediction report,* it is shown that $\vec{H}_a(\vec{r})$ is given by

$$\vec{H}_a(\vec{r}) = \frac{ikJ_o}{4\pi} \frac{e^{ikD_1}}{D_1^2} \left[x\hat{e}_z - (z-h)\hat{e}_x \right] \tag{8}$$

where $\hat{e}_x$, $\hat{e}_y$, and $\hat{e}_z$ denote unit vectors in the x, y, and z directions respectively, J_o is a parameter which measures relative phase and amplitude, and D_1 is the distance from the antenna to the observation point r:

$$D_1 = \left[x^2 + (y-y_a)^2 + (z-h)^2 \right]^{\frac{1}{2}} \tag{9}$$

To take into account reflections from the ground plane (z = 0) we use simple image theory to obtain the image field $\vec{H}_a^*(\vec{r})$:

$$\vec{H}_a^*(\vec{r}) = \frac{ikJ_o}{4\pi} \frac{e^{ikD_2}}{D_2^2} \left[x\hat{e}_z - (z+h)\hat{e}_x \right] \tag{10}$$

where D_2 is the distance from the image of the transmitting dipole to the field point $\vec{r}$:

$$D_2 = \left[x^2 + (y-y_a)^2 + (z+h)^2 \right]^{\frac{1}{2}} \tag{11}$$

The total field intensity H_i at $\vec{r}$ is just the sum of the direct ($\vec{H}_a$) and ground reflected ($\vec{H}_a^*$) signals:

$$\vec{H}_i(\vec{r}) = \vec{H}_a(\vec{r}) + \vec{H}_a^*(\vec{r}) \tag{12}$$

Note that on the ground plane (z = 0), the z component of $\vec{H}_i$ vanishes identically.

---

* ILS Glide Slope Performance Predictions, Vol. B, FAA-RD-74-157.B, S. Morin, D. Newsom, D. Kahn, L. Jordan, September 1974.

The field H_i determined by Equations (8), (10), and (12) can now be substituted into Equation (7) and the integral can be performed over the illuminated surface of the scattering structure to give the scattered field at the receiver location r_1. Actually, only the z component of the scattered field need be calculated since the receiving antenna responds primarily to the horizontal component of electric field which is proportional to the z component of the magnetic field. It should be noted that for a complete solution, the contribution of the image of the scattering structure must also be calculated. We will assume that the receiver is always in the far field of the scattering structure so that the following asymptotic form of the gradient of the Green's function is applicable:

$$\vec{\nabla} G(\vec{r}_1,\vec{r}) \approx - ik\ (\vec{r}_1-\vec{r})\ \frac{e^{ik|\vec{r}_1-\vec{r}|}}{|\vec{r}_1-\vec{r}|^2} \tag{13}$$

Substituting Euqations (8), (10), (12) and (13) into Equation (7) and taking the z-component of the resulting vector equation, we obtain the following expressions for $H_{sz}(r_1)$, the z-component of scattered magnetic field at the receiver point r_1:

$$H_{sz}(\vec{r}_1) = \frac{k^2 J_o}{8\pi^2} \left[I_1+I_2+I_3+I_4 \right] \tag{14}$$

where

$$I_1 = \int_{S_+} \frac{F_1}{D_1^2 R_1^2}\ e^{ik(R_1+D_1)}\ ds \tag{15}$$

$$I_2 = - \int_{S_+} \frac{F_2}{D_2^2 R_1^2}\ e^{ik(R_1+D_2)}\ ds \tag{16}$$

$$I_3 = -\int_{S_+} \frac{F_1}{D_1^2 R_2^2} \, e^{ik(R_2+D_1)} \, ds \tag{17}$$

$$I_4 = \int_{S_+} \frac{F_2}{D_2^2 R_2^2} \, e^{ik(R_2+D_2)} \, ds \tag{18}$$

$$D_1 = \left[x^2 + (y-y_a)^2 + (z-h)^2 \right]^{\frac{1}{2}} \tag{19}$$

$$D_2 = \left[x^2 + (y-y_a)^2 + (z+h)^2 \right]^{\frac{1}{2}} \tag{20}$$

$$R_1 = \left[(X_1-x)^2 + (Y_1-y)^2 + (Z_1-z)^2 \right]^{\frac{1}{2}} \tag{21}$$

$$R_2 = \left[(X_1-x)^2 + (Y_1-y)^2 + (Z_1+z)^2 \right]^{\frac{1}{2}} \tag{22}$$

$$F_1 = n_2 x(Y_1-y) + \left[n_1 x + n_3(z-h) \right](X_1-x), \tag{23}$$

$$F_2 = n_2 x (Y_1-y) + \left[n_1 x + n_3(z+h) \right](X_1-x) \tag{24}$$

In Equations (14) through (24), the coordinates (X_1, Y_1, Z_1) denote the coordinates of the aircraft, (x, y, z) the coordinates of some source point on the surface of the scattering structure and (n_1, n_2, n_3) the components of the unit outward normal to the surface of the scatterer at the point (x, y, z). The integrals I_3 and I_4 represent the contributions of the image of the scattering structure in the ground plane $z = 0$. Note the following relationships among the four integrals:

$$\begin{aligned} I_1 \; (X_1, Y_1, Z_1) &= -I_3 \; (X_1, Y_1, -Z_1) \\ I_2 \; (X_1, Y_1, Z_1) &= -I_4 \; (X_1, Y_1, -Z_1) \end{aligned} \tag{25}$$

Consequently, when $Z_1 = 0$, $H_{sz}(\vec{r}_1) \equiv 0$ as it should be.

The direct numerical integration of the integrals I_1, I_2, I_3, and I_4 for an arbitrary scattering structure would in general require an inordinate amount of computer time. However, certain simplifying assumptions can be made which considerably expedite the evaluation of these integrals. Specifically, we will assume that any scattering surface can be adequately represented by a series of interconnecting plane facets. By definition, the unit normal vector $\hat{n}$ will be constant over each facet. The exact size, shape, and orientation of these facets will depend upon the surface characteristics of the particular scatterer. In turn, each facet can be broken up into a series of interconnected rectangular pieces. If these rectangular pieces are made small enough, the integrals I_1, I_2, I_3 and I_4 can be evaluated analytically for each piece and then the results summed over the whole surface of the scatterer to give H_{sz}. To illustrate these procedures, we will now evaluate the integral I_1 for an arbitrarily oriented rectangular plate. In the course of this evaluation, we will discuss the size restrictions on such plates.

In Figure 2, a rectangular facet typical of those making up the surface of some scatterer has been drawn. We will evaluate the integral I_1 of Equation (15) for such a facet in the Fraunhofer approximation. The unit vectors $\hat{\eta}$ and $\hat{\xi}$ lie in the plane of the facet, are orthonormal, and define the direction of the outward normal $\hat{n}$:

$$\hat{n} = \hat{\eta} \times \hat{\xi}$$

The center point of the facet (x_o, y_o, z_o) will be used as a local origin of coordinates for the integrations which are to be performed. The integral I_1 is given by

$$I_1 = \int_{S_+} \frac{F_1}{D_1^2 R_1^2} e^{ik(D_1+R_1)} \, ds \qquad (26)$$

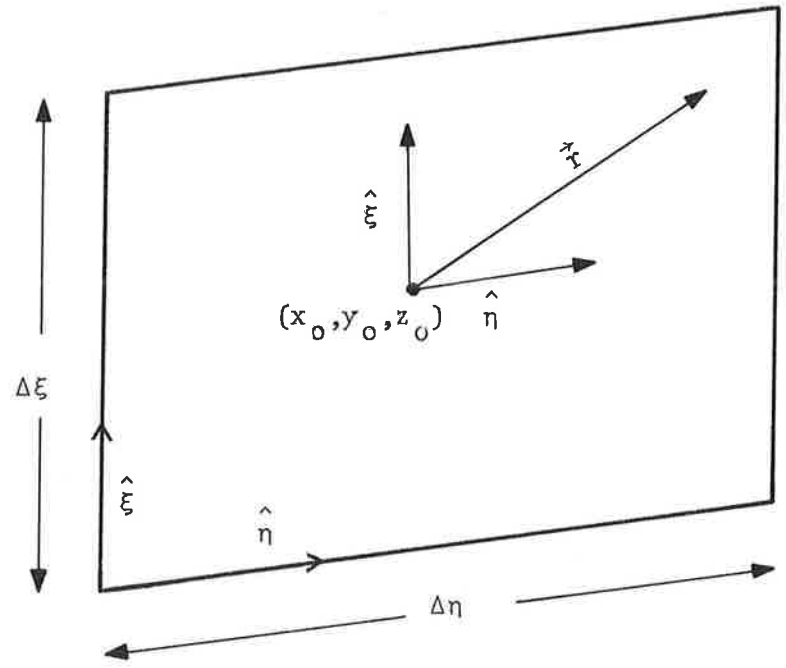

FIGURE 2. REPRESENTATION OF RECTANGULAR FACET

where

$$F_1 = n_2 x (Y_1-y) + \left[n_1 x + n_3(z-h)\right](\vec{X}_1-x) \tag{27}$$

$$D_1 = \left[x^2 + (y-y_a)^2 + (z-h)^2\right]^{1/2} \tag{28}$$

$$R_1 = \left[(X_1-x)^2 + (Y_1-y)^2 + (Z_1-z)^2\right]^{1/2} \tag{29}$$

Clearly, the distances D_1 and R_1 denote, respectively, the length of the vector $\vec{D}_1$ from the antenna to a point (x, y, z) on the surface of the facet and the length of the vector $\vec{R}_1$ from the point (x, y, z) to the receiver. From Figure 2, it is seen that the vector D_1 can be represented as follows:

$$\vec{D}_1 = \vec{D}_{10} + \vec{r} \tag{30}$$

where

$$\vec{D}_{10} = X_o\hat{e}_x + (y_o-y_a)\hat{e}_y + (z_o-h)\hat{e}_z \tag{31}$$

and

$$\vec{r} = \eta\hat{\eta} + \xi\hat{\xi} \tag{32}$$

and the ranges of the variables η and ξ are $-\frac{\Delta\eta}{2} \leq \eta \leq \frac{\Delta\eta}{2}$ and $-\frac{\Delta\xi}{2} \leq \xi \leq \frac{\Delta\xi}{2}$. From Equation (30), we have

$$D_1 = D_{10}\left(1 + \frac{r^2+2\vec{D}_{10}\cdot\vec{r}}{D_{10}^2}\right)^{1/2} \tag{33}$$

Normally, D_{10} is on the order of thousands of feet and r is of the order of tens of feet so that the radical in Equation (33) can be expanded in powers of r/D_{10} to give D_1 approximately as a function of η and ξ. To terms of second order in r/D_{10}, we obtain

$$D_1 \approx D_{10} + \eta\cos\alpha + \xi\cos\beta + \frac{r^2}{2D_{10}} - \frac{(\hat{D}_{10}\cdot r)}{2D_{10}} \tag{34}$$

where

$$\hat{D}_{10} = \vec{D}_{10}/D_{10} \tag{35}$$

$$\cos\alpha = D_{10}\cdot\hat{\eta} \tag{36}$$

$$\cos\beta = \hat{D}_{10}\cdot\hat{\xi} \tag{37}$$

The numbers $\cos\alpha$ and $\cos\beta$ are the direction cosines of D_{10} relative to $\hat{\eta}$ and $\hat{\xi}$. In the Fraunhofer approximation which we will use, it is assumed that the quatratic terms of Equation (33) are small compared to a wavelength for any point (x, y, z) on the surface of the facet so that we can write to a good approximation:

$$D_1 = D_{10} + \eta\cos\alpha + \xi\cos\beta \tag{38}$$

It can be shown that the largest value attainable by the quadratic terms in Equation (33) on the facet's surface is

$$\Delta = \frac{(\Delta\eta)^2}{8\,D_{10}}\sin^2\alpha + \frac{(D\xi)^2}{8\,D_{10}}\sin^2\beta + \frac{\Delta\eta\Delta\xi}{4}\left|\cos\alpha\,\cos\beta\right| \tag{39}$$

Equation (38) should provide a good approximation for the distance D_1 as a function of η and ξ as long as $\Delta\eta$ and $\Delta\xi$ are chosen so that Δ in Equation (39) is small compared to the wavelength λ. We will return to this important requirement later.

Similarly, the vector $\vec{R}_1$ can be represented as follows:

$$\vec{R}_1 = \vec{R}_{10} - \vec{r} \tag{40}$$

$$\text{where } \vec{R}_{10} = (X_1-x_o)\hat{e}_x+(Y_1-y_o)\hat{e}_y+(Z_1-z_o)\hat{e}_z \tag{41}$$

Thus, in the Fraunhofer approximation, we find

$$R_1 \simeq R_{10} - \eta\cos\alpha - \xi\cos\delta \tag{42}$$

$$\cos \alpha = \hat{R}_{10} \cdot \hat{\eta} \tag{43}$$

$$\cos \delta = \hat{R}_{10} \cdot \hat{\xi} \tag{44}$$

where $$\hat{R}_{10} = \vec{R}_{10}/R_{10} \tag{45}$$

In Equation (42), we have ignored terms of second order and higher in r/R_{10}.

One final approximation which we will make is that $\Delta\eta$ and $\Delta\xi$ are sufficiently small compared with D_{10} and R_{10}, that the variation of the amplitude function $F_1/D_1^2R_1^2$ in Equation (26) can be ignored This is normally an excellent approximation. Consequently, we will assume that for any point on the surface of the facet we can write

$$F_1/D_1^2R_1^2 \approx F_{10}/D_{10}^2R_{10}^2 \tag{46}$$

where F_{10}, D_{10}, and R_{10}, are the values of F_1, D_1, and R_1 at the center point (x_o, y_o, z_o).

Substituting Equations (38), (42), and (46) into Equation (26) yields the following approximate expression for I_1;

$$I_1 = \frac{F_{10}}{D_{10}^2R_{10}^2} e^{ik(D_{10}+R_{10})} \int_{-\Delta\eta/2}^{+\Delta\eta/2} e^{ik\eta(\cos\alpha - \cos\gamma)} d\eta \int_{-\Delta\xi/2}^{+\Delta\xi/2} e^{ik\xi(\cos\beta - \cos\delta)} d\xi \tag{47}$$

Performing the integrals indicated in Equation (47), we finally obtain the following approximate expression for I_1:

$$I_1 = \frac{4F_{10}}{D_{10}^2R_{10}^2} \frac{e^{ik(D_{10}+R_{10})}}{k^2} \times \frac{\sin\left\{\frac{k\Delta\eta}{2}(\cos\alpha - \cos\gamma)\right\} \sin\left\{k\frac{\Delta\xi}{2}(\cos\beta - \cos\delta)\right\}}{(\cos\alpha - \cos\gamma)(\cos\beta - \cos\delta)} \tag{48}$$

A similar treatment of the integrals I_2, I_3, and I_4 ultimately lead to the following approximate expression for the scattered magnetic field intensity at the receiver due to the rectangular facet:

$$H_{sz}(\vec{r}_1) = \frac{J_o}{2\pi^2} \frac{F_{10} e^{ik(D_{10}+R_{10})}}{D_{10}^2 R_{10}^2} \frac{\sin(kA\Delta\eta/2)\sin(kB\Delta\xi/2)}{A\,B}$$

$$- \frac{J_o}{2\pi^2} \frac{F_{20} e^{ik(D_{20}+R_{10})}}{D_{20}^2 R_{10}^2} \frac{\sin(kA_1\Delta\eta/2)\sin(kB_1\Delta\xi/2)}{A_1 B_1}$$

$$- \frac{J_o}{2\pi^2} \frac{F_{10} e^{ik(D_{10}+R_{20})}}{D_{10}^2 R_{20}^2} \frac{\sin(kA_2\Delta\eta/2)\sin(kB_2\Delta\xi/2)}{A_2 B_2}$$

$$+ \frac{J_o}{2\pi^2} \frac{F_{20} e^{ik(D_{20}+R_{20})}}{D_{20}^2 R_{20}^2} \frac{\sin(kA_3\Delta\eta/2)\sin(kB_3\Delta\xi/2)}{A_3 B_3} \qquad (49)$$

where F_{10}, F_{20}, D_{10}, D_{20}, R_{10} and R_{20} denote the values of F_1, F_2 D_1, D_2, R_1, and R_2 at (x_o, y_o, z_o) and the parameters A, A_1, A_2, A_3, B, B_1, B_2, and B_3 are defined as follows:

$$A = \cos\alpha - \cos\gamma \qquad B = \cos\beta - \cos\delta \qquad (50)$$

$$A_1 = \cos\alpha_1 = \cos\gamma \qquad B_1 = \cos\beta_1 - \cos\delta \qquad (51)$$

$$A_2 = \cos\alpha - \cos\gamma_1 \qquad B_2 = \cos\beta - \cos\delta_1 \qquad (52)$$

$$A_3 = \cos\alpha_1 - \cos\gamma_1 \qquad B_3 - \cos\beta_1 - \cos\delta_1 \qquad (53)$$

and the angles appearing in Equations (50) through (53) are defined as follows:

$$\vec{D}_{10} = x_o \hat{e}_x + (y_o - y_a)\hat{e}_y + (z_o - h)\hat{e}_z \qquad (54)$$

$$\vec{R}_{10} = (X_1 - x_o)\hat{e}_x + (Y_1 - y_o)\hat{e}_y + (Z_1 - z_o)\hat{e}_z \qquad (55)$$

$$\vec{D}_{20} = x_o \hat{e}_x + (y_o - y_a)\hat{e}_y + (z_o + h)\hat{e}_z \tag{56}$$

$$\vec{R}_{20} = (X_1 - x_o)\hat{e}_x + (Y_1 - y_o)\hat{e}_y - (Z_1 + z_0)\hat{e}_z \tag{57}$$

and

$$\cos\alpha = \frac{\vec{D}_{10}}{D_{10}} \cdot \hat{\eta} \quad , \quad \cos\beta = \frac{\vec{D}_{10} \cdot \hat{\xi}}{D_{10}} \tag{58}$$

$$\cos\alpha_1 = \frac{\vec{D}_{20} \cdot \hat{\eta}}{D_{20}} \quad , \quad \cos\beta_1 = \frac{\vec{D}_{20} \cdot \hat{\xi}}{D_{20}} \tag{59}$$

$$\cos\alpha = \frac{\vec{R}_{10} \cdot \hat{\eta}}{R_{10}} \quad , \quad \cos\delta = \frac{\vec{R}_{10} \cdot \hat{\xi}}{R_{10}} \tag{60}$$

and

$$\cos\alpha_1 = \frac{\vec{R}_{20} \cdot \hat{\eta}}{R_{20}} \quad , \quad \cos\delta_1 = \frac{\vec{R}_{20} \cdot \hat{\xi}}{R_{20}} \tag{61}$$

The total scattered field at the receiver is obtained by summing up the contributions from all of the rectangular facets which make up the surface of the scattering structure. Segmenting the surface of a scatterer into rectangular facets and then applying the approximate closed form solution in Equation (49) to each facet represents a far more efficient procedure for calculating the scattered field at the receiver than attempting to directly numerically integrate Equations (14) through (18).

We now return to the question raised earlier of the size restrictions upon the facets. Clearly, one would like to maximize the area of each facet in order to minimize computer running time. The principal restriction upon the size of the facets is that Δ_η and $\Delta\xi$ must not be so large that the Fraunhofer approximation, upon which the approximate formula (49) is based, is violated. That is, the quadratic path length difference terms like those in Equation (34)

must be small compared to the wavelength λ for all points on the surface of the facet to which Equation (49) is to be applied. Thus, in choosing appropriate values for $\Delta\xi$ and $\Delta\xi$, we are essentially faced with an optimization problem with a constraint. Specifically, we want to maximize the area $\Delta\eta\Delta\xi$ of the facet while keeping the quadratic path length difference terms less than some prescribed value. For example, for the path length D_1, the maximum value of the quadratic path length difference term is given by

$$\Delta = \frac{(\Delta\eta)^2}{8\,D_{10}}\sin^2\alpha + \frac{(\Delta\xi)^2}{8\,D_{10}} + \frac{\Delta\eta\Delta\xi}{4}\left|\cos\alpha\cos\beta\right| \qquad (62)$$

Depending upon the sign of $\cos\alpha\cos\beta$, this value will be achieved at two of the four corners of the rectangular facet. At all other points, the quadratic path length terms will be less than Δ, but always positive. We can optimize our choice of $\Delta\eta$ and $\Delta\xi$ by maximizing $\Delta\eta\,\Delta\xi$ subject to the condition that Δ in Equation (62) be some fractional part of a wavelength. This problem has been solved in closed form using Lagrange multipliers. The optimization procedure must be applied to the quadratic path length difference terms affecting all four distances (D_1, D_2, R_1, R_2) and then from the resulting set of solutions the smallest values of $\Delta\eta$ and $\Delta\xi$ are chosen. A subroutine has been written to carry out the optimization procedure.

Of course, the scattered fields must be calculated for each dipole in the array, the parameter J_o being varied to take into account the exact phase and amplitude ratios among the various elements and, along with J_o, the height h and y-offset y_a of each element. Our program automatically offsets the elements of an array to correct for the effects of proximity phase lag. The y-coordinates of the elements are adjusted so that all dipoles are at the same slant distance from the touchdown point on the runway directly opposite the array.

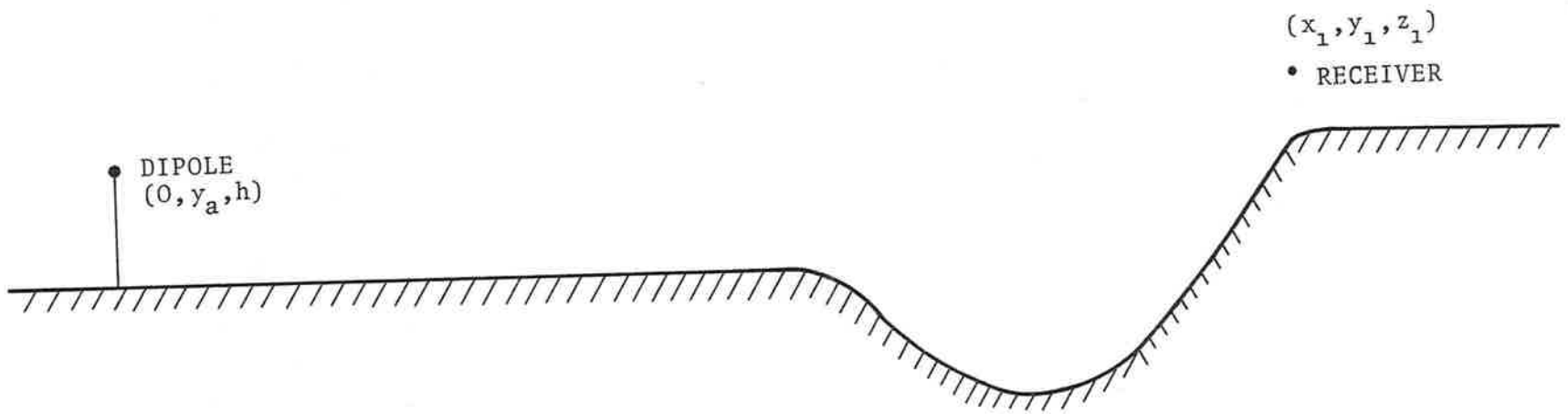

FIGURE 3. TYPICAL PROFILE OF ONE-DIMENSIONAL TERRAIN VARIATION

will generate the ground reflected signals at the carrier frequency. 90Hz modulated frequency, and the 150Hz modulated frequency. These signals are then combined with the incident signals directly from the antennas to give what we have been calling the direct fields, the fields which would be measured at the reeeiver assuming that no scatterers (hangars, hillsides, etc.) were present. These direct signals are then combined with the scattered signals calculated using the techniques of Part A and the resulting total signals are used in Equation (65) to calculate C.D.I. Again, if the terrain profile is perfectly flat or nearly so, Equation (63) can be used to calculate the direct signals.

3. NUMERICAL RESULTS

Before presenting some sample numerical results illustrating the predictions of our model, we will first review the characteristics of the three main types.of image glide slope arrays; the null reference, the sideband reference, and the capture effect arrays.

The null reference array is the simplest of the image glide slope systems. It consists of two transmitting antennas whose heights are in the ratio of 2:1. The upper antenna is fed sideband only signal, the 150 Hz and the 90 Hz components being of equal amplitude but 180° out of phase. The lower antenna is fed both carrier and sideband. The carrier signal is nominally 40% modulated. The ratio of the sideband currents in the upper antenna to the sideband currents in the lower antenna is typically 0.3. The sideband ratio of 0.3 would nominally yield a 1.4° course width (full deflection 0.7° above or below the glide path). Let

I_c, I_{150}, and I_{90} denote the current amplitudes fed to the antennas at the carrier frequency, the 150 Hz modulated frequency, and the 90 Hz modulated frequency, respectively. The null reference array parameters discussed above can be summarized as follows:

Carrier Antenna	Sideband Antenna
Height = h	Height = 2h
$I_c = 1$	$I_c = 0$
$I_{150} = 0.4$	$I_{150} = 0.12$
$I_{90} = 0.4$	$I_{90} = -0.12$

Note that all current amplitudes have been normalized relative to the carrier current amplitude ($I_c = 1$).

The sideband reference array employs two transmitting dipoles whose heights are in the ratio of 3:1. If the lower antenna is positioned at 1/2 the height of the lower antenna of the null reference array and if the upper antenna is positioned at 3/4 of the height of the upper antenna of the null reference array, the same glide angle is produced. Modulated carrier (40% modulated) is fed to the lower antenna. Both antennas are fed separate sideband signals. The separate sideband signals fed to the two antennas are equal in amplitude but are 180° out of phase. The amplitude ratio of the separate sideband signal to the carrier sideband signal is typically 0.3. This ratio produces a nominal course width of 1.4° as in the case of the null reference array. The sideband reference parameters are summarized below.

Lower Antenna	Upper Antenna
Height = h	Height = 3h
$I_c = 1$	$I_c = 0$
$I_{150} = 0.28$	$I_{150} = 0.12$
$I_{90} = 0.52$	$I_{90} = -0.12$

Note that the I_{150} and I_{90} current amplitudes given above for the lower antenna represent the sums of the carrier sideband and separate sideband signsls (I_{150} = .4 - .12 = .28, I_{90} = .4 + .12 = .52). All current amplitudes have been normalized relative to the carrier signal amplitude.

The capture effect glide slope array consists of three transmitting antennas whose heights are in the ratios of 1:2:3. If the lower and middle antennas are set at the same heights as the null reference antennas, the same glide angle is produced. We will not treat the clearance signal which provides a strong fly up signal at low approach angles but has little effect upon the glide angle and course width. Concerning the primary signal, the modulated carrier is fed to both the lower and middle antennas. The modulated carrier fed to the middle antenna has half the amplitude and is 180° out of phase with the modulated carrier fed to the lower antenna. The carrier signals are nominally 40% modulated. In addition, all three antennas are fed separate sideband signals. The separate sideband signals fed to the lower and upper antennas have half the amplitude and are 180° out of phase with the separate sideband signal fed to the middle antenna. The ratio of the separate sideband signal fed to the middle antenna to the carrier sideband signal in the lower antenna is typically 0.3. This ratio yields nominally a course width of 1.4° as in the case of the null reference array. The capture effect array parameters are summarized below.

Lower Antenna	Middle Antenna
Height = h	Height = 2h
I_c = 1	I_c = -0.5
I_{150} = 0.34	I_{150} = -0.08
I_{90} = 0.46	I_{90} = -0.32

Upper Antenna

Height = 3h
I_c = 0
I_{150} = -0.06
I_{90} = 0.06

Note that the I_{150} and I_{90} current amplitudes given above represent the sums of the carrier sideband and separate sideband signals. Again, all values have been normalized relative to the carrier amplitude in the lower antenna.

It should be noted here that our computer program automatically offsets the elements of each glide slope array to correct for the effects of proximity phase lag. The y coordinates of the elements are adjusted so that all dipoles are at the same slant distance from the touchdown point on the runway directly opposite the array. For each array, one element is held fixed while the other elements are offset relative to the fixed one. For the null reference and sideband reference arrays, the lower element is held fixed while for the capture array, the middle element is held fixed. The amount of the offset for each dipole can be calculated approximately in the following manner. Let y_a and h denote, respectively, the y-coordinate and height of the fixed antenna element. The y-displacement, ε, of any other element in the array relative to the fixed one is given approximately by:

$$\varepsilon = \frac{h^2 - H^2}{2y_a} \tag{66}$$

where H is the height of the element which is to be offset.

For the present study, the wavelength λ was set at 3 feet. All arrays were positioned 300 feet from the centerline of the runway. The heights of the array elements were set at 14.33 feet and 28.66 feet (approximately 5λ and 10λ) for the null reference array, 7.17 feet and 21.5 feet (approximately 2.5λ and 7.5λ) for the sideband reference array, and 14.33 feet, 28.66 feet, and 42.99 feet (approximately 5λ, 10λ, and 15λ) for the capture effect array. Under normal circumstances, a glide angle of 3° would be produced by all three arrays.

To illustrate the performance of our multipath model, the glide slope course deragation caused by a large, flat reflecting surfaee (perhaps the side of a large hangar or the side of a hill) has been calculated. The structure was taken to be 300 feet long and 100 feet high and was oriented parallel to the runway centerline. The structure was positioned 200 feet from the runway centerline in the y-direction, on the opoosite side of the centerline from the glide slope array. The near edge of the structure was displaced 1000 feet in the x-direction from the touchdown point. The geometry of the configuration is depicted in Figure 4.

In Figures 5, 6, and 7 are plotted the C.D.I. signal as a function of the horizontal distance from touchdown for each of the three arrays for the arrangement depicted in Figure 4. In each case, the receiver followed the nominal 3^{o} zero C.D.I. hyperbola. The results for all three arrays are very similar. Our model predicts large high frequency, alternating fly up and fly down signals near the end of the flight path roughly between 1700 feet and 1800 feet from touchdown. This region in fact corresponds almost exactly to the region of specular reflection as predicted by geometrical optics. Note that the excursions are large enough to saturate the receiver over much of the affected range (full scale deflection = 150 microamps). The excursions are clearly highly localized and damp out very rapidly as the aircraft leaves the specular reflection zone. The narrowness of the pattern (i.e., the lack of broadening due to diffraction and the rapid damping of the side lobes) is undoubtedly attributable to the large size of the scatterer relative to the scattering wavelength.

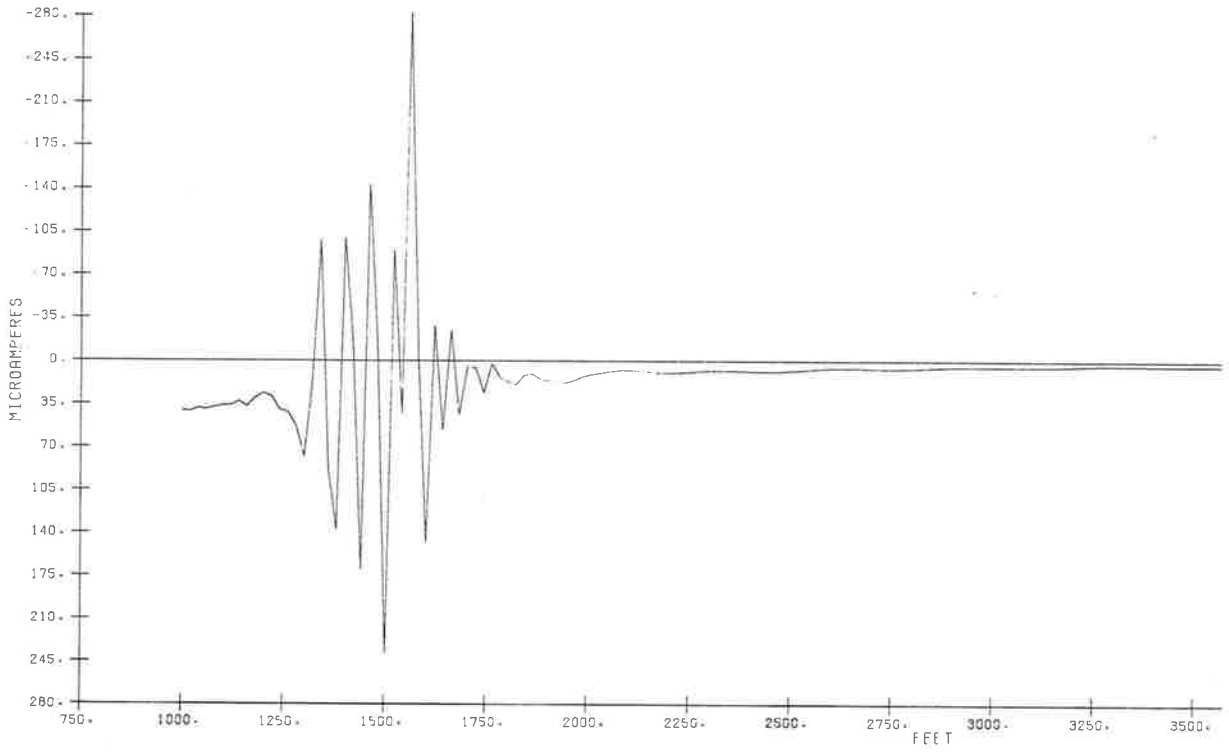

FIGURE 6. SIDEBAND REFERENCE ARRAY, FLYABILITY RUN

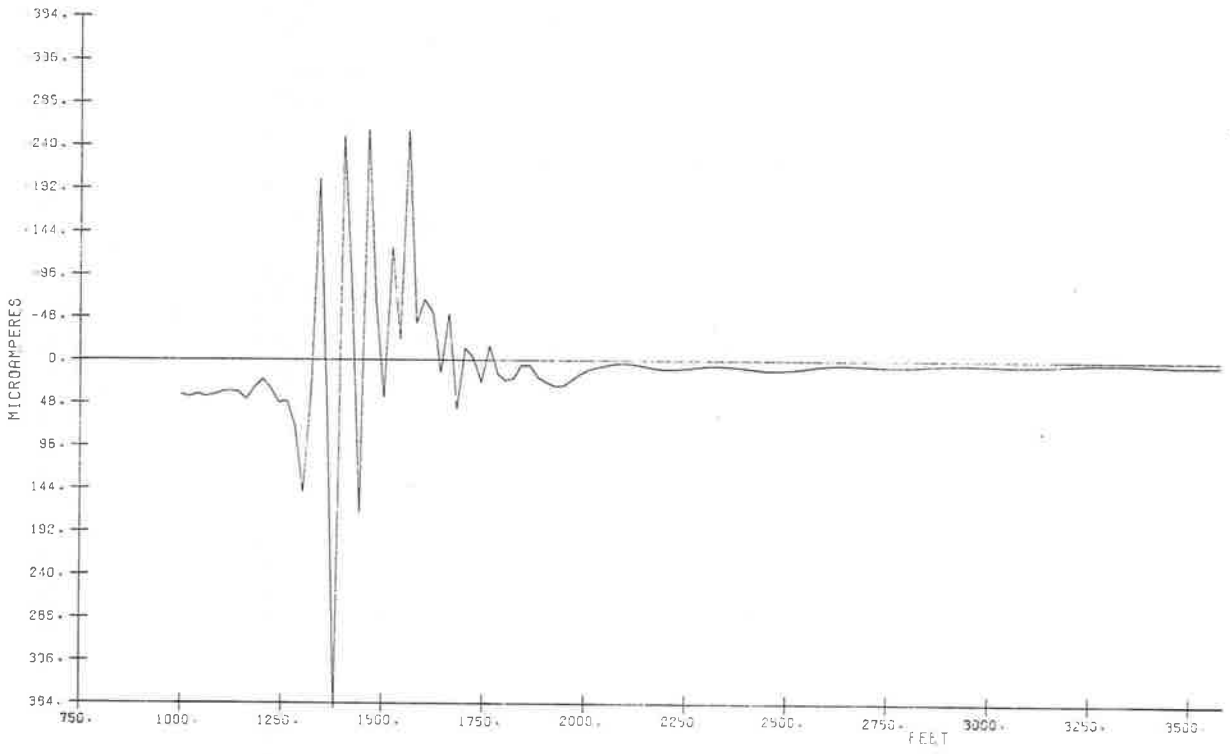

FIGURE 7. CAPTURE EFFECT ARRAY, FLYABILITY RUN

PROGRAM ILSVEN.F4

```
      DIMENSION ILABL(8)
      DIMENSION IPTDAT(33)
      COMMON /PLXT/ NRP,RXMN,RXMX,RXFT,RXLT,RYMN,RYMX,RYFT,RYLT,
     1RZMN,RZMX,RZFT,RZLT,RTMN,RTMX,RTFT,RTLT,
     2AIMN,AIMX,AIFT,AILT,ARMN,ARMX,ARFT,ARLT,
     3ADIN,ADIX,ADIF,ADIL,
     4ADRN,ADRX,ADRF,ADRL
      EQUIVALENCE (IPTDAT(1),NRP)
      IMPLICIT COMPLEX (C)
      DIMENSION X(20),Y(20),Z(20)
      DIMENSION CF1(20),CF2(20),CF3(20)
      IMPLICIT DOUBLE PRECISION (D)
      COMMON /REC/RX,RY,RZ,RT,NSIZE
      REAL LAMBDA
      COMMON /GROUND/ K,X1(20),Z1(20),X2(0/20),Z2(0/20),IEL
      COMMON /ANT/AX,AY,AZ,LAMBDA,DAK,DPI
      COMMON /VAL/ HR,HI
C
C       THIS VALUE OF TWO PI IS INITIALIZED THIS WAY TO AVOID USING
C BLOCK DATA
      DPI=6.283185307179586476 9
C
C       THIS OPENS THE OUTPUT FILE
      CALL OFILE(1,'STRIP')
C
C       THIS SUBROUTINE OPENS THE FLIGHT PATH FILE AND RETURNS WITH
C THE FLIGHT PATH PLOT LABEL (ILABL) AND TIME CONSTANT (TAU)
C THE FILE WAS SET UP WITH JOVRAX SO THIS SUBROUTINE AND INPUT ARE
C USED TO FACILITATE MODIFACTIONS
      CALL IF(ILABL,TAU)
1000  FORMAT(8A5,F)
      WRITE(1,1000) ILABL,TAU
C
C       THIS SECTION INITIALIZES SOME CONSTANTS
      NRP=0
C
C       THIS SECTION INPUTS THE GROUND STRIPS DECSRIPTIONS
      CALL IFILE(20,'GRND')
      READ(20,1000) ILABL
      WRITE(1,1000) ILABL
      READ(20) K,X1,Z1,X2,Z2
      CALL RELEAS (20)
C
C       THIS SECTION INPUTS THE ANTENNA FILE NAME TO BEUSED
C AND THEN INPUTS THE ANTENNA ELEMENT DESCRIPTIONS
      WRITE(5,2001)
2001  FORMAT(' INPUT ANTENNA FILE NAME:',$)
      READ(5,2000) ILBL
2000  FORMAT(A5)
      CALL IFILE(20,ILBL)
      READ(20,1000) ILABL
      WRITE(1,1000) ILABL
      READ(20) LAMBDA,NEL,(X(I),Y(I),Z(I),CF1(I),CF2(I),CF3(I),I=1,NEL)
```

```
      WRITE(1) LAMBDA,NEL,(X(I),Y(I),Z(I),CF1(I),CF2(I),CF3(I),I=1,NEL)
      CALL RELEAS (20)
      SQRT2L=1./SQRT(2.*LAMBDA)
      TEMP2=LAMBDA
      DAK=DPI/DBLE(LAMBDA)
      SAK=SNGL(DAK)
C
C       THIS IS THE MAIN LOOP FOR THE SIMULATION.  THE RECEIVER
C LOCATION IS READ IN BY INPUT.  THE DATA IS IN COMMON 'REC'
C THE INPUT BEING DONE BY JOVRAX.  IF THERE ARE NO MORE RECEIVER
C POINTS THE SUBROUTINE RETURNS TO 200.
201   CALL INPUT(*200)
C
C       THIS SECTION INITIALIZES THE COMPLEX AMPLITUDES FOR
C THE RECEIVED FIELD AS FOLLOWS:
C       CFR1    CARRIER WITH 'REAL' GROUND
C       CFR2    150 HZ SIDEBAND WITH 'REAL' GROUND
C       CFR3    90HZ SIDEBAND WITH 'REAL' GROUND
C       CFS1    CARRIER WITH 'IDEAL' FLAT GOUND PLANE
C       CFS2    150HZ WITH 'IDEAL' GROUND
C       CFS3    90 HZWITH 'IDEAL' GROUND
      CFR1=(0.,0.)
      CFR2=(0.,0.)
      CFR3=(0.,0.)
      CFS1=(0.,0.)
      CFS2=(0.,0.)
      CFS3=(0.,0.)
      RZ=SQRT(RX*RX+RZ*RZ)
C
C       THIS LOOP IS OVER THE ELEMENTS OF THE ANTENNA
C THE COMPLEX FIELDS ARE SUMMED IN CFR1,CFR2 ETC.
      DO 3 IEL=1,NEL
C
C       THESE ARE THE LOCATION COORDINATES OF THE ANTENNA ELEMENTS
C AND CONSTANTS USED IN THE STRIP INTEGRATION
      AX=X(IEL)
      AY=Y(IEL)
      AZ=Z(IEL)
      DELX=RX-AX
      DELY=RY-AY
      DELZ=RZ-AZ
      DR=DSQRT(DELX*DELX+DELY*DELY+DELZ*DELZ)
      R=SNGL(DR)
      DR=DR*DAK
      IL=DR/DPI
C
C       THIS SECTION INITIALIZES  HR AND HI TO INCLUDE THE
C SEMI-INFINITE PEAK GROUND PLANE
       TEMP2=DR-DBLE(FLOAT(IL))*DPI
      TEMP=RZ+AZ
      F1=SQRT(TEMP*TEMP+AY*AY)
      F2=-RX*TEMP/(F2*F1)
      TC=SQRT(1.+AY*AY/(TEMP*TEMP))
```

```
      TD=TC*AZ
      R1=R2*TC
      S=SQRT((1./R2+1./AZ)/(TC*TC*TC))
      G=RX/(TD*TD*R1*R1*S)
      TEMP=SAK*F1
      SF=SIN(TEMP)
      FC=COS(TEMP)
      TEMP=AZ*G/DAK/F2
C
C       HR AND HI ARE THE REAL AND IMAGINARY PARTS OF THE COMPLEX
C 'GAIN' FACTOR OF THE GROUND SURFACE SCATTERING TO THE RECIEVER
C LOCATION
      HR=-TEMP*(SF+FC/(DAK*TD))
      HI=TEMP*(FC-SF/(DAK*TD))
C
C       THIS SUBROUTINE SUMS THE 'GAIN' FACTOR FOR EACH STRIP OF
C THE GROUND SURFACE
      CALL SCAT
C
C       THIS SECTION INCLUDES THE EFFECT OF THE DIRECT RADIATION FROM
C THE ANTENNA ELEMENT AT THE RECEIVER
      HR=HR*SQRT2L
      HI=HI*SQRT2L
      TEMP=DELX/(R*R)
      SF=SIN(TEMP2)
      FC=COS(TEMP2)
C
C       CTEMP IS THE COMPLEX GAIN FACTOR INCLUDING ALL RADIATION FROM
C THIS ELEMENT
      CTEMP=CMPLX(-TEMP*SF+HR-HI,TEMP*FC+HR+HI)*.5/LAMBDA
C
C       THIS SECTION ACCUMULATES THE FIELDS OF THE VARIOUS FREQUENCIES
      CFS1=CFS1+CTEMP*CF1(IEL)
      CFS2=CFS2+CTEMP*CF2(IEL)
      CFS3=CFS3+CTEMP*CF3(IEL)
      ALPH=SAK*2.*AZ*RZ/R
      CTEMP=TEMP*.5/LAMBDA*CMPLX(-SF,FC)*
     1CMPLX((1.-COS(ALPH)),-SIN(ALPH))
      CFR1=CFR1+CTEMP*CF1(IEL)
      CFR2=CFR2+CTEMP*CF2(IEL)
      CFR3=CFR3+CTEMP*CF3(IEL)
3     CONTINUE
      WRITE(1,2003) RX,RY,RZ,RT,CFR1,CFR2,CFR3,CFS1,CFS2,CFS3
2003  FORMAT(4F,,6E13.6,/,6E13.6)
      GO TO 201
C
C       THIS IS THE TERMINATION SECTION.  THE INITIAL RECORD ON
C THE OUTPUT FILE IS WRITTEN AND THE PROGRAM TERMINATES.
200   CALL RELEAS (1)
      CALL EXIT
      STOP
      END
```

CONSTANTS

0	2036220077325	1	1560420550061	2	0000000030001	3	5185122440440	4	0000000000010				
5	000000000024	6	436451642100	7	0000000000000	10	0000000003000						

COMMON

NRP	/PLXT	/+0	RXMN	/PLXT	/+1	RXMX	/PLXT	/+2	RXFT	/PLXT	/+3	RXLT	/PLXT	/+4
RYMN	/PLXT	/+5	RYMX	/PLXT	/+6	RYFT	/PLXT	/+7	RYLT	/PLXT	/+10	RZMN	/PLXT	/+11
RZMX	/PLXT	/+12	RZFT	/PLXT	/+13	RZLT	/PLXT	/+14	RTMN	/PLXT	/+15	RTMX	/PLXT	/+16
RTFT	/PLXT	/+17	RTLT	/PLXT	/+20	AIMN	/PLXT	/+21	AIMX	/PLXT	/+22	AIFT	/PLXT	/+23
AILT	/PLXT	/+24	ARMN	/PLXT	/+25	ARMX	/PLXT	/+26	ARFT	/PLXT	/+27	ARLT	/PLXT	/+30
ADIN	/PLXT	/+31	ADIX	/PLXT	/+32	ADIF	/PLXT	/+33	ADIL	/PLXT	/+34	ADRN	/PLXT	/+35
ADRX	/PLXT	/+36	ADRF	/PLXT	/+37	ADRL	/PLXT	/+40	RX	/REC	/+0	RY	/REC	/+1
RZ	/REC	/+2	RT	/REC	/+3	NSIZE	/REC	/+4	N	/GROUND	/+0	X1	/GROUND	/+1
Z1	/GROUND	/+25	X2	/GROUND	/+51	Z2	/GROUND	/+76	IEL	/GROUND	/+123	AX	/ANT	/+0
AY	/ANT	/+1	AZ	/ANT	/+2	LAMBDA	/ANT	/+3	DAK	/ANT	/+4	DP1	/ANT	/+5
HR	/VAL	/+0	HI	/VAL	/+1	IPTDAT	/PLXT	/+0						

SUBPROGRAMS

FORSE.	.JREF	DFILE	IF	ALPHD.	ALPHI.	FLOUT.	FLIPT.	IFILE	RINGR.	RELEAS	SORT	DBUF	DFD.2	SNGL
INPUT	DSQRT	DFM.2	DFM.4	DFA.2	DFM.6	DFMM.2	IDINT	FLOAT	DFM.0	DFS.0	SIN	COS	DFD.4	DFA.4
DFS.4	SCAT	CMPLX	CFD.0	CFM.2	CFM.0	EXIT								

SCALARS

DPI	6		TAU	1017		NRP	0		N	0		ILBL	1020	
LAMBDA	3		NEL	1021		I	1022		SQRT2L	1023		TEMP2	1024	
DAK	4		SAK	1025		CFR1	1026		CFR2	1030		CFR3	1032	
CFS1	1034		CFS2	1036		CFS3	1040		R2	1042		PX	0	
RZ	2		IEL	123		AX	0		AY	1		AZ	2	
DELX	1043		DELY	1045		PY	1		DELZ	1047		DR	1051	
R	1053		IL	1054		TEMP	1055		F1	1056		F2	1057	
TC	1060		TD	1061		P1	1062		S	1063		G	1064	
SF	1065		FC	1066		HR	0		HI	1		CFR0	1067	
ALPH	1071		PT	3		RXMN	1		RXMX	2		RXFT	3	
RXLT	4		RYMN	5		RYMX	6		RYFT	7		RYLT	10	
RZMN	11		RZMX	12		RZFT	13		RZLT	14		RTMN	15	
RTMX	16		RTFT	17		RTLT	20		AIMN	21		AIMX	22	
AIFT	23		AILT	24		ARMN	25		ARMX	26		ARFT	27	
ARLT	30		ADIN	31		ADIX	32		ADIF	33		ADIL	34	
ADRN	35		ADRX	36		ADRF	37		ADRL	40		NSIZE	1	

ARRAYS

ILABL	1072		IPTDAT	0		X	1102		Y	1126		Z	1152	
CF1	1176		CF2	1246		CF3	1316		X1	1		Z1	25	
X2	51		Z2	76										

X1	15	41				
X2	15	41				
Y	10	53	54	90		
Z	10	53	54	91		
Z1	15	41				
Z2	15	41				
3P	85	148				
200P	65	155				
201P	65	151				
1000P	31	32	39	40	51	52
2000P	48	49				
2001P	46	47				
2003P	149	150				

```
    1          C
    2          C       THIS SUBROUTINE OPENS THE FLIGHT PATH FILE AND INPUTS THE
    3          C FLIGHT PATH PLOT LABEL AND THE INERTIAL TIME CONSTANT
    4          C
    5          C       THIS SUBROUTINE INPUTS THE RECEIVER LOCATION
    6          C COORDINATES OF THE NEXT POINT ON THE FLIGHT PATH.  IF THERE
    7          C ARE NO MORE POINTS THE SUBROUTINE EXITS TO THE
    8          C END RETURN POINT
    9                SUBROUTINE IF(ILABL,TAU)
   10                DIMENSION ILABL(8)
   11                COMMON/REC/ DUM(4),NSIZE
   12                CALL JOVSET(1,'PATH.DAT',NS)
   13                WRITE(5,1000) NS
   14           1000 FORMAT(15,' RECORDS IN PATH.DAT',/)
   15                NSIZE=(NS-8)/4
   16                CALL JOVWI(1,ILABL,8,0)
   17                CALL JOVWI(1,TAU,1,0)
   18                RETURN
   19                END

      CONSTANTS

      0       000000000001    1       502032444134    2       422u3242u100    3       000000000000    4       000000000010

      GLOBAL DUMMIES

      ILABL   66              TAU     67

      COMMON

      DUM     /REC   /+0      NSIZE   /REC   /+4

      SUBPROGRAMS

      JOVSET  INTO.   INTI.   JOVWI

      SCALARS

      IF      70              NS      71              NSIZE   4               TAU     67

      ARRAYS

      ILABL   66              DUM     0


DUM          11
IF            9
ILABL         9      10      16
JOVSET       12
JOVWI        16      17
NS           12      13      15
NSIZE        11      15
REC          11
TAU           9      17
```

```
 1000P      13      14

      1                SUBROUTINE INPUT($)
      2                COMMON /REC/ RX(4),NSIZE
      3                IF(NSIZE .LE. 0) RETURN 1
      4                CALL JOVWI(1,RX,4,0)
      5                NSIZE=NSIZE-1
      6                RETURN
      7                END

     CONSTANTS

     0        000000000001    1        000000000004    2        000000000000

     COMMON

     RX       /REC    /+0     NSIZE    /REC    /+4

     SUBPROGRAMS

     JOVWI

     SCALARS

     INPUT    36              NSIZE    4

     ARRAYS

     RX       0


 INPUT        1
 JOVWI        4
 NSIZE        2       3       5
 REC          2
 RX           2       4
```

```
      C
      C       THIS SUBROUTINE SUMS THE EFFECTS OF THE STRIPS THAT MAKE
      C UP HE GROUNDSURFACE.  THERE ARE 'K' STRIPS DESCRIBED IN COMMON
      C GROUND AS FOLLOWS:
      C       X1(I)   THE X-COORDINATE OF THE LEADING EDGE OF THE I'TH STRIP
      C       Z1(I)   THE Z-COORDINATE OF THE LEADING EDGE OF THE I'TH STRIP
      C       X2(I)   THE X-COORDINATE OF THE ENDING EDGE OF THE I'TH STRIP
      C       Z2(I)   THE Z-COORDINATE OF THE ENDING EDGE OF THE I'TH STRIP
            SUBROUTINE SCAT
            COMMON /REC/ RX,RY,RZ
            COMMON /ANT/AX,AY,AZ
            COMMON /GROUND/ K,X1(20),Z1(20),X2(20/20),Z2(20/20),ILL
            COMMON /SEG/ XX1,ZZ1,XX2,ZZ2,N
      C
      C       THESE ARE INITIAL VALUES FOR THE PARAMETERS USED IN SHADOWING
            SLOPE=-1.
            PHIE=-1.
      C
      C       THIS IS THE LOOP OVER THE STRIPS
            DO 1 I=1,K
      C
      C       THESE ARE THE VALUES TO BE USED IN THE STRIP
      C INTEGRATION SUBROUTINE
      C       XX1     LEADING X-COORDINATE
      C       ZZ1     LEADING Z-COORDINATE
      C       XX2     TRAILING X-COORDINATE
      C       ZZ2     TRAILING Z-COORDINATE
            XX1=X1(I)
            ZZ1=Z1(I)
            XX2=X2(I)
            ZZ2=Z2(I)
      C
      C       THIS IS A TEST TO SEE IF THE SUMMATION OVER THE GROUND
      C STRIPS HAS REACHED THE RECEIVER LOCATION.  IF IT HAS THE SUMSATION
      C IS STOPPED.  THIS IS TO GIVE THE EFFECT OF FORWARD LOOKING RECEIVER
      C ANTENNA PATTERN.
            IF( XX1 .GE. RX) GO TO 6
      C
      C       IF THE RECIEVER IS LOCATED OVER THE MIDDLE PORTION OF A STRIP
      C THE STRIP WILL BE INTEGRATE ONLY UP TO THE VALUE OF THE
      C RECEIVER X-COORDINATE
            IF(XX2 .LE. RX) GO TO 5
            ZZ2=ZZ1+(RX-XX1)*(ZZ2-ZZ1)/(XX2-XX1)
            XX2=RX
      5     CONTINUE
      C
      C       THIS SECTION DOES THE SHADOWING.  IF PART OR ALL OF THE STRIP
      C IS IN THE SHADOW OF A PREVIOUS STRIP, THIS STRIP WILL BE ELIMINATED
      C OR MASKED TO GIVE THE EFFECT OF SHADOWING.
            DELX=XX2-AX
            IF(DELX .LE. 0.) GO TO 3
            PHIE=(AZ-ZZ2)/DELX
            IF(SLOPE .LT. 0.) GO TO 3
```

```
                IF(PHIE .GE. SLOPE) GO TO 1
                PHIB=(AZ-ZZ1)/(XX1-AX)
                IF( PHIB .LE. SLOPE) GO TO 3
                IF( XX1 .EQ. XX2) GO TO 4
                A=(ZZ2-ZZ1)/(XX2-XX1)
                B=ZZ1-A*(XX1-AX)
                XX1=(AZ-B)/(A+SLOPE)+AX
      4         ZZ1=-SLOPE*(XX1-AX)+AZ
      C
      C           THIS SUBROUTINE WILL INTEGRATE OVER THE STRIP THE
      C COMPLEX 'GAIN' EFFECT OF THIS STRIP WILL BE ADDED TO HR AND HI
      C IN COMMON 'VALL'
      3         CALL SUM
                SLOPE=PHIE
      1         CONTINUE
      6         RETURN
                END

CONSTANTS

0       201400000000

COMMON

RX      /REC    /+0     RY      /REC    /+1     RZ      /REC    /+2     AX      /ANT    /+0     AY      /ANT    /+1
AZ      /ANT    /+2     K       /GROUND/+0      X1      /GROUND/+1      Z1      /GROUND/+25     X2      /GROUND/+51
Z2      /GROUND/+76     IEL     /GROUND/+123    XX1     /SEG    /+0     ZZ1     /SEG    /+1     XX2     /SEG    /+2
ZZ2     /SEG    /+3     N       /SEG    /+4

SUBPROGRAMS

SUM

SCALARS

SCAT    143             SLOPE   144             PHIE    145             1       146             M       0
XX1     0               ZZ1     1               XX2     2               ZZ2     3               PX      0
DELX    147             AX      0               AZ      2               PHIB    150             A       151
B       152             RY      1               RZ      2               AY      1               IEL     123
N       4

ARRAYS

X1      1               Z1      25              X2      51              Z2      76
```

A	58	59	60								
ANT	11										
AX	11	50	55	59	60	61					
AY	11										
AZ	11	52	55	60	61						
B	59	60									
DELX	50	51	52								
GROUND	12										
I	20	28	29	30	31						
IEL	12										
K	12	20									
N	13										
PHIB	55	56									
PHIE	17	52	54	67							
REC	10										
RX	10	37	42	43	44						
RY	10										
RZ	10										
SCAT	9										
SEG	13										
SLOPE	16	53	54	56	60	61	67				
SUM	66										
X1	12	28									
X2	12	30									
XX1	13	28	37	43	55	57	58	59	60	61	
XX2	13	30	42	43	44	50	57	58			
Z1	12	29									
Z2	12	31									
ZZ1	13	29	43	55	58	59	61				
ZZ2	13	31	43	52	58						

1P	20	54	68		
3P	51	53	56	66	
4P	57	61			
5P	42	45			
6P	37	69			

```
      C
      C       THIS SUBROUTINE INTEGRATES OVER THE SURFACE STRIP DEFINED
      C BY X1,Z1,X2,Z2 IN COMMON 'SEG', TO GIVE THE FIELD EFFECT
      C OF THEANTENNA ELEMENT IN COMMON 'ANT' AT RECIEVER DEFINED
      C IN COMMON 'REC'.  THE VARIABLES ARE AS FOLLOWS:
      C       AX      ANTENNA X-COORDINATE
      C       AY      ANTENNA Y-COORDINATE
      C       AZ      ANTENNA Z-COORDINATE
      C       LAMBDA  WAVELENGTH OF CARRIER
      C       AK      TWO*PI/LAMBDA
      C       DPI     TWO*PI (DOUBLE PRECISION)
      C       RX      RECEIVER X-COORDINATE
      C       RY      RECEIVER Y-COORDINATE
      C       RZ      RECEIVER Z-COORDINATE
      C       HR      REL PART OF 'GAIN' FACTOR
      C       HI      IMAGINARY PART OF 'GAIN' FACTOR
      C       X1      LEADING EDGE OF STRIP'S X-COORDINATE
      C       Z1      LEADING Z-COORDINATE
      C       X2      TRAILING EDGE X-COORDINATE
      C       Z2      TRAILING Z-COORDINATE
      C THE INTEGRATION IS PERFORMED BY A MODIFIED TRAPIZOID RULE.
      C THE SPACING BETWEEN POINTS ALONG THE VARIABLE OF INTEGRATION
      C IS VARIED BY THE RATE OF CHANGE OF THE INTEGRAND.
            SUBROUTINE SUM
            COMMON /SEG/ X1,Z1,X2,Z2,A
            DOUBLE PRECISION A1,A2,B1,B2,XL,AY2
            REAL  JR,JI,JOR,JOI,JNR,JNI
            REAL LAMBDA
             DOUBLE PRECISION AK,DPI,DR
            COMMON /ANT/AX,AY,AZ,LAMBDA,AK,DPI
            COMMON /REC/RX,RY,RZ
            COMMON /VAL/HR,HI
            REAL L3,L10
      C
      C       THIS IS THE INITIALIZATION SECTION
            AY2=DBLE(AY)*DBLE(AY)
            AKK=SNGL(AK)
            SE=Z2-Z1
            CE=X2-X1
      C
      C       XMAX IS THE LENGTH ALONG THE SURFACE OF THE STRIP
            XMAX=SQRT(SE*SE+CE*CE)
      C
      C       THESE ARE THE SIN AND COS OF THE ANGLE THE STRIP MAKES WITH
      C A HORIZONTAL PLANE
            SE=SE/XMAX
            CE=CE/XMAX
            JR=0.
            JI=0.
      C
      C       XL IS THE VARIABLE OF INTEGRATION.  IT IS THE DISTANCE
      C ONG THE SURFACE OF THE STRIP STARTING FROM THE LEADING EDGE
            XL=0.
```

```
      NX=1
      IT=0
C
C       THESE ARE THE LOWER AND UPPER BOUNDS FOR THE SPACING BETWEEN
C POINTS ALONG THE VARIABLE OF INTEGRATION
      L3= LAMBDA/24.
      L10=20.*LAMBDA
      A1=RX-X1
      A2=RZ-Z1
      B1=X1
      B2=Z1-AZ
      A=A1
      TEMP=A2
       A= SQRT(A*A+TEMP*TEMP)
      B=B1
      TEMP=B2
      B= SQRT(B*B+TEMP*TEMP)
      TEMP=A+B
      DR=DSQRT(DBLE(TEMP)*DBLE(TEMP)+DBLE(AY*AY))
      C=DR
      DR=DR*AK
      I=DR/DPI
      F=DR-DBLE(FLOAT(I))*DPI
      C=C/TEMP
      D=C*B
      R=C*A
       S=SQRT((1./A+1./B)/C/C/C)
      G=A1/D/D/R/R/S
      TEMP=G/(AKK*D)
      CF=COS(F)
      SF=SIN(F)
      JOR=G*CF-TEMP*SF
      JOI=G*SF+TEMP*CF
      AP=(-A1*CE-A2*SE)/A
      BP=(B1*CE+B2*SE)/B
C
C       FP IS THE DERIVATIVE OF THE PHASE FUNCTION
C OF THE INTEGRAND
      FP=ABS((AP+BP)/C)
C
C       DL IS DELTA XL
      DL=L3/FP
      IF(DL .GT. L10) DL=L10
      IF(DL .LT. L3) DL=L3
      XL=XL+DL
C
C       THIS IS THE LOOP OVER THE SURFACE OF THE STRIP.  XL IS
C INCREMENTED BY DL (OF VARIABLE SIZE) UNTIL THE END OF THE STRIP
C IS REACHED (XMAX)
    1 CONTINUE
C
C       THIS SECTION CALCULATE VARIOUS TERMS USED IN EVALUATING THE
C INTEGRAND.  THE AMPLITUDE AND PHASE FUNCTION
```

```
      C ARE EVALUATED SEPARATELLY.  THE DERIVATIVE OF THE PHASE FUNCTION
      C IS EVALUATED TO DETERMINE THE SIZE FOR DELTA X
            DLSE=DL*SE
            DLCE=DL*CE
            A1=A1-DLCE
            A2=A2-DLSE
            B1=B1+DLCE
            B2=B2+DLSE
            A=A1
             TEMP=A2
            A= SQRT(A*A+TEMP*TEMP)
            B=B1
            TEMP=B2
            B= SQRT(B*B+TEMP*TEMP)
            TEMP=A+B
            DR=DSQRT(DBLE(TEMP)*DBLE(TEMP)+DBLE(AY*AY))
            C=SNGL(DR)/TEMP
            DR=DR*AK
            I=DR/DPI
      C
      C       THIS IS THE PHASEE ANGLE "MODULO TWO PI"
            F=DR-DBLE(FLOAT(I))*DPI
            D=C*B
            R=C*A
            S=SQRT((1./A+1./B)/C)/C
            G=A1/(D*D*R*R*S)
      C
      C       THIS IS THE AMPLITUDE FUNCTION
            TEMP=G/(AKK*D)
            CF=COS(F)
            SF=SIN(F)
      C
      C       THIS IS THE REAL PART OF THE INTEGRAND FOR THE
      C INTEGRATION VARIABLE VALUE OF XL
            JNR=G*CF-TEMP*SF
      C
      C       THIS IS THE IMAGINARY PART
            JNI=G*SF+TEMP*CF
            TEMP=DL
      C
      C       THESE ARE THE REAL AN IMAGINARY PARTS OF THE THE SUMMATION
      C OF THE TRAPIZOIDS MAKING UP THE APPROXIMATION TO THE INTEGRAL
            JR=JR+(JOR+JNR)*TEMP
            JI=JI+(JOI+JNI)*TEMP
             IF(IT .NE. 0) GO TO 2
            JOR=JNR
            JOI=JNI
            AP=(-A1*CE-A2*SF)/A
             BP=(B1*CE+B2*SE)/B
      C
      C     FP IS THE DERIVATIVE OF THE PHASE FUNCTION
            FP=ABS((AP+BP)/C)
      C
```

```
160           C       DL IS DELTA X AND IS LIMITED BY THE BOUNDS L3,L10
161                 DL=L3/FP
162                 IF(DL .GT. L10) DL=L10
163                 IF(DL .LT. L3) DL=L3
164                 NX=NX+1
165           C
166           C       THE VARIABLE OF INTGRATION IS INCREMENTED AND IF THE END OF THE
167           C STRIP IS REACHED THE LAST TRAPIZOID IS ADDED
168                 XL=XL+DL
169                 IF( XL .LT. XMAX) GO TO 1
170                 DL=XMAX+DL-XL
171                 XL=XMAX
172                 IT=1
173                 GO TO 1
174           C
175           C       THIS SECTION ADDS THE FIELD EFFECT FROM THE STRIP TO THE
176           C TOTAL FIELD SUM AND TEH SUBROUTINE TERMINATES
177           2     CONTINUE
178                 N=NX
179                 TEMP=((Z1-AZ)*CE-X1*SE)/2.
180                 HR=HR+JR*TEMP
181                 HI=HI+JI*TEMP
182                 RETURN
183                 END

      CONSTANTS

      0       205600000000

      COMMON

      X1      /SEG    /+0     Z1      /SEG    /+1     X2      /SEG    /+2     Z2      /SEG    /+3     X       /SEG    /+4
      AX      /ANT    /+0     AY      /ANT    /+1     AZ      /ANT    /+2     LAMBDA  /ANT    /+3     AR      /ANT    /+4
      DPI     /ANT    /+6     RX      /REC    /+0     RY      /REC    /+1     RZ      /REC    /+2     HR      /VAL    /+0
      HI      /VAL    /+1

      SUBPROGRAMS

      DBLE    DFM.0   SNGL    SQRT    DSQRT   DFA.0   DFMM.2  DFD.2   IDINT   FLOAT   DFS.0   DFD.6   COS     SIN     DFM.4
      DFM.6   DFA.4   DFD.4   ABS     DFAM.2  DFS.2

      SCALARS

      SUM     1064            AY2     1065            AY      1       AAR     1067            AR      4
      SE      1070            Z2      3               Z1      1       CE      1071            X2      2
      X1      0               XMAX    1072            JR      1073    JI      1074    XL      1075
      NX      1077            IT      1100            L3      1101    LAMBDA  3       L10     1102
      A1      1103            RX      0               A2      1105    RZ      2       BI      1107
      B2      1111            AZ      2               A       1113    TEMP    1114    R       1115
      DR      1116            C       1120            I       1121    DPI     6       F       1122
      D       1123            R       1124            S       1125    G       1126    CF      1127
      SF      1130            JOR     1131            JOI     1132    AP      1133    HP      1134
      FP      1135            DL      1136            DLSE    1137    DLCE    1140    JAR     1141
```

JNI 1142 N 4 HR 0 HI 1 AX 0
RY 1

A	65	67	71	79	80	87	115	117	121	130	131	154
A1	26	61	65	81	87	111	115	132	154			
A2	26	62	66	87	112	116	154					
ABS	92	158										
AK	29	30	37	74	124							
AKK	37	82	135									
ANT	30											
AP	87	92	154	158								
AX	30											
AY	30	36	72	122								
AY2	26	36										
AZ	30	64	179									
B	68	70	71	78	80	88	118	120	121	129	131	155
B1	26	63	68	88	113	118	155					
B2	26	64	69	88	114	119	155					
BP	88	92	155	158								
C	73	77	78	79	80	92	123	129	130	131	158	
CE	39	42	47	87	88	110	154	155	179			
CF	83	85	86	136	141	144						
COS	83	136										
D	78	81	82	129	132	135						
DBLE	36	72	76	122	128							
DL	95	96	97	98	109	110	145	161	162	163	168	170
DLCE	110	111	113									
DLSE	109	112	114									
DPI	29	30	75	76	125	128						
DR	29	72	73	74	75	76	122	123	124	125	128	
DSQRT	72	122										
E	76	83	84	128	136	137						
FLOAT	76	128										
FP	92	95	158	161								
G	81	82	85	86	132	135	141	144				
HI	32	181										
HR	32	180										
I	75	76	125	128								
IT	55	151	172									
JI	27	49	150	181								
JNI	27	144	150	153								
JNR	27	141	149	152								
JOI	27	86	150	153								
JOR	27	85	149	152								
JR	27	48	149	180								
L10	33	60	96	162								
L3	33	59	95	97	161	163						
LAMBDA	28	30	59	60								
N	25	178										
NX	54	164	178									
R	79	81	130	132								
REC	31											
RX	31	61										
RY	31											
RZ	31	62										
S	80	81	131	132								

PROGRAM MOLE.F4

```
      DIMENSION ILABL(8)
      DIMENSION IPTDAT(33)
      COMMON /PLXT/ NRP,RXMN,RXMX,RXFT,RXLT,RYMN,RYMX,RYFT,RYLT,
     1RZMN,RZMX,RZFT,RZLT,RTMN,RTMX,RTFT,RTLT,
     2AIMN,AIMX,AIFT,AILT,ARMN,ARMX,ARFT,ARLT,
     3ADIR,ADIX,ADIF,ADIL,
     4ADRR,ADRX,ADRF,ADRL
      EQUIVALENCE (IPTDAT(1),NRP)
      IMPLICIT COMPLEX (C)
      DIMENSION X(20),Y(20),Z(20)
      DIMENSION CF1(20),CF2(20),CF3(20)
      IMPLICIT DOUBLE PRECISION (D)
      COMMON /REC/RX,RY,RZ,RT,NSIZE
      REAL LAMBDA
      COMMON /ANT/AX,AY,AZ,LAMBDA,DAK,DPI
      COMMON /VAL/ HR,HI
      COMMON /GRND/ P(3,4),Y(3)
C
C       THIS VALUE OF TWO PI IS INITIALIZED THIS WAY TO AVOID USING
C BLOCK DATA
      DPI=6.2831853071795864769
      WRITE(5,2001)
2001  FORMAT(' INPUT FILE NAME:',$)
      READ(5,2000) ILBL
2000  FORMAT(A5)
      CALL IFILE(20,ILBL)
      WRITE(5,2002)
2002  FORMAT(' OUTPUT FILE NAME:',$)
      READ(5,2000) ILBL
      CALL OFILE(1,ILBL)
      READ(20,1000) ILABL,TAU
      WRITE(1,1000) ILABL
      DO 3 I=1,2
      READ(20,1000) ILABL
3     WRITE(1,1000) ILABL
1000  FORMAT(8A5,F)
      READ(20) LAMBDA,NEL,(X(I),Y(I),Z(I),CF1(I),CF2(I),CF3(I),I=1,NEL)
      WRITE(1) LAMBDA,NEL,(X(I),Y(I),Z(I),CF1(I),CF2(I),CF3(I),I=1,NEL)
      DAK=DPI/DBLE(LAMBDA)
201   READ(20,2005,END=200) RX,RY,RZ,RT,
     1CFR1,CFR2,CFR3,CFS1,CFS2,CFS3
2005  FORMAT(4F,/,6E13.6,/,6E13.6)
      READ(5,3000) P
3000  FORMAT(3G)
      DO 5 I=1,NEL
      AX=X(I)
      AY=Y(I)
      AZ=Z(I)
      CTEMP=(0.,0.)
      CALL INTR2(CTEMP)
      CT=CTEMP*CF1(I)
      CFR1=CFR1+CT
      CFS1=CFS1+CT
```

```
                CT=CTEMP*CF2(I)
                CFR2=CFR2+CT
                CFS2=CFS2+CT
                CT=CTEMP*CF3(I)
                CFS3=CFS3+CT
                CFR3=CFR3+CT
          5     CONTINUE
                WRITE(1,2005) RX,RY,RZ,RT,CFR1,CFR2,CFR3,CFS1,CFS2,CFS3
                GO TO 201
          C
          C       THIS IS THE TERMINATION SECTION.  THE INITIAL RECORD ON
          C THE OUTPUT FILE IS WRITTEN AND THE PROGRAM TERMINATES.
          200   CALL RELEAS (1)
                CALL EXIT
                STOP
                END

CONSTANTS

0       203622077325    1       150042055061    2       000000000024    3       000000000001    4       000000000000
5       000000000000

COMMON

NRP     /PLXT   /+0     RXMN    /PLXT   /+1     RXMX    /PLXT   /+2     RXFT    /PLXT   /+3     RXLT    /PLXT   /+4
RYMN    /PLXT   /+5     RYMX    /PLXT   /+6     RYFT    /PLXT   /+7     RYLT    /PLXT   /+10    RZMN    /PLXT   /+11
RZMX    /PLXT   /+12    RZFT    /PLXT   /+13    RZLT    /PLXT   /+14    RTMN    /PLXT   /+15    RTMX    /PLXT   /+16
RTFT    /PLXT   /+17    RTLT    /PLXT   /+20    AIMN    /PLXT   /+21    AIMX    /PLXT   /+22    AIFT    /PLXT   /+23
AILT    /PLXT   /+24    ARMN    /PLXT   /+25    ARMX    /PLXT   /+26    ARFT    /PLXT   /+27    ARLT    /PLXT   /+30
ADIN    /PLXT   /+31    ADIX    /PLXT   /+32    ADIF    /PLXT   /+33    ADIL    /PLXT   /+34    ADRN    /PLXT   /+35
ADRX    /PLXT   /+36    ADRF    /PLXT   /+37    ADRL    /PLXT   /+40    RX      /REC    /+0     RY      /REC    /+1
RZ      /REC    /+2     RT      /REC    /+3     NSIZE   /REC    /+4     AX      /ANT    /+0     AY      /ANT    /+1
AZ      /ANT    /+2     LAMBDA  /ANT    /+3     DAK     /ANT    /+4     DPI     /ANT    /+5     NR      /VAL    /+0
HI      /VAL    /+1     P       /GRND   /+0     N       /GRND   /+14    IPTDAT  /PLXT   /+0

SUBPROGRAMS

FORSE.  .JBFF   ALPHD.  ALPHI.  IFILE   OFILE   FLOUT.  FLIRT.  BINRR.  DBLE    DFD.2   EXD.    ALLIO.  IBIN2   CFS.2
RELEAS  EXIT

SCALARS

DPI     6               ILBL    363             TAU     364             I       365             LAMBDA  3
NEL     366             DAK     4               RX      0               RY      1               RZ      2
RT      3               CFR1    367             CFR2    371             CFR3    373             CFS1    375
CFS2    377             CFS3    401             AX      0               AY      1               AZ      2
CTEMP   403             CT      405             NRP     0               RXMN    1               RXMX    2
RXFT    3               RXLT    4               RYMN    5               RYMX    6               RYFT    7
RYLT    10              RZMN    11              RZMX    12              RZFT    13              RZLT    14
RTMN    15              RTMX    16              RTFT    17              RTLT    20              AIMN    21
AIMX    22              AIFT    23              AILT    24              ARMN    25              ARMX    26
ARFT    27              ARLT    30              ADIN    31              ADIX    32              ADIF    33
ADIL    34              ADRN    35              ADRX    36              ADRF    37              ADRL    40
```

NSIZE	4		HR	0		HI	1				
ARRAYS											
ILABL	407		IPTDAT	0		X	417	Y	443	Z	467
CF1	513		CF2	563		CF3	633	F	0	G	14

RELEAS	66				
RT	13	40	61		
RTFT	3				
RTLT	3				
RTMN	3				
RTMX	3				
RX	13	40	61		
RXFT	3				
RXLT	3				
RXMN	3				
RXMX	3				
RY	13	40	61		
RYFT	3				
RYLT	3				
RYMN	3				
RYMX	3				
RZ	13	40	61		
RZFT	3				
RZLT	3				
RZMN	3				
RZMX	3				
TAU	31				
VAL	16				
X	10	37	38	46	
Y	10	37	38	47	
Z	10	37	38	48	

3P	33	35			
5P	45	60			
200P	40	66			
201P	40	62			
1000P	31	32	34	35	36
2000P	24	25	29		
2001P	22	23			
2002P	27	28			
2005P	40	42	61		
3000P	43	44			

```
    1                SUBROUTINE NORMAL(V1,V2,V3,V4,R)
    2                DIMENSION V1(1),V2(1),V3(1),V4(1)
    3                X1=V2(1)-V1(1)
    4                X2=V3(1)-V1(1)
    5                Y1=V2(2)-V1(2)
    6                Y2=V3(2)-V1(2)
    7                Z1=V2(3)-V1(3)
    8                Z2=V3(3)-V1(3)
    9                X=Y1*Z2-Y2*Z1
   10                Y=Z1*X2-Z2*X1
   11                Z=X1*Y2-Y1*X2
   12                R=SQRT(X*X+Y*Y+Z*Z)
   13                V4(1)=X/R
   14                V4(2)=Y/R
   15                V4(3)=Z/R
   16                RETURN
   17                END
```

GLOBAL DUMMIES

V1	133	V2	134	V3	135	V4	136	R	137		

SUBPROGRAMS

SQRT

SCALARS

NORMAL	141	X1	142	X2	143	Y1	144	Y2	145		
Z1	146	Z2	147	X	150	Y	151	Z	152		
R	137										

ARRAYS

V1	133	V2	134	V3	135	V4	136				

NORMAL	1							
R	1	12	13	14	15			
SQRT	12							
V1	1	2	3	4	5	6	7	8
V2	1	2	3	5	7			
V3	1	2	4	6	8			
V4	1	2	13	14	15			
X	9	12	13					
X1	3	10	11					
X2	4	10	11					
Y	10	12	14					
Y1	5	9	11					
Y2	6	9	11					
Z	11	12	15					
Z1	7	9	10					
Z2	8	9	10					

```
    1                 DOUBLE PRECISION FUNCTION DIST(X,Y)
    2                 DIMENSION X(1),Y(1)
    3                 DOUBLE PRECISION R,TEMP
    4                 R=0.
    5                 DO 1 I=1,3
    6                 TEMP=X(I)-Y(I)
    7           1     R=R+TEMP*TEMP
    8                 DIST=DSQRT(R)
    9                 RETURN
   10                 END

        GLOBAL DUMMIES

        X       56              Y       57

        SUBPROGRAMS

        DFM.2   DFAM.2  DSQRT

        SCALARS

        DIST    60              R       62              I       64              TEMP    65

        ARRAYS

        X       56              Y       57


DIST        1       8
DSQRT       8
I           5       6
R           3       4       7       8
TEMP        3       6       7
X           1       2       6
Y           1       2       6


    1P      5       7
```

PROGRAM INT2.F4

```
      SUBROUTINE INTR2(CTEMP)
      DATA DX,DY/23.,40./
      DIMENSION XTA(3),ZTA(3)
      DOUBLE PRECISION D10,D20,R10,R20
      COMPLEX A,B
      DOUBLE PRECISION DR1,DR2
      COMPLEX CTEMP,CCT,CCX,CCY,CCX0
      REAL N,LAMBDA,N1,N2,N3
      COMMON /GRND/ P(3,4),N(3)
      EQUIVALENCE (N(1),N1),(N(2),N2),(N(3),N3)
      DOUBLE PRECISION DAK,DPI
      COMMON /REC/ XR,YR,ZR
      COMMON /ANT/XA,YA,ZA,LAMBDA,DAK,DPI
      EQUIVALENCE (P11,P(1,1)),(P12,P(1,2)),(P21,P(2,1))
      EQUIVALENCE (P24,P(2,4)),(P31,P(3,1)),(P34,P(3,4))
      LOGICAL TEST
      DATA TEST/.TRUE./
      IF(TEST) CALL NORMAL(P11,P12,P(1,4),N(1),TEMP)
      TEST=.FALSE.
      ZA2=2.*ZA
      TPI=SNGL(DPI)
      AK=SNGL(DAK)
      CTEMP=(0.,0.)
      DELX=DX
      DG0=DIST(D(1,1),D(1,2))
      IX=DG0/DELX
      IF(IX .LT. 0) IX=-IX
      IF(IX .LT. 1) IX=1
      IX=((IX+1)/2)*2
      DELX=DG0/FLOAT(IX)
      XTA(1)=(P(1,2)-P(1,1))/DG0
      XTA(2)=(P(2,2)-P(2,1))/DG0
      XTA(3)=(P(3,2)-P(3,1))/DG0
      DG0X=XTA(1)*DELX
      DG0Y=XTA(2)*DELX
      DG0Z=XTA(3)*DELX
      DG1=DIST(P(1,1),P(1,4))
      DELZ=DY
      IZ=DG1/DELZ
      IF(IZ .LT. 0) IZ=-IZ
      IF(IZ .LT. 1) IZ=1
      IZ=((IZ+1)/2)*2
      DELZ=DG1/FLOAT(IZ)
      ZTA(1)=(P(1,4)-P(1,1))/DG1
      ZTA(2)=(P(2,4)-P(2,1))/DG1
      ZTA(3)=(P(3,4)-P(3,1))/DG1
      DG1X=ZTA(1)*DELZ
      DG1Y=ZTA(2)*DELZ
      DG1Z=ZTA(3)*DELZ
      DO 1 IXX=1,IX
      FX=FLOAT(IXX)-.5
      XS=P(1,1)+FX*DG0X
      YS=P(2,1)+FX*DG0Y
```

```
      ZS=P(3,1)+FX*DG0Z
      DO 2 IZZ=1,IZ
      FZ=FLOAT(IZZ)-.5
      XS=XS+FZ*DG1X
      YS=YS+FZ*DG1Y
      ZS=ZS+FZ*DG1Z
      CC6=XR-XS
      CC7=XS-XA
      TEMP=YR-YS
      TEMP2=ZR-ZS
      TEMP3=ZR+ZS
      DR1=DBLE(CC6*CC6)+DBLE(TEMP*TEMP)
      DR2=DR1+DBLE(TEMP3*TEMP3)
      DR1=DR1+DBLE(TEMP2*TEMP2)
      R12=DR1
      R22=DR2
      R10=DSQRT(DR1)
      R20=DSQRT(DR2)
      R1=R10
      R2=R20
      TEMP=YS-YA
      TEMP2=ZS-ZA
      TEMP3=ZS+ZA
      DR1=DBLE(CC7*CC7)+DBLE(TEMP*TEMP)
      DR2=DR1+DBLE(TEMP3*TEMP3)
      DR1=DR1+DBLE(TEMP2*TEMP2)
      D12=DR1
      D22=DR2
      D10=DSQRT(DR1)
      D20=DSQRT(DR2)
      D1=D10
      D2=D20
      F10=N2*XS*(YR-YS)+(N1*XS+N3*(ZS-ZA))*(XR-XS)
      F20=F10+N3*(XR-XS)*ZA2
      COSA=(XTA(1)*CC7+XTA(2)*(YS-YA)+XTA(3)*(ZS-ZA))/D1
      COSA1=(XTA(1)*CC7+XTA(2)*(YS-YA)+XTA(3)*(ZS+ZA))/D2
      COSG=(XTA(1)*CC6+XTA(2)*(YR-YS)+XTA(3)*(ZR-ZS))/R1
      COSG1=(XTA(1)*CC6+XTA(2)*(YR-YS)+XTA(3)*(ZR+ZS))/R2
      COSB=(ZTA(1)*CC7+ZTA(2)*(YS-YA)+ZTA(3)*(ZS-ZA))/D1
      COSB1=(ZTA(1)*CC7+ZTA(2)*(YS-YA)+ZTA(3)*(ZS+ZA))/D2
      COSD=(ZTA(1)*CC6+ZTA(2)*(YR-YS)+ZTA(3)*(ZR-ZS))/R1
      COSD1=(ZTA(1)*CC6+ZTA(2)*(YR-YS)+ZTA(3)*(ZR+ZS))/R2
      CH=COSA-COSG
      CH1=COSA-COSG1
      CH2=COSA1-COSG
      CH3=COSA1-COSG1
      C=COSB-COSD
      C1=COSB-COSD1
      C2=COSB1-COSD
      C3=COSB1-COSD1
      D10=D10*DAK
      D20=D20*DAK
      R10=R10*DAK
```

```
                R20=R20*DAK
                ID=D10/DPI
                D1=D10-DBLE(FLOAT(ID))*DPI
                ID=D20/DPI
                D2=D20-DBLE(FLOAT(ID))*DPI
                ID=R10/DPI
                R1=R10-DBLE(FLOAT(ID))*DPI
                ID=R20/DPI
                R2=R20-DBLE(FLOAT(ID))*DPI
                TEMP=F10*SIN(AK*CH*DELX*.5)*SIN(AK*C*DELZ*.5)/(CH*C*D12*R12)
                CTEMP=CTEMP+TEMP*CEXP(CMPLX(0.,D1+R1))
                TEMP=F10*SIN(AK*CH1*DELX*.5)*SIN(AK*C1*DELZ*.5)/(CH1*C1*D12*R22)
                CTEMP=CTEMP-TEMP*CEXP(CMPLX(0.,D1+R2))
                TEMP=F20*SIN(AK*CH2*DELX*.5)*SIN(AK*C2*DELZ*.5)/(CH2*C2*D22*R12)
                CTEMP=CTEMP-TEMP*CEXP(CMPLX(0.,D2+R1))
                TEMP=F20*SIN(AK*CH3*DELX*.5)*SIN(AK*C3*DELZ*.5)/(CH3*C3*D22*R22)
                CTEMP=CTEMP+TEMP*CEXP(CMPLX(0.,D2+R2))
          2     CONTINUE
          1     CONTINUE
                CTEMP=CTEMP*2./(TPI*TPI)
                ICC=IX*IZ
                RETURN
                END

      CONSTANTS

      0         000000000000    1         000000000000    2         000000000001    3         000000000002

      GLOBAL DUMMIES

      CTEMP     1341

      COMMON

      P         /GRND   /+0     N         /GRND   /+14    XR        /REC    /+0     YR        /REC    /+1     ZR        /REC    /+2
      XA        /ANT    /+0     YA        /ANT    /+1     ZA        /ANT    /+2     LAMBDA    /ANT    /+3     DAK       /ANT    /+4
      DPI       /ANT    /+6     N1        /GRND   /+14    N2        /GRND   /+15    N3        /GRND   /+16    D11       /GRND   /+0
      P12       /GRND   /+3     P21       /GRND   /+1     P24       /GRND   /+12    P31       /GRND   /+7     P34       /GRND   /+13

      SUBPROGRAMS

      NORMAL    SNGL    DIST    D         IFIX    FLOAT   DBLE    DFA.0   DFAM.0  DSQRT   DFM.2   DFD.2   IFIX    DFM.0   DFS.0
      SIN       CEXP    CMPLX   CFM.0     CFD.4

      SCALARS

      INTR2     1347            DX        1350            DY        1351            TEST      1352            PI1       0
      P12       3               TEMP      1353            ZA2       1354            ZA        2               IPI       1355
      DPI       6               AK        1356            DAK       4               CTEMP     1341            DELX      1357
      DG0       1360            IX        1361            DG0X      1362            DG0Y      1363            DG0Z      1364
      DG1       1365            DELZ      1366            IZ        1367            DG1X      1370            DG1Y      1371
      DG1Z      1372            IXX       1373            FX        1374            XS        1375            YS        1376
      ZS        1377            IZZ       1400            FZ        1401            CC0       1402            XR        0
```

CC7	1403	XA	0	YR	1	TEMP2	1404	ZR	2
TEMP3	1405	DR1	1406	DR2	1410	R12	1412	R22	1413
R10	1414	R20	1416	R1	1420	R2	1421	YA	1
D12	1422	D22	1423	D10	1424	D20	1426	G1	1430
D2	1431	F10	1432	R2	15	M1	14	R3	16
F20	1433	COSA	1434	COSA1	1435	COSC	1436	COSC1	1437
COSB	1440	COSB1	1441	COSD	1442	COSD1	1443	CH	1444
CH1	1445	CH2	1446	CH3	1447	C	1450	C1	1451
C2	1452	C3	1453	ID	1454	ICC	1455	DAMPDA	3
P21	1	P24	12	P31	2	P34	13		

ARRAYS

XTA	1456	ZTA	1461	P	0	M	14

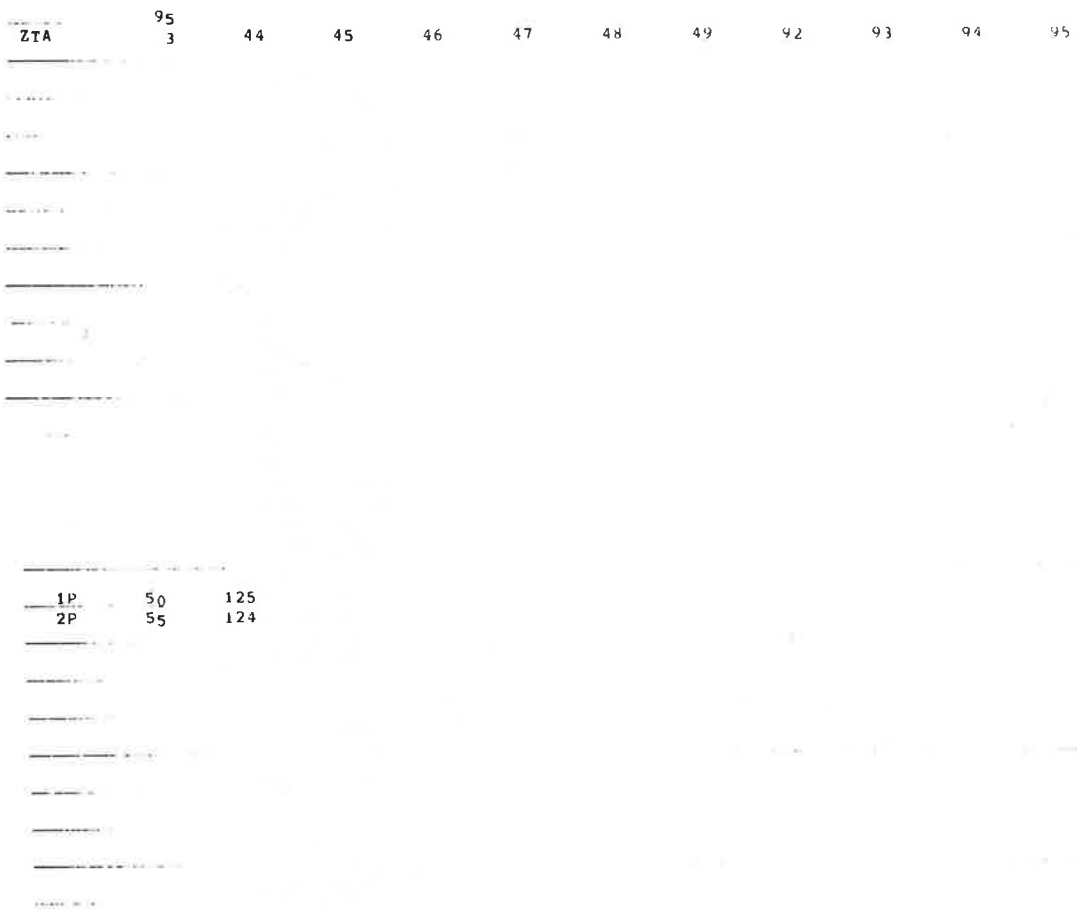
95
ZIA
3
44
45
46
47
48
49
92
93
94
95
1P
2P
50
55
125
124

PROGRAM GLDCDI.F4

```
      1               DIMENSION ILABL(8)
      2               DIMENSION IPTDAT(33)
      3               COMMON /PLXT/ NRP,RXMN,RXMX,RXFT,RXLT,RYMN,RYMX,RYFT,RYLT,
      4              1RZMN,RZMX,RZFT,RZLT,RTMN,RTMX,RTFT,RTLT,
      5              2AIMN,AIMX,AIFT,AILT,ARMN,ARMX,ARFT,ARLT,
      6              3ADIN,ADIX,ADIF,ADIL,
      7              4ADRN,ADRX,ADRF,ADRL
      8               EQUIVALENCE (IPTDAT(1),NRP)
      9               IMPLICIT COMPLEX (C)
     10               DIMENSION X(20),Y(20),Z(20)
     11               DIMENSION CF1(20),CF2(20),CF3(20)
     12               IMPLICIT DOUBLE PRECISION (D)
     13               COMMON /REC/RX,RY,RZ,RT,NSIZE
     14               REAL LAMBDA
     15               COMMON /GROUND/ K,X1(20),Z1(20),X2(0/20),Z2(0/20),IEL
     16               COMMON /ANT/AX,AY,AZ,LAMBDA,DAK,DPI
     17               COMMON /VAL/ HR,HI
     18         C
     19         C       THIS VALUE OF TWO PI IS INITIALIZED THIS WAY TO AVOID USING
     20         C BLOCK DATA
     21               DPI=6.28318530717958864769
     22               WRITE(5,2001)
     23         2001  FORMAT(' INPUT FILE NAME:',$)
     24               READ(5,2000) ILBL
     25         2000  FORMAT(A5)
     26               CALL IFILE(20,ILBL)
     27               WRITE(5,2002)
     28         2002  FORMAT(' OUTPUT FILE NAME:',$)
     29               READ(5,2000) ILBL
     30               CALL OFILE(1,ILBL)
     31               WRITE(1) IPTDAT
     32               READ(20,1000) ILABL,TAU
     33               WRITE(1,1000) ILABL
     34               DO 3 I=1,2
     35               READ(20,1000) ILABL
     36         3     WRITE(1,1000) ILABL
     37         1000  FORMAT(8A5,F)
     38               READ(20) LAMBDA,NEL,(X(I),Y(I),Z(I),CF1(I),CF2(I),CF3(I),I=1,NEL)
     39         201   READ(20,2005,END=200) RX,RY,RZ,RT,
     40              1CFR1,CFR2,CFR3,CFS1,CFS2,CFS3
     41         2005  FORMAT(4F,/,6E13.6,/,6E13.6)
     42         C
     43         C       AFTER THE FIELDS HAVE BEEN ACCUMULATED FOR ALL THE ELEMENTS
     44         C THE CDI'S ARE CALCUATED
     45         C       ACDR    CDI FOR THE GROUND SURFACE
     46         C       ACDI    CDI FOR 'IDEAL' GROUND PLANE
     47               ACDR=857.14*REAL((CFR2-CFR3)/CFR1)
     48               ACDI=857.14*REAL((CFS2-CFS3)/CFS1)
     49         C
     50         C       NCRP IS THE COUNT OF THE RECEIVERPOINTS
     51               NRP=NRP+1
     52               IF(NRP .NE. 1) GO TO 4
     53         C
```

```
      C       THIS SECTION INITIALIZES THE MAXIMUN AND MINIMUM VALUES
      C OF THE VARIOUS RANGE AND DOMAIN VARIABLES,  THESE ARE
      C USED IN THE PLOTTING PROGRAM TO SCALE THE PLOTS.  AFTER THE
      C RUN IS FINISHED THEY WILL BE OUTPUT IN PLACE OF THE
      C INITIAL DUMMY RECORD
            ADDI=ACDI
            ADDR=ACDR
            T0=RT
            ADIX=ACDI
            ADIN=ACDI
            ADIF=ACDI
            ADRX=ACDR
            ADRN=ACDR
            ADRF=ACDR
            RXFT=RX
            RYFT=RY
            RZFT=RZ
            RTFT=RT
            AIFT=ACDI
            ARFT=ACDR
            RXMN=RX
            RXMX=RX
            RYMN=RY
            RYMX=RY
            RZMN=RZ
            RZMX=RZ
            RTMN=RT
            RTMX=RT
            AIMX=ACDI
            AIMN=ACDI
            ARMX=ACDR
            ARMN=ACDR
      C
      C       THIS SECTION UDPDATES THE MAXIMUM AND MINIMUM VALUES
      4     CONTINUE
            RXLT=RX
            RYLT=RY
            RZLT=RZ
            RTLT=RT
            AILT=ACDI
            ARLT=ACDR
            IF(RX .LT. RXMN) RXMN=RX
            IF(RX .GT. RXMX) RXMX=RX
            IF(RY .LT. RYMN) RYMN=RY
            IF(RY .GT. RYMX) RYMX=RY
            IF(RZ .GT. RZMX) RZMX=RZ
            IF(RZ .LT. RZMN) RZMN=RZ
            IF(RT .GT. RTMX) RTMX=RT
            IF(RT .LT. RTMN) RTMN=RT
            IF(ACDI .GT. AIMX) AIMX=ACDI
            IF(ACDI .LT. AIMN) AIMN=ACDI
            IF(ACDR .GT. ARMX) ARMX=ACDR
            IF(ACDR .LT. ARMN) ARMN=ACDR
```

```
107               CON=EXP((T0-RT)/TAU)
108         C
109         C       THIS  SECTION SIMULATE THE EFFECT OF THE ELECTICAL AND
110         C MECHANICAL 'INERTIA' OF THE ILS
111         C RECEIVER SYSTEM FOR DYNAMIC SIMULATION
112               T0=RT
113               ADDI=CON*(ADDI-ACDI)+ACDI
114               ADDR=CON*(ADDR-ACDR)+ACDR
115               IF(ADDI .LT. ADIN) ADIN=ADDI
116               IF(ADDI .GT. ADIX) ADIX=ADDI
117               ADIL=ADDI
118               IF(ADDR .LT. ADRN) ADRN=ADDR
119               IF(ADDR .GT. ADRX) ADRX=ADDR
120               ADRL=ADDR
121         C
122         C       THIS IS THE OUTPUT OF THE REAL AND 'IDEAL' , STATIC
123         C AND DYNAMIC CDI'S WWITH THE RECEIVER COORDINATES
124               WRITE(1,2003) RX,RY,RZ,RT,ACDI,ACDR,ADDI,ADDR
125         2003  FORMAT(8F)
126               GO TO 201
127         C
128         C       THIS IS THE TERMINATION SECTION,  THE INITIAL RECORD OF
129         C THE OUTPUT FILE IS WRITTEN AND THE PROGRAM TERMINATES.
130         200   CALL RELEAS (1)
131               ENCODE (9,2006,ILABL(1)) ILBL
132         2006  FORMAT(A5,'.DAT')
133               CALL DEFINE FILE(1,25,I,ILABL(1))
134               WRITE(1#1) IPTDAT
135               CALL RELEAS (1)
136               CALL EXIT
137               STOP
138               END

      CONSTANTS

      0       203622077325    1       150042055061    2       000000000024    3       000000000001    4       212553443656
      5       000000000031

      COMMON

      NRP     /PLXT   /+0     RXMN    /PLXT   /+1     RXMX    /PLXT   /+2     RXFT    /PLXT   /+3     RXLT    /PLXT   /+4
      RYMN    /PLXT   /+5     RYMX    /PLXT   /+6     RYFT    /PLXT   /+7     RYLT    /PLXT   /+10    RZMN    /PLXT   /+11
      RZMX    /PLXT   /+12    RZFT    /PLXT   /+13    RZLT    /PLXT   /+14    RTMN    /PLXT   /+15    RTMX    /PLXT   /+16
      RTFT    /PLXT   /+17    RTLT    /PLXT   /+20    AIMN    /PLXT   /+21    AIMX    /PLXT   /+22    AIFT    /PLXT   /+23
      AILT    /PLXT   /+24    ARMN    /PLXT   /+25    ARMX    /PLXT   /+26    ARFT    /PLXT   /+27    ARLT    /PLXT   /+30
      ADIN    /PLXT   /+31    ADIX    /PLXT   /+32    ADIF    /PLXT   /+33    ADIL    /PLXT   /+34    ADRN    /PLXT   /+35
      ADRX    /PLXT   /+36    ADRF    /PLXT   /+37    ADRL    /PLXT   /+40    RX      /REC    /+0     RY      /REC    /+1
      RZ      /REC    /+2     RT      /REC    /+3     NSIZE   /REC    /+4     N       /GROUND/+0      X1      /GROUND/+1
      Z1      /GROUND/+25     X2      /GROUND/+51     Z2      /GROUND/+76     ISL     /GROUND/+123    AX      /ANT    /+0
      AY      /ANT    /+1     AZ      /ANT    /+2     LAMBDA  /ANT    /+3     DAR     /ANT    /+4     DPI     /ANT    /+5
      HR      /VAL    /+0     HI      /VAL    /+1     IPTDAT  /PLXT   /+0

      SUBPROGRAMS
```

PARSE. VADDR.	.JBFF DEFINE	ALPHO. RECNO.	ALPHI. RANAC.	IFILE EXIT	OFILE	BINWR.	FLOAT.	FLIST.	END.	REAL	CFD.2	EXP	CF-.2	RELEAS
SCALARS														
DPI	6		ILBL	567		TAU	570		1	571		LA[illegible]	3	
NEL	572		RX	0		RY	1		RZ	2		RI	3	
CFR1	573		CFR2	575		CFR3	577		CFS1	601		CFS2	603	
CFS3	605		ACDR	607		ACDI	610		GRP	0		ADDI	611	
ADDR	612		T0	613		ADIX	32		ADIA	31		ADIF	33	
ADRX	36		ADRN	35		ADRF	37		RXFT	3		RYFT	7	
RZFT	13		RTFT	17		AIFT	23		ARFT	27		RXI	1	
RXMX	2		RYMN	5		RYMX	6		RZMN	11		RZMX	12	
RTMN	15		RTMX	16		AIMX	22		AIMN	21		ARMX	26	
ARMN	25		RXLT	4		RYLT	10		RZLT	14		RILT	20	
AILT	24		ARLT	30		CON	614		ADIL	34		ADMI	10	
NSIZE	4		K	0		IEL	123		AX	0		AY	1	
AZ	2		DAK	4		HR	0		HI	1				
ARRAYS														
ILABL	616		IPTDAT	0		X	626		Y	652		Z	676	
CF1	722		CF2	772		CF3	1042		X1	1		Z1	25	
X2	51		Z2	76										

PROGRAM GLDPLT.F4

```
      1                 DIMENSION ITYPE(3,2)
      2                 DATA ITYPE/'STATI','C VAL','UES','DYNAM','IC VA','LUES'/
      3                 DATA PID,PRD/'CDID','THEOD'/
      4                 DIMENSION SPACE(4),IAX(2,3)
      5                 DATA SPACE/1.,2.,2.5,5./
      6                 DATA IAX/'DEGRE','ES',' FEET','      ','SECON','DS'/
      7                 DATA PRX,PRY,PRZ,PRT,PAI,PAR/
      8                1'RX','RY','RZ','RT','CDI','THEO'/
      9                 DIMENSION IPTDAT(33)
     10                 COMMON /PTXYN/NRP,RXMN,RXMX,RXFT,RXLT,RYMN,RYMX,RYFT,RYLT,
     11                1RZMN,RZMX,RZFT,RZLT,RTMN,RTMX,RTFT,RTLT,
     12                2AIMN,AIMX,AIFT,AILT,ARMN,ARMX,ARFT,ARLT,
     13                3ADIN,ADIX,ADIF,ADIL,ADRN,ADRX,ADRF,ADRL
     14                 EQUIVALENCE (IPTDAT(1),NRP)
     15                 DIMENSION ILABL(8)
     16                 DATA XLEN,YLEN,ITIC/20.,8.,21/
     17                 DIMENSION DY1(2000)
     18                 DIMENSION DX(2000),DY(2000)
     19                 NAMELIST /FRED/ YLENG,YDEL,YSC,DMIN,DMAX,DEL,IP,XSC
     20                 CALL PLOTS(IBUF,360,16)
     21           3     WRITE(5,1006)
     22        1006     FORMAT(' INPUT FILE NAME AND AXIS TYPES:',$)
     23                 READ(5,1005) NAME,ISX,ISY,BOUND
     24        1005     FORMAT(A5,I,I,F)
     25                 IF(ISY .LT. 1) GO TO 204
     26                 IF(ISY .GT. 2) GO TO 204
     27                 IF(ISX .LT. 1) GO TO 204
     28                 IF(ISX .GT. 3) GO TO 204
     29                 CALL PLOT(0.,-12.,-3)
     30                 CALL PLOT(0.,1.,-3)
     31                 I=0
     32                 CALL IFILE(20,NAME)
     33                 READ(20) IPTDAT
     34                 WRITE(3,1002) NRP
     35        1002     FORMAT(' THERE ARE',I5,' RECEIVER POINTS.',/)
     36                 WRITE(3,1003)
     37        1003     FORMAT(14X,'MIN',9X,'MAX',9X,'FIRST',8X,'LAST',/)
     38        1004     FORMAT(1X,A5,1X,4F12.4)
     39                 WRITE(3,1004) PRX,RXMN,RXMX,RXFT,RXLT
     40                 WRITE(3,1004) PRY,RYMN,RYMX,RYFT,RYLT
     41                 WRITE(3,1004) PRZ,RZMN,RZMX,RZFT,RZLT
     42                 WRITE(3,1004) PRT,RTMN,RTMX,RTFT,RTLT
     43                 WRITE(3,1004) PAI,AIMN,AIMX,AIFT,AILT
     44                 WRITE(3,1004) PAR,ARMN,ARMX,ARFT,ARLT
     45                 WRITE(3,1004) PID,ADIN,ADIX,ADIF,ADIL
     46                 WRITE(3,1004) PRD,ADRN,ADRX,ADRF,ADRL
     47                 GASD=0.
     48                 GASU=0.
     49                 GACN=0.
     50                 DO 7 II=1,3
     51                 READ(20,100) ILABL
     52                 WRITE(3,101) ILABL
     53        101      FORMAT(1X,8A5)
```

```
      100   FORMAT(8A5)
            CALL SYMBOL(0.,0.,.2,ILABL,90.,40)
      7     CALL PLOT(.3,0.,-3)
            CALL SYMBOL(0.,0.,.2,ITYPE(1,ISY),90.,15)
            CALL PLOT(2.,0.,-3)
      1     READ(20,1000,END=2) X,Y,Z,I,C,R,CD,RD
      1000  FORMAT(8F)
            TEMP=SQRT(X*X+Y*Y)
            IF((TEMP .LT. 3500.) .OR. (TEMP .GT. 20720.)) GO TO 60
            GASU=GASU+C
            GASD=GASD+CD
            GACN=GACN+1.
      60    CONTINUE
            I=I+1
            GO TO (300,301) ISY
      300   CONTINUE
            DY(I)=C
            DY1(I)=R
            GO TO 302
      301   DY(I)=CD
            DY1(I)=RD
      302   CONTINUE
            GO TO (200,201,202) ISX
      200   DX(I)=ATAN2(Z,SQRT(X*X+Y*Y))*57.2953
            GO TO 199
      201   DX(I)=X
            GO TO 199
      202   DX(I)=T
            GO TO 199
      199   IF(I .NE. 1) GO TO 198
            DMIN=DX(I)
            DMAX=DX(I)
      198   DMIN=AMIN1(DMIN,DX(I))
            DMAX=AMAX1(DMAX,DX(I))
      1001  FORMAT(5X,3F)
            IF( I .LT. 2000) GO TO 1
      2     IF(I .LT. 2) GO TO 3
            YLENG=AMAX1(AIMX,ABS(BOUND),-AIMN,8.)
            IF(ABS(BOUND) .LT. 1.E-4) GO TO 10
            YDEL=YLENG
            GO TO 11
      10     YLENG=AMAX1(YLENG,ARMX,-ARMN)
            YDEL=FLOAT(IFIX(YLENG/YLEN))
            YLENG=YDEL*YLEN
      11    CALL AXIS3(0.,0.,-YLENG,YLENG,YDEL,YLEN,
           1'MICROAMPERES',12,0,0.,YSC)
            IP=IFIX(ALOG10(DMAX-DMIN))-1
            POW=10.**IP
            DO 120 J=1,4
            DEL=SPACE(J)*POW
            IT=IFIX(DMAX/DEL-1.)+1-IFIX(DMIN/DEL)
            IF(IT .LT. ITIC) GO TO 121
      120   CONTINUE
```

```
                DMIN=FLOAT(IFIX(DMIN/DEL))*DEL
                DMAX=FLOAT(IFIX(-.1+DMAX/DEL)+1)*DEL
                IP=-IP+1
                IF(IP .LT. 0) IP=0
                CALL AXIS3(0.,0.,DMAX,DMIN,DEL,-XLEN,TAX(1,ISX),7,IP,0.,XSC)
                CALL PLOT(0.,YLEN/2.,-3)
                CALL PLOT(XLEN,0.,2)
                WRITE(5,FRED)
                CALL PLOT((DX(1)-DMIN)/XSC,DY(1)/YSC,3)
                WRITE(3,1001) DX(1),DY(1),DY1(1)
                GASU=GASU*.7/GACN/150.
                GASD=GASD*.7/GACN/150.
                WRITE(3,1007) GASU,GASD,GACN
1007            FORMAT(' STATIC MEAN ANGLE ERROR=',E,/
               1' DYNAMIC MEAN ANGLE ERROR=',E,10X,'COUNT=',F6.0)
                DO 4 J=2,I
                WRITE(3,1001) DX(J),DY(J),DY1(J)
4               CALL PLOT((DX(J)-DMIN)/XSC,DY1(J)/YSC,2)
                IF(BOUND .LT. 0.) GO TO 8
                ISW=2
                CALL PLOT((DX(1)-DMIN)/XSC,DY1(1)/YSC,3)
                DO 6 J=2,I
                CALL PLOT((DX(J)-DMIN)/XSC,DY1(J)/YSC,ISW)
6               ISW=5-ISW
8               CALL PLOT(XLEN+2.,-5.,-3)
                GO TO 3
204             CALL PLOT(3.,0.,999)
                CALL EXIT
                STOP
                END
```

CONSTANTS

0	000000000550	1	000000000020	2	204600000000	3	000000000000	4	201400000000
5	000000000024	6	176631463146	7	207550000000	10	000000000050	11	177463146314
12	000000000017	13	202400000000	14	217503600000	15	214665400000	16	206712271436
17	204400000000	20	163643334272	21	466230351236	22	406332442744	23	426464020100
24	000000000000	25	000000000014	26	175631463146	27	000000000007	30	000000000002
31	000000000003	32	200546314631	33	210454000000	34	203500000000	35	202600000000
36	000000001747								

COMMON

NRP	/PTXXN /+0	RXMN	/PTXXN /+1	RXMX	/PTXXN /+2	RXFT	/PTXXN /+3	RXLT	/PTXXN /+4
RYMN	/PTXXN /+5	RYMX	/PTXXN /+6	RYFT	/PTXXN /+7	RYLT	/PTXXN /+10	RZMN	/PTXXN /+11
RZMX	/PTXXN /+12	RZFT	/PTXXN /+13	RZLT	/PTXXN /+14	RTMN	/PTXXN /+15	RTMX	/PTXXN /+16
RTFT	/PTXXN /+17	RTLT	/PTXXN /+20	AIMN	/PTXXN /+21	AIMX	/PTXXN /+22	AIFT	/PTXXN /+23
AILT	/PTXXN /+24	ARMN	/PTXXN /+25	ARMX	/PTXXN /+26	ARFT	/PTXXN /+27	ARLT	/PTXXN /+30
ADIN	/PTXXN /+31	ADIX	/PTXXN /+32	ADIF	/PTXXN /+33	ADIL	/PTXXN /+34	ADRN	/PTXXN /+35
ADRX	/PTXXN /+36	ADRF	/PTXXN /+37	ADRL	/PTXXN /+40	IPTOAT	/PTXXN /+0		

SUBPROGRAMS

	FORSE.	.JBFF	ALLIO.	PLOTS	ALPHD.	ALPHI.	INTO.	INTI.	FLOAT.	PRINT.	PLOT	IFILE	PINOP.	SYMBOL	END.
	SQRT	ATAN2	AMINI	AMAX1	ABS	FLOAT	IFIX	AXIS3	ALOG10	EXP2.2	SPLST.	EXIT			
	SCALARS														
	PID	1230		PRD	1231		PRX	1232		PPY	1233		PRZ	1234	
	PRT	1235		PAI	1236		PAR	1237		XLEN	1240		YLEN	1241	
	ITIC	1242		YLENG	1243		YDEL	1244		YSC	1245		[illegible]	1246	
	DMAX	1247		DEL	1250		IP	1251		XSC	1252		IHOR	1253	
	NAME	1254		ISX	1255		ISY	1256		NORMD	1257		1	1260	
	NRP	0		RXMN	1		RXMX	2		RXLT	3		RXLT	4	
	RYMN	5		RYMX	6		RYFT	7		RYLT	10		RZMN	11	
	RZMX	12		RZFT	13		PZLT	14		PTMN	15		PTMX	16	
	RIFT	17		RTLT	20		AIMN	21		AIMX	22		AIFT	23	
	AILT	24		ARMN	25		ARMX	26		AFFT	27		AFLT	30	
	ADIN	31		ADIX	32		ADIF	33		ADIL	34		ADRO	35	
	ADRX	36		ADRF	37		AORL	40		GASO	1261		GASO	1262	
	GACN	1263		II	1264		X	1265		Y	1266		Z	1267	
	T	1270		C	1271		R	1272		CU	1273		RU	1274	
	TEMP	1275		POW	1276		J	1277		IT	1300		ISK	1301	
	ARRAYS														
	ITYPE	1302		SPACE	1310		IAX	1314		IPTDAT	0		TLAST	1322	
	DY1	1332		DX	5252		DY	11172							

```
                CALL SYMBOL(XXC,YYC,.12,BCD,90.*W2,NCH)
                IF(PWR.EQ.0.) RETURN
                CALL WHERE (XQ,YQ,XXCX)
                CALL SYMBOL(XQ,YQ,.12,5H * 10,90.*W2,5)
                CALL WHERE (XQ,YQ,XXCX)
                X = XQ + (XXC-.08-XQ)*W2
                Y = YQ + (YYC+.08-YQ)*W1
                CALL NUMBER(X,Y,.09,PWR,90.*W2,-1)
                RETURN
             50 DELN = 1.E-3*10.**PWR/CINCH
                N=NCR/5
                WRITE(5,1000) AMAX,AMIN,DELA,PWR,(BCD(I),I=1,N)
           1000 FORMAT(1H0,27HINSUFFICIENT RANGE FOR AXIS ,
               1/,1X,4G,/,1X,13A5)
                CALL EXIT
                RETURN
                END
```

CONSTANTS

0	175631463146	1	167406111564	2	160517426542	3	201771n314n31	4	000000000003
5	201400000000	6	174631463146	7	177463146314	10	176463146314	11	000000000002
12	000000000000	13	175753412172	14	177702436560	15	176534121727	16	177702436560
17	201244030540	20	000000000000	21	000000000005	22	175567534121	23	175566507534

GLOBAL DUMMIES

XQ	656	YQ	657	AMAX	660	AMIN	661	DELA	662
AINCH	663	BCD	664	NCR	665	NDEC	666	PWR	667
DELN	670								

SUBPROGRAMS

SIGN	IABS	ABS	IFIX	FLOAT	PLOT	EXP3.2	EXP2.2	ANINT	NUMBER	SYMBOL	WHERE	ALOG10	ALOG	ALOGI
EXIT														

SCALARS

AXIS3	673	HT	674	DELX	675	DELA	662	AMAX	660
AMIN	661	W1	676	W2	677	W3	700	NEXP	701
NCH	702	NCR	665	PWR	667	CINCH	703	AINCH	663
NUM	704	ANC	705	XQ	656	YQ	657	DELN	670
ANUM	706	X	707	Y	710	XXC	711	I	712
II	713	IMORE	714	NDEC	666	CENTER	715	OFF	716
XC	717	YC	720	BST	721	XXC	722	YYC	723
XQ	724	YQ	725	XXCX	726	N	727		

ARRAYS

BCD 664

ABS	11	12	30	34									
AINCH	1	11	17										
AMAX	1	4	12	13	15	65							
AMIN	1	4	12	13	15	23	65						
AMIN1	37												
ANC	16	22	37	48	49								
ANUM	23	28	30	33	34	46							
AXIS3	1												
BCD	1	2	54	65									
BST	51	52	53										
CENTER	38	40	52										
CINCH	11	13	16	51	63								
DELA	1	4	65										
DELN	1	22	63										
DELX	4	12	13	15	22	23	28						
EXIT	68												
FLOAT	16	37	38	51									
HT	3	37	38	42	46	53							
I	27	37	65										
IABS	9												
IFIX	15	37											
II	29	30	31	33	34	36	37	38					
IMORE	35	36											
N	64	65											
NCH	9	51	54										
NCR	1	9	14	64									
NDEC	1	35	46										
NEXP	8	10	51										
NUM	15	16	27										
NUMBER	46	61											
OFF	39	42	52										
PLOT	21	43	44	45	47								
PWR	1	10	22	55	61	63	65						
SIGN	4												
SYMBOL	54	57											
W1	5	20	37	38	42	44	45	48	52	53	54		
W2	6	18	40	42	44	45	49	52	53	54	57	59	61
W3	7	14	40	42	52	53							
WHERE	56	58											
X	24	40	43	44	45	47	48	59	61				
XO	1	21	43	44	45	46	47	52					
XC	40	41	46										
XM	26	41	52										
XQ	56	57	58	59									
XXC	52	54	59										
XXCX	56	58											
Y	25	42	43	44	45	47	49	60	61				
YO	1	21	43	44	45	46	47	53					
YC	42	46	53										
YQ	56	57	58	60									
YYC	53	54	60										

5p	17	20
10p	19	21
20p	30	33
25p	30	32
40p	27	50
50p	12	63
1000p	65	66

175copies

FAA-76-17
REPORT NO. FAA-RD-76-136

MEASUREMENT OF THE ATCRBS SURFACE INTERROGATION ENVIRONMENTS AT CHICAGO O'HARE AND LOS ANGELES INTERNATIONAL AIRPORTS

M. J. Moroney
H. J. Glynn

U.S. Department of Transportation
Transportation Systems Center
Kendall Square
Cambridge MA 02142

JULY 1976

INTERIM REPORT

Prepared for

U.S. DEPARTMENT OF TRANSPORTATION
FEDERAL AVIATION ADMINISTRATION
Systems Research and Development Service
Washington DC 20591

NOTICE

This document is disseminated under the sponsorship of the Department of Transportation in the interest of information exchange. The United States Government assumes no liability for its contents or use thereof.

NOTICE

The United States Government does not endorse products or manufacturers. Trade or manufacturers' names appear herein solely because they are considered essential to the object of this report.

Technical Report Documentation Page

1. Report No.	2. Government Accession No.	3. Recipient's Catalog No.
FAA-RD-76-136		

4. Title and Subtitle	5. Report Date
MEASUREMENT OF THE ATCRBS SURFACE INTERROGATION ENVIRONMENTS AT CHICAGO O'HARE AND LOS ANGELES INTERNATIONAL AIRPORTS	July 1976
	6. Performing Organization Code
7. Author(s)	8. Performing Organization Report No.
M. J. Moroney and H. J. Glynn	DOT-TSC-FAA-76-17
9. Performing Organization Name and Address	10. Work Unit No. (TRAIS)
U.S. Department of Transportation Transportation Systems Center Kendall Square Cambridge MA 02142	FA621/R6134
	11. Contract or Grant No.
	13. Type of Report and Period Covered
12. Sponsoring Agency Name and Address	Interim Report June-October 1975
U.S. Department of Transportation Federal Aviation Administration Systems Research and Development Service Washington DC 20591	14. Sponsoring Agency Code

15. Supplementary Notes

16. Abstract

The Transportation Systems Center is conducting a program to develop a surface surveillance sensor that uses replies from ATCRBS transponders. The operation of this system can be affected by surface interrogations at major airports where such a system might eventually be deployed. Consequently, tests were conducted at Chicago O'Hare and Los Angeles International Airports to measure the surface interrogation environment and to determine the number of interrogators causing surface transponders to reply.

This report describes the tests that were performed, presents the analysis of collected data, and offers conclusions pertinent to future operational ASTC systems.

17. Key Words	18. Distribution Statement
ATCRBS, Airport Surface Traffic Control, ASTC, ASDE, Surface Surveillance	DOCUMENT IS AVAILABLE TO THE U.S. PUBLIC THROUGH THE NATIONAL TECHNICAL INFORMATION SERVICE, SPRINGFIELD, VIRGINIA 22161

19. Security Classif. (of this report)	20. Security Classif. (of this page)	21. No. of Pages	22. Price
Unclassified	Unclassified	42	

Form DOT F 1700.7 (8-72) Reproduction of completed page authorized

PREFACE

The test series described in this report is part of a comprehensive program at the Transportation Systems Center (TSC) to investigate and evaluate factors bearing on the development of a surface surveillance system that operates with replies from ATCRBS transponders. This program is being conducted by the Airport Surface Traffic Control (ASTC) Program Office at TSC and is sponsored by the Federal Aviation Administration (FAA) through the Systems Research and Development Service. One of the factors being investigated is the ATCRBS interrogation rate for vehicles on the surface of airports. The surface surveillance system would function in the dead time of local ASR(s) in order to be compatible with ATCRBS. It is expected that this method of operation will be technically feasible unless high surface interrogation rates exist due to radiation from surrounding ATCRBS sites. Analytical studies have indicated that the surface interrogation environments at Chicago O'Hare and Los Angeles International Airports might be very severe. It was necessary, therefore, to measure exactly the surface interrogation rates at these airports since both are candidates for advanced surface surveillance systems.

The test program was carried out by the following team:

H. R. Jackson, Federal Aviation Administration-National Aviation Facilities Experimental Center
J. D. Vinatieri, The Mitre Corporation
P. J. Woodall, Bendix Communications Division.

Our endeavors were greatly facilitated by cooperation from the Federal Aviation Administration Adminstration, the O'Hare Airport Administration Office and the Los Angeles Airport Management Office. In particular we wish to acknowledge the interest, encouragement and efforts of Mr. Jim Burns and Mr. Norm Oleson, FAA, Chicago O'Hare Airport; Mr. Jim Donovan, O'Hare Airport Administration Office; Mr. Frank Scollick, Mr. Doug LePage and Mr. Bob Curtis, FAA Los Angeles International Airport.

METRIC CONVERSION FACTORS

Approximate Conversions to Metric Measures

Symbol	When You Know	Multiply by	To Find	Symbol
		LENGTH		
in	inches	2.5	centimeters	cm
ft	feet	30	centimeters	cm
yd	yards	0.9	meters	m
mi	miles	1.6	kilometers	km
		AREA		
in^2	square inches	6.5	square centimeters	cm^2
ft^2	square feet	0.09	square meters	m^2
yd^2	square yards	0.8	square meters	m^2
mi^2	square miles	2.6	square kilometers	km^2
	acres	0.4	hectares	ha
		MASS (weight)		
oz	ounces	28	grams	g
lb	pounds	0.45	kilograms	kg
	short tons (2000 lb)	0.9	tonnes	t
		VOLUME		
tsp	teaspoons	5	milliliters	ml
Tbsp	tablespoons	15	milliliters	ml
fl oz	fluid ounces	30	milliliters	ml
c	cups	0.24	liters	l
pt	pints	0.47	liters	l
qt	quarts	0.95	liters	l
gal	gallons	3.8	liters	l
ft^3	cubic feet	0.03	cubic meters	m^3
yd^3	cubic yards	0.76	cubic meters	m^3
		TEMPERATURE (exact)		
°F	Fahrenheit temperature	5/9 (after subtracting 32)	Celsius temperature	°C

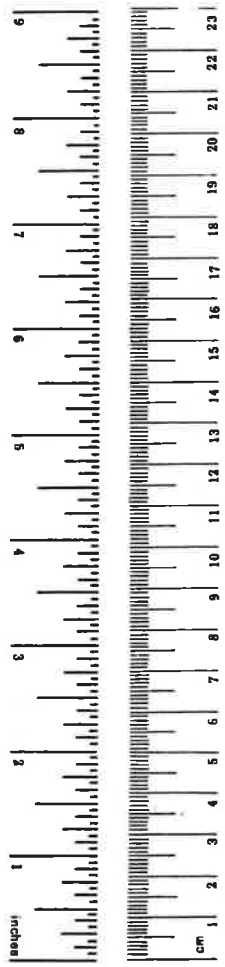

Approximate Conversions from Metric Measures

Symbol	When You Know	Multiply by	To Find	Symbol
		LENGTH		
mm	millimeters	0.04	inches	in
cm	centimeters	0.4	inches	in
m	meters	3.3	feet	ft
m	meters	1.1	yards	yd
km	kilometers	0.6	miles	mi
		AREA		
cm^2	square centimeters	0.16	square inches	in^2
m^2	square meters	1.2	square yards	yd^2
km^2	square kilometers	0.4	square miles	mi^2
ha	hectares (10,000 m^2)	2.5	acres	
		MASS (weight)		
g	grams	0.035	ounces	oz
kg	kilograms	2.2	pounds	lb
t	tonnes (1000 kg)	1.1	short tons	
		VOLUME		
ml	milliliters	0.03	fluid ounces	fl oz
l	liters	2.1	pints	pt
l	liters	1.06	quarts	qt
l	liters	0.26	gallons	gal
m^3	cubic meters	35	cubic feet	ft^3
m^3	cubic meters	1.3	cubic yards	yd^3
		TEMPERATURE (exact)		
°C	Celsius temperature	9/5 (then add 32)	Fahrenheit temperature	°F

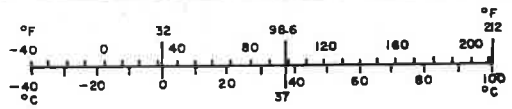

CONTENTS

ILLUSTRATIONS

TABLES

LIST OF ABBREVIATIONS AND SYMBOLS

ARSR	Air Route Surveillance Radar
ARTCC	Air Route Traffic Control Center
ASR	Airport Surveillance Radar
ASTC	Airport Surface Traffic Control
ATC	Air Traffic Control
ATCRBS	Air Traffic Control Radar Beacon System
BCN	Beacon
DAS	Data Acquisition Subsystem
IFR	Instrument Flight Rules
ISLS	Interrogate Side Lobe Suppression
I^2SLS	Improved Interrogate Side Lobe Suppression
NAFEC	National Aviation Facilities Experimental Center
NAS	National Airspace System
NM	Nautical Mile
PRF	Pulse Repetition Frequency
RSLS	Receive Side Lobe Suppression
TRACON	Terminal Radar Control
TSC	Transportation Systems Center
SLS	Side Lobe Suppression
VFR	Visual Flight Rules

1. INTRODUCTION

1.1 PURPOSE OF THE MEASUREMENT PROGRAM

The purpose of measuring the Surface Interrogation Environment at Chicago O'Hare (ORD) and at Los Angeles Airport (LAX) was to enlarge the body of data previously collected at the NAFEC and Logan Airports. The O'Hare and Los Angeles airports were selected because they are representative of large hubs and are candidates for installation of an operational ATCRBS-based Airport Surface Traffic Control (ASTC) system. Furthermore, O'Hare Airport is being considered for advanced testing of the brassboard model ATCRBS-based Surface Trilateration Data Acquisition Subsystem presently being built by TSC for planned feasibility tests at NAFEC. O'Hare also is a candidate site for installation and checkout of the Tower Automated Ground Surveillance (TAGS) system which will be the advanced ASTC system based on ATCRBS-trilateration as the primary surveillance sensor. Hence, there was a need to measure the interference environment at O'Hare. On the other hand, it has been suggested that the severity of the surface interrogation environment at Los Angeles might preclude the operation of an ATCRBS-based ASTC system. Indeed, analytical studies indicated that as many as ten interrogators might have line-of-sight coverage of the Los Angeles airport surface. Measurements at this site were needed to validate the analytical results and to provide valuable data representative of a heavy surface interrogation environment. The tests at both airports were performed in accordance with the test plan of reference 1.

1.2 PREVIOUS TESTS

The tests performed at these airports were similar to those previously made at Logan Airport and reported in Reference 2. Measurements were made using portable equipment which could easily be transported by automobile to various locations on the airport surface. This equipment was used to gather information on interrogation and improved interrogate side lobe suppression (I^2SLS)* rates occurring for a surface transponder at designated airport locations.

---

*ISLS generally refers to Interrogate Side Lobe Suppression whereby the P_2 pulse is radiated from an omni antenna. The FAA has widely implemented a system known as "improved ISLS" (I^2SLS). In this system, a portion of the P_1 signal is radiated along with P_2 through the omni antenna to suppress all transponders within the omni coverage volume not in the mainbeam. The equipment used in this test program does not differentiate between the two types, but simply records all suppression events occurring in the transponder whether from ISLS or I^2SLS. Henceforth, in this document, the transponder suppression rate will be referred to as the I^2SLS suppression rate. Reference 1, pages 2 and 3, describe both suppression systems in more detail.

1.3 TEST OBJECTIVES

The objectives for this test program were: (1) to collect data at ORD and LAX airports and (2) perform a detailed analysis of the data in order to: (a) provide a first order assessment of the extent to which a surface operated transponder is interrogated by existing ATCRBS interrogators; (b) determine the uniformity of the surface transponder interrogation rate as a function of airport surface location; and (c) determine the number of interrogators in the vicinity of each airport causing surface transponder interrogations.

The field test data were obtained from a specially constructed test unit containing an instrumented transponder and associated electronics. This equipment provided data relative to the surface interrogation rate and I^2SLS rate and, through post-test analysis, provided a measure of the number of interrogators illuminating each test point.

Specifically, the test objectives were as follows:

a. To take multiple counts of the number of interrogations and suppressions occurring during specified time intervals at several airport locations. These counts were later compared and analyzed.

b. To determine the periodicity of bursts of interrogations occurring during specified time intervals, and to compare these periodicities with known beacon interrogator scan rates. By means of this procedure the number of interrogators illuminating a given test location was determined.

2. DATA COLLECTION

2.1 METHOD OF APPROACH

As previously stated, tests were made at the Chicago O'Hare and Los Angeles airports. In general, the same three basic steps were used at each airport site. First, a preliminary meeting was held at which the test team, composed of representatives from TSC, FAA, MITRE and the Bendix Communications Division, were introduced to FAA and Airport Authority operating personnel. A briefing was given by TSC to explain the purpose of the visit, the objectives of the ASTC program at TSC and the relationship of data that would be collected at the airports to the overall program. At this meeting, the manner in which data would be gathered on the airport surface was stressed and the interface between the test team, ATC controllers and Airport Authority personnel was discussed in detail. Also at this meeting, the operating characteristics (e.g., scan rate, PRF, stagger) of the local ASR beacon(s) were reviewed and the location and identity of the ASR and ARSR beacons in the airport vicinity which might have line of sight to the airport surface were noted.

Second, the test data was collected over a period of one to one and one-half days by driving an instrumented transponder to the planned test points. The test team and test equipment were driven on the airport surface by an authorized driver in a vehicle supplied by the FAA or the Airport Authority.

Third, a departure briefing was held at the conclusion of the test data gathering. Highlights of the testing were discussed and an attempt was made to give a very preliminary assessment of the interrogator environment based on a cursory examination of the data. It was emphasized that the data analysis would take several weeks and the test results for both airports would be presented in a final report.

2.2 TEST EQUIPMENT

At both airports portable equipment (see Figure 2-1) was employed to obtain measurements at selected locations. A major component of this equipment was a transponder (see Appendix A) which had been modified to provide outputs from its decoder circuitry in order to allow counts to be made of: (1) the number of valid interrogations received and (2) the number of suppressions which occurred during a prescribed time interval. The time interval was selectable in 0.1 second increments from 0.1 seconds to 10.0 seconds and the equipment had provision for recording in sequence the counts for 61 such intervals. At the conclusion of 61 intervals, the total count was printed and the counter automatically reset in preparation for the next test sequence.

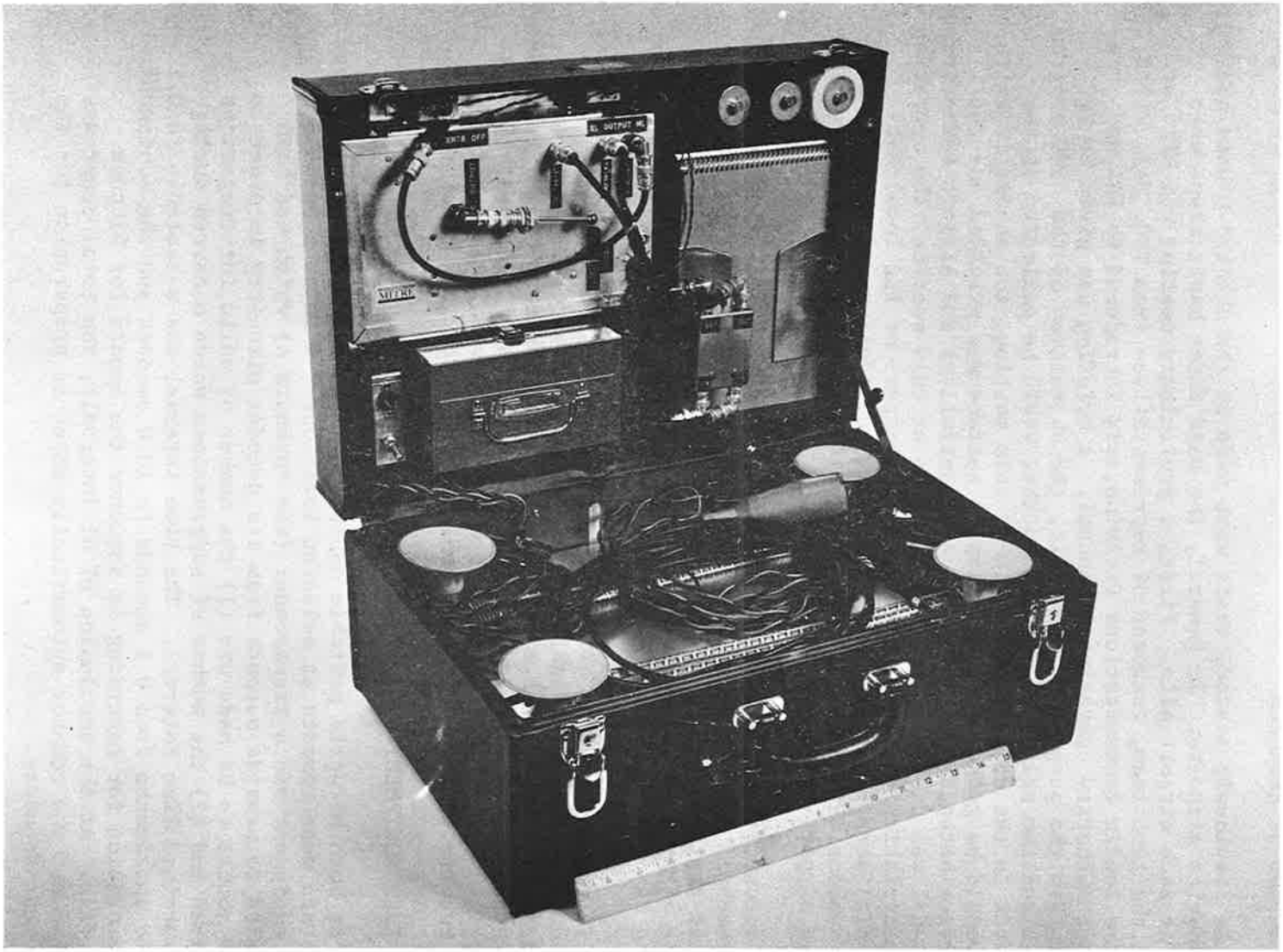

FIGURE 2-1. PACKAGING OF EQUIPMENT SHOWING STORAGE OF ANTENNA GROUND PLANE AND ALL NECESSARY CABLES

The equipment was designed so that it could be easily installed and operated in an ordinary surface vehicle such as an automobile or truck for rapid transportation to each test point. Set up time in the vehicle required only 5 to 10 minutes. A stub antenna was mounted on an aluminum ground plane which contained four suction cups. This antenna assembly was placed on the roof of the vehicle and held in place by two clamps fastened to the vehicle's rain gutter. Power for the equipment was provided by the 12 volt car battery either through battery cables and clips or by means of a plug inserted into the cigarette lighter.

Figures 2-1 and 2-2 illustrate the packaging of the equipment. Figure 2-1 shows the equipment with the necessary cables, antenna and ground plane packaged in a single case. The transponder can be seen mounted in the lid of the case and the counter electronics and strip printer are shown directly beneath the antenna ground plane. Figure 2-2 shows the equipment as it is set up at an airport site with the exception, of course, that the antenna and ground plan will be fastened to the roof of a vehicle. The counter electronics can be clearly seen and the strip printer is shown immediately to the left of the electronic assembly.

Before starting the series of measurements at O'Hare and Los Angeles, the transponder was bench tested at MITRE. This bench test showed the transponder to have a sensitivity of -72 dbm and a power output of 220 watts. These values are within the ATCRBS national standard* and thus the interrogation and I^2SLS counts obtained are representative of typical operational values. In addition, the portable equipment was checked out at Logan airport prior to the initiation of these tests. This field check provided verification that the transponder and counter electronics were properly interfaced and were accurately recording the surface interrogation rate.

2.3 SURFACE TEST PROCEDURES

Testing was accomplished using the portable test equipment to record the number of successful interrogations occurring in a specified time interval and the number of successful sidelobe suppressions received by the transponder during a specified time interval. After the equipment was installed in the test vehicle a check was made to verify its readiness. Once installed, the equipment, including the antenna fastened to the roof and the battery

---

*U.S. National Standard for the IFF Mark X Air Traffic Control Radar Beacon System Characteristics (ATCRBS), AC No. 00-27, Jan. 1969

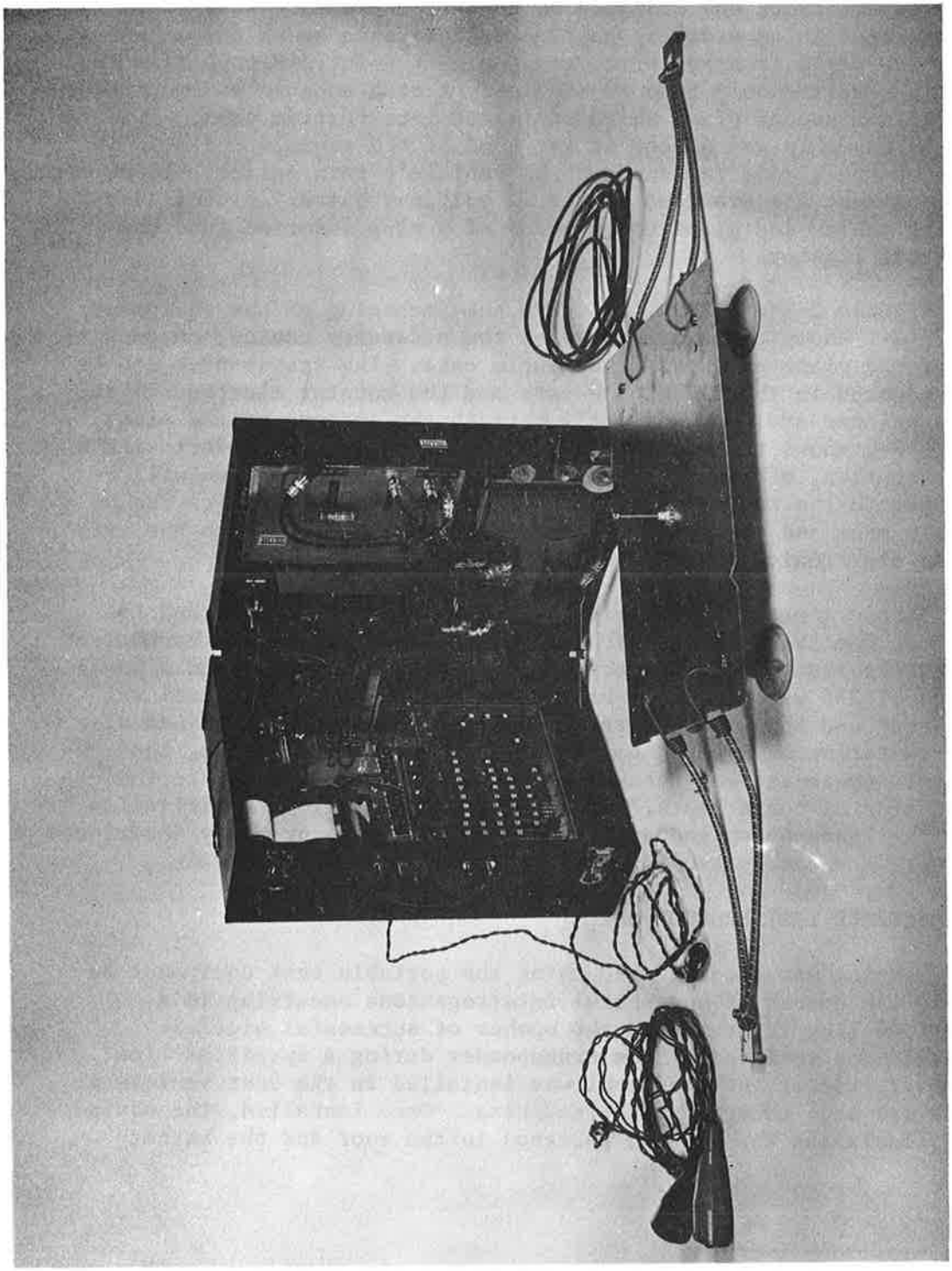

FIGURE 2-2. EQUIPMENT SHOWN WITH TRANSPONDER ANTENNA AND GROUND PLANE REMOVED

connection, remained in place while the vehicle travelled between test locations. In this way a minimum amount of time was required at each test point since the equipment was ready for data collection when the vehicle arrived at each test point. At both airports, the vehicle was driven by an experienced driver familiar with the airport runway and taxiway system. In addition the test team had VHF communications with ground controllers to request and receive clearances when needed to proceed to specific test points.

The surface interrogation and suppression rate due to each interrogator illuminating the airport surface was measured by taking interrogation counts over time intervals of 0.5 second and sidelobe suppression counts over time intervals of 1.0 seconds. Using this procedure, interrogation counts were made in a 30.5 second period based on data collected for 61 intervals. In general, Airport Surveillance Radar (ASR) interrogators have a scan rate in the order of 4 seconds and Air Route Surveillance Radar (ARSR) interrogators have a scan rate of about 12 seconds. A 30.5 second sample therefore provided for roughly 7 scans of ASR beacon data and 2-3 scans of ARSR data. During the post-test analysis, the strip printer tapes containing 0.5 second counts for each of the 61 intervals recorded were examined for periodicity of interrogation counts to determine the number of ASR and ARSR beacon interrogators illuminating the field.

The I^2SLS counts measured over time intervals of 1.0 second provided data relative to the suppression rates of surface transponders, and were correlated with interrogation counts and known PRFs for interrogators in the vicinity of the airport. This provided an additional aid in evaluating the surface interrogation environment.

Total counts of the number of interrogation and I^2SLS events during the 30.5 second data collection period also were printed on the paper tapes. In addition, another sample was collected using a 1.0 second sampling rate to measure total suppression and interrogation counts. Light emitting diodes (LED) were used to indicate total counts over the 61 second test period rather than the paper tape readout.

Although original test points were located directly on runway and taxiway surfaces and would have required the test vehicle to be parked at these locations for periods of five to ten minutes, interference with normal airport surface operations was effectively eliminated by parking the vehicle on access roads and grass areas adjacent to test points. Thus test points in Figures 3-1 and 3-4 represent only approximate locations where measurements were made. In this manner, the performance of these tests did not obstruct the normal flow of surface traffic and conversely surface traffic did not impede the collection of data.

Data Recording Requirements

In the test vehicle, a record (log) of all significant events which occurred during the test was maintained. This log included the following types of data:

- Test point number
- Date
- Time-of-day
- Run number
- Average interrogation and I^2SLS counts for each run
- Comments such as equipment malfunctions and difficulties observed.

It also was a required procedure that each paper tape produced by the test equipment was annotated with the following data:

- Test point number
- Time-of-day
- Interrogation or I^2SLS data
- Time interval used to collect data
- Run number at each location.

3. DATA ANALYSIS

3.1 GENERAL APPROACH

The equipment used to collect the data was different than that used in earlier tests (see References 2 and 3), but provided the means for collecting data with greater precision than that previously obtained. These data included not only the average surface interrogation rates similar to those obtained at Logan and Atlantic City airports but also individual bursts of interrogations as each radar scanned the airport surface. These data were useful in determining how many interrogators actually illuminated the airport surface. Individual interrogation bursts were analyzed to assess the effective interrogation beamwidth of individual interrogators. This provided a means to discriminate between interrogations from ASR beacons and ARSR beacons. Bursts also were examined for periodicities equal to scan rates of nearby interrogators. This helped to develop an approximation of the number of interrogators with line-of-sight to the airport surface. This estimate was substantiated by correlating the SLS total count with the sum of the PRF's for nearby interrogators.

Once the analysis had established the number of interrogators illuminating the surface, the test data was compared with analytical data. Analytical results on the number of interrogators illuminating each airport surface had been derived by using the known locations of interrogators in the vicinity of each airport and by examining topographical maps to determine those interrogators with probable line-of-sight coverage of the airport surface. This method was suspect because factors such as the limited information on the topographical maps, their date, and unknowns such as recent construction around the airport perimeter which could block or shield the surface from interrogations. In the analysis, peripheral interrogators were assumed to contribute to the surface transponder interrogation rate. The results from this test series established a measure of the validity of predicting surface interrogation rates for any airport based on anything other than a measurement of the surface environment.

Data which have been collected at Logan and Atlantic City Airports (NAFEC) were designed to assess the extent of the interrogation and side lobe suppression of surface vehicle transponders at various airport locations. NAFEC offered the opportunity to examine these effects under various conditions of interrogator population ranging from one to three beacon interrogators. In addition, data were collected during the NAFEC test series for various configurations of ASR and ARSR beacon interrogators. Logan Airport, on the other hand, offered the opportunity for examination of surface interrogation rates at higher surface traffic volumes.

One result of the previous tests was the generation of several interrogation maps of each airport surface showing the surface vehicle interrogation rates at various locations on the airport surface. Since the O'Hare and Los Angeles tests were designed to extend these results and thereby increase the data base, the final step in the analysis was a comparison of data obtained at O'Hare and Los Angeles with data previously obtained at Logan and NAFEC.

3.2 SURFACE INTERROGATION ANALYSIS

Data collection consisted of counting the number of interrogation and SLS events occurring in the instrumented transponder. As previously explained, the types of data collected at each test location were:

a. Interrogation counts at 0.5 seconds using paper tape

b. Total interrogations for 30.5 seconds using paper tape

c. Total I^2SLS counts for 30.5 seconds using paper tape.

d. Total interrogations for 61 seconds using LED

e. Total I^2SLS counts for 61 seconds using LED.

3.2.1 Chicago O'Hare Data

3.2.1.1 Surface Interrogation and SLS Map. Interrogations of the surface transponder occurred in bursts as the O'Hare ASR interrogator scanned the airport. These data have been broken down into the average number of replies per ASR scan and the average replies per second. An interrogation map for the 25 test points showing the replies per second and SLS counts per second is presented in Figure 3-1. Two numbers are shown at each test point. The top number is the number of successful interrogations (replies generated) per second. The bottom number is the number of SLS counts generated per second.

From Figure 3-1 it can be seen that the average surface interrogation rate at O'Hare is very low; generally ranging between 7 and 13 counts per second. This indicates that the only source of surface interrogations was the local O'Hare ASR interrogator. This can be confirmed by observing that the SLS counts which show an average of 408 per second is very close to the average O'Hare PRF of 423 per second. Moreover, the sum of the average interrogation rate (12.8) and the average SLS rate (408) is seen to be 421 per second versus the known PRF of 423 per second. This provides a better than 98% correlation. A comparison of the O'Hare data with Logan Data reveals that although O'Hare has only a single ASR interrogator, as opposed to

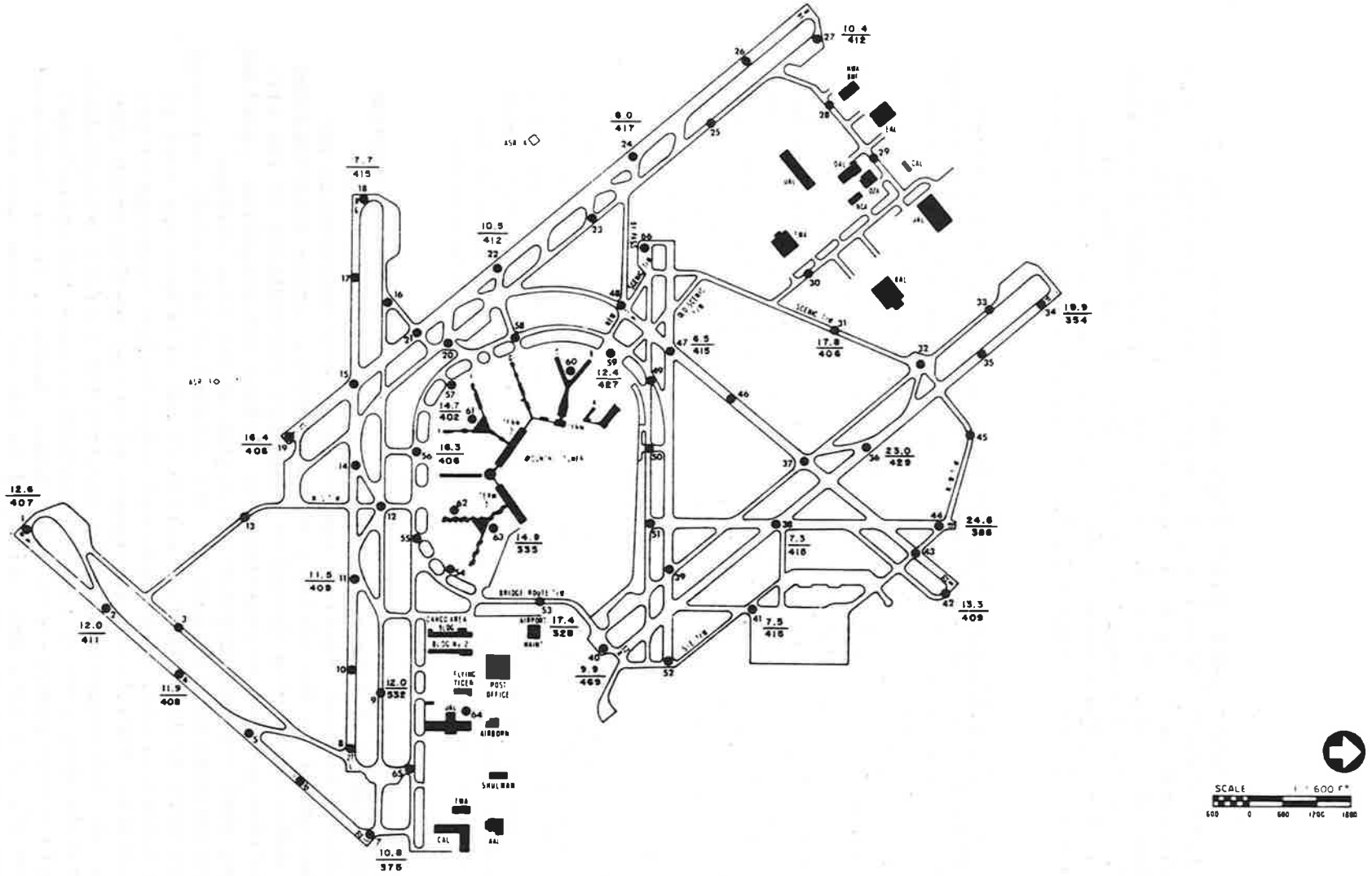

Figure 3-1 SURFACE INTERROGATION MAP FOR CHICAGO O'HARE AIRPORT

the single ASR single ARSR interrogator environment at Logan, the average reply rate for O'Hare is 13, compared to 9.5 for Logan. This can be explained by the fact that the average number of replies per scan triggered by the O'Hare ASR interrogator is somewhat higher than that triggered by the Logan ASR interrogator suggesting that the beamwidth of the O'Hare interrogator is greater than that at Logan. Nevertheless, the reply rate at O'Hare is consistently at a very low value.

3.2.1.2 Effective Interrogation Beamwidth. Figure 3-2 shows a typical example of the temporal distribution of replies triggered from the surface transponder. Replies are seen to occur in bursts of 40 to 50 at periodic intervals of approximately 4.5 seconds. This coincides very well with the O'Hare scan rate of 4.62 seconds. The average number of replies per scan is 40 which is considerably larger than the 18.5 per scan previously measured at Logan. The differences between these two values must be regarded with some reservations because the reply per scan data for Logan was inferred based upon total reply counts measured over 70 scans whereas a high sampling rate approach was employed at O'Hare. Nevertheless, the average reply rate has been shown to be slightly higher for O'Hare. Hence there is a great likelihood that the reply per scan counts are, in fact, higher for O'Hare than Logan.

3.2.1.3 Number of Interrogators. Examination of Figure 3-2 clearly shows that only one interrogator is triggering replies since only one set of interrogation bursts is present with a periodic rate of 4.5 seconds and essentially no interrogations are present between these bursts. Thus, it can be concluded that only the local O'Hare ASR interrogator is successful in triggering surface transponder replies.

In the previous analytical study which was performed to provide data on the number of interrogators within line-of-sight to the O'Hare airport surface, vertical contour maps were constructed for each interrogator in the vicinity of the airport. Those interrogators with an unobstructed view (based on available information) of the airport were then assumed to contribute to surface interrogation, provided, of course, that the interrogator was active at the time surface interrogation data were collected. The results of this study indicated that there were 12 interrogators within 25 nmi of O'Hare and that of these 12 interrogators, 8 probably had line-of-sight coverage of the O'Hare surface. This is not substantiated by the results which show that only one interrogator actively interrogates surface transponders. It is possible that some of the 8 interrogators were not operational while surface measurements were being made. However, as was indicated in Section II, test data were collected on two successive days and for several time periods. Thus, it seems reasonable to conclude that

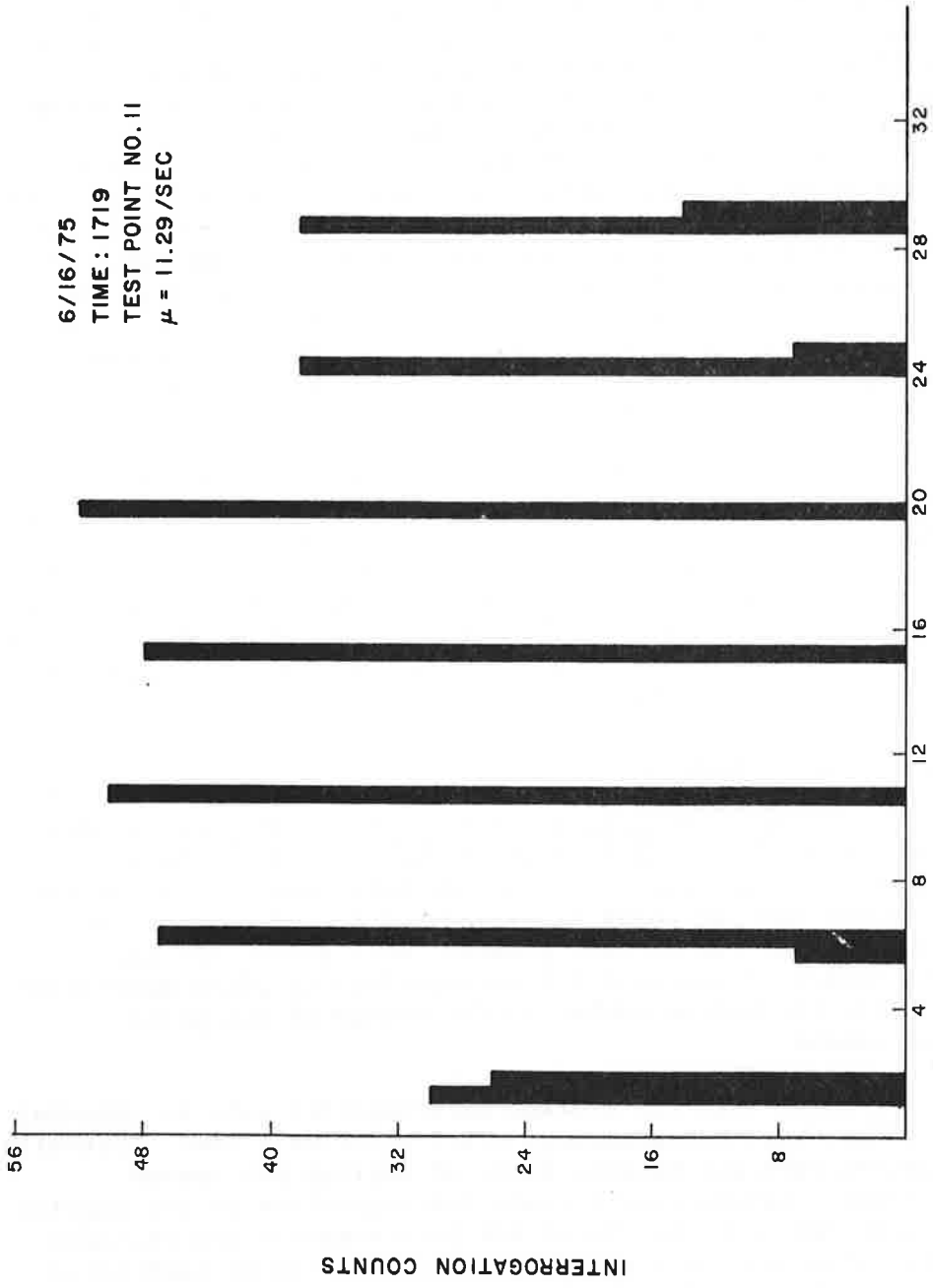

Figure 3-2 TYPICAL INTERROGATION HISTOGRAM FOR O'HARE AIRPORT

the nominal surface interrogation environment at O'Hare is composed of a single ASR interrogator. Furthermore, based on these results, the use of topographical maps and known interrogator locations as a means for estimating the surface interrogation environment at a given airport does not appear to be reliable. In fact, the examination of topographical maps indicated that the McCook ARSR located approximately 10.5 nmi southwest of the airport would have line-of-sight coverage of the airport surface and thus contribute to the surface interrogation environment. Since this interrogator was known to be operational at all times, but was not observed in the test data, it must be concluded that the interrogator does not radiate energy to the airport surface. Once again, this can be accounted for by the many additional variables such as man-made obstructions, antenna patterns, etc., that were not taken into account in the analytical studies.

Finally, on one occasion there seemed to be a second interrogator triggering surface replies. These data are shown in Figure 3-3. In the histogram, the O'Hare ASR interrogations are still present at a 4.5 second periodicity, but now additional replies are generated at a periodicity of approximately 10 seconds. These interrogations may have come from the McCook ARSR interrogator or possibly from a nearby military installation. In any event these additional interrogations were observed only on this one occasion.

3.2.2 Los Angeles International Data

3.2.2.1 Surface Interrogation and SLS Map. The same analysis technique previously described in Section 3.2.1 for the O'Hare data was also used for the Los Angeles data. An interrogation map of the replies per second and SLS gates generated per second is shown in Figure 3-4 for each of the 16 test points. Here again, the top number is the number of successful interrogations (replies generated) per second, while the bottom number is the number of SLS gates generated per second.

Figure 3-4 shows that the average interrogation rate is somewhat higher than O'Hare but, nevertheless, still relatively low. Typically, the interrogation rate was between 20 to 30 replies per second. Subsequent analysis showed that surface interrogations at Los Angeles were caused principally by two local ASR interrogators and one ARSR interrogator. Although these three interrogators can be identified in the data, the SLS rate is only 767 per second, which is roughly equivalent to the sum of the average PRF for both local ASR interrogators. Thus, the I^2SLS of the ARSR interrogator is not actively suppressing surface transponders at Los Angeles even though this interrogator is triggering surface transponder replies.

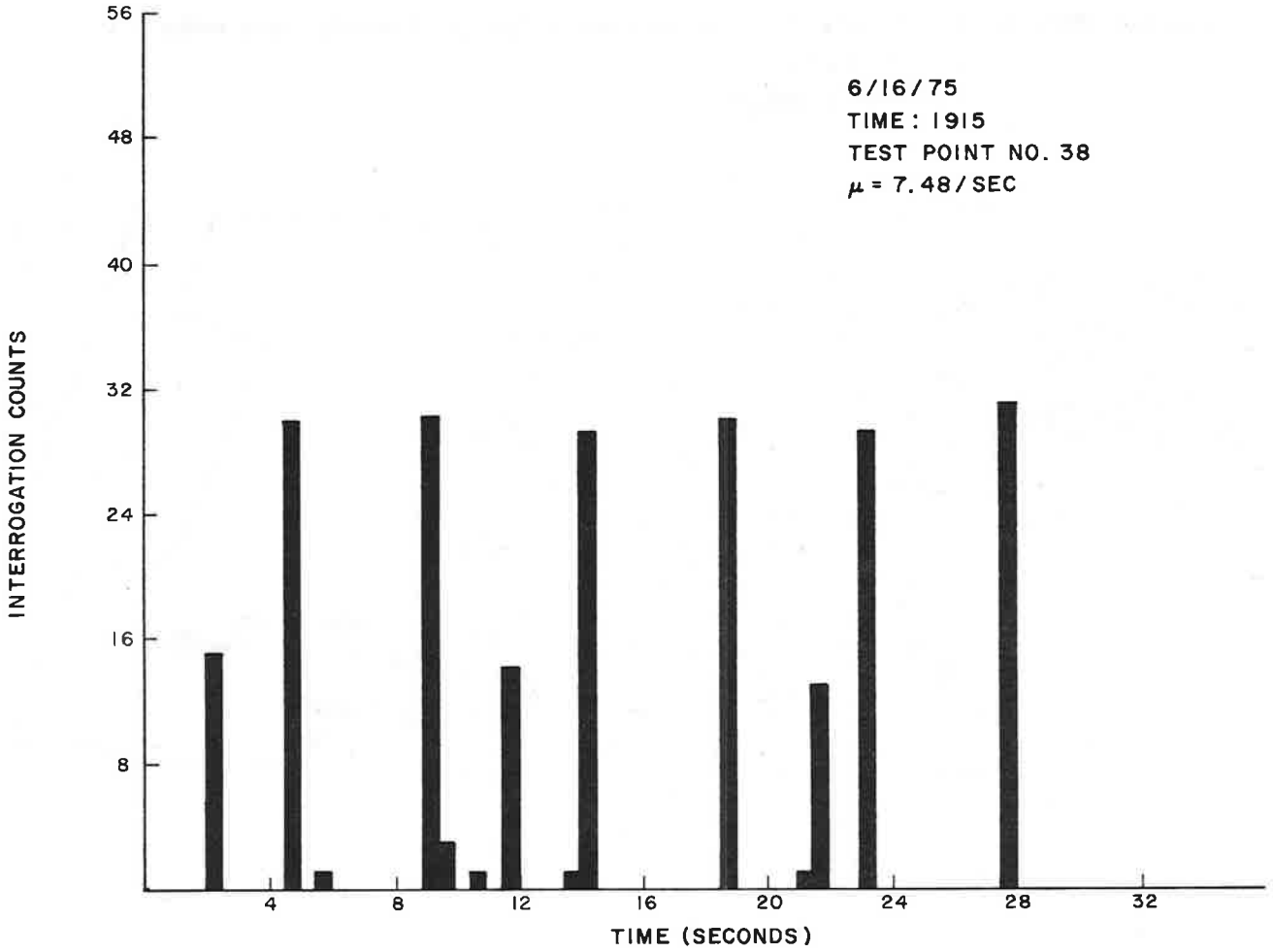

Figure 3-3 INTERROGATION HISTOGRAM FOR O'HARE AIRPORT SHOWING BURST FROM TWO INTERROGATORS

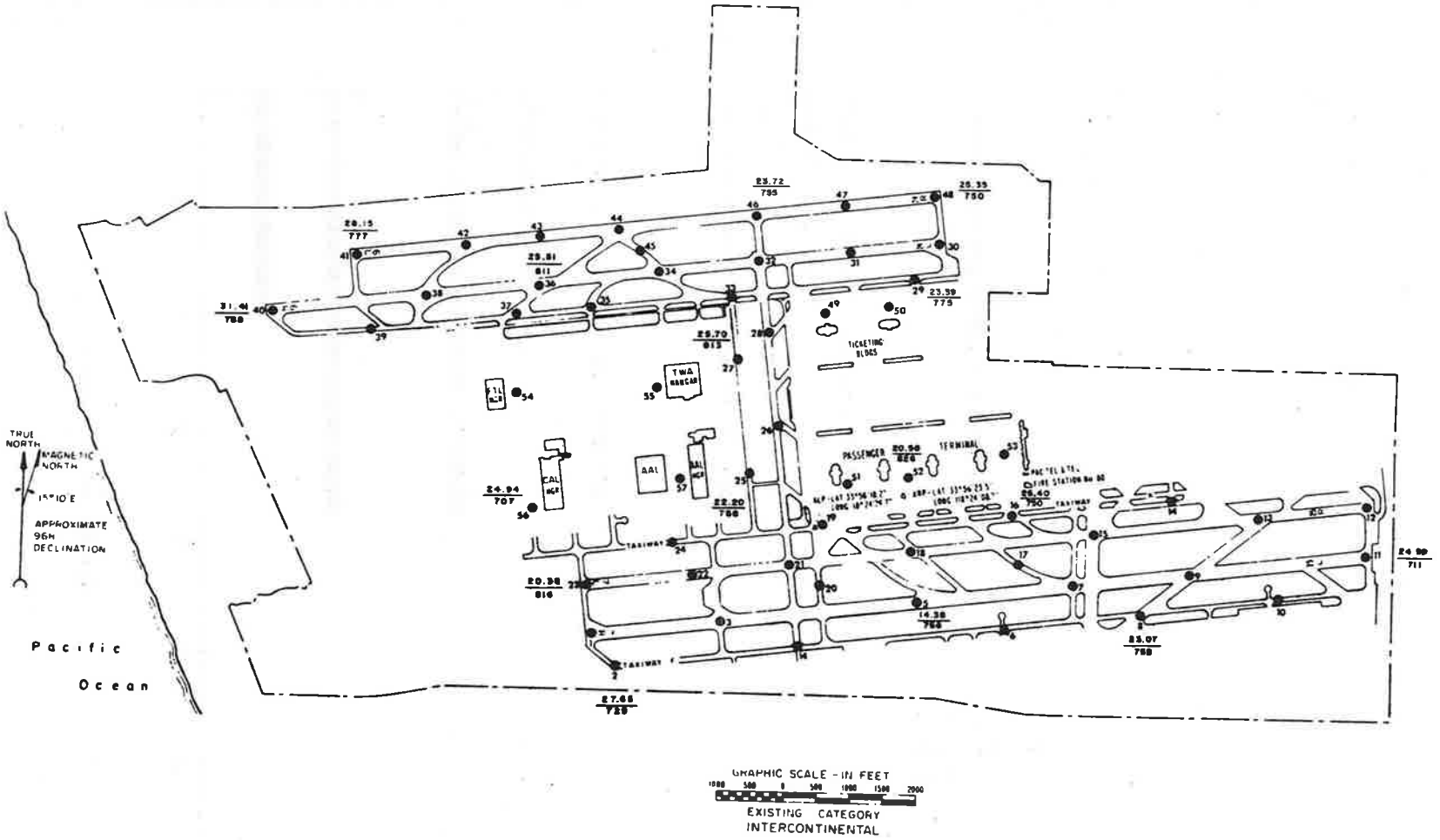

Figure 3-4 SURFACE INTERROGATION MAP FOR LOS ANGELES INTERNATIONAL AIRPORT

3.2.2.2 Effective Interrogation Beamwidth. Figure 3-5 shows a typical example of the temporal distribution of replies triggered from the surface transponder at LAX. Three sets of interrogation bursts are evident. Two sets have periodicities of roughly 4.8 seconds corresponding to the scan rates of the Los Angeles ASR-7 and ASR-4 beacon interrogators. It was not possible with this test data to determine the particular interrogator responsible for each set of interrogation bursts. The third set has a periodicity of 12 seconds and is in good agreement with the 12 second scan rate of the ARSR interrogator located approximately 5 miles southwest of the airport.

Examination of the number of interrogations in each burst reveals that for both ASR interrogators there are about 32 interrogations per scan. This is somewhat less than the O'Hare ASR interrogator which triggered around 48 replies per scan, but it is more than the 18.5 per scan generated by the Logan ASR interrogator. The ARSR interrogator caused 70 to 80 replies per scan and seems to be consistent with the beamwidth and scan rate for this radar. Between interrogation bursts the environment was relatively clean. The data presented in Figure 3-5 was collected at 0120 local time. It is interesting to observe that data collected at the same test location at 1123 the following morning show nearly identical results. Nevertheless, the distribution of data from test point to test point shows more variations than that previously experienced at either O'Hare or Logan. For example, the average reply rate was seen to vary from a high of 53 per second at test point 7 to a low of 19 at test point 14 (see Appendix C). This can be attributed to the numerous buildings on the airport surface which for various locations can cause shielding for either the ASR-7 or ASR-4 interrogators.

3.2.2.3 Number of Interrogators. The surface interrogation environment at Los Angeles as depicted in Figure 3-5 is due principally to three interrogators: 2 ASR interrogators and one ARSR interrogator. Analytical studies indicated that 19 interrogators are within 25 nmi of LAX, and of these, 10 had line-of-sight to the airport surface. This again points out the hazards in attempting to use analytical techniques to predict the surface interrogation environment at airports.

Although the nominal environment at Los Angeles was seen to be three interrogators, this was not always the case. The first test period at Los Angeles from 1600 to 2051 on June 16 provided data which indicated very high interrogation rates in the order of 80 to 90 per second and for every test point with the exception of test location number 8. A typical example of the data collected during this period is shown in Figure 3-6 for test location 25. It can be seen that interrogation bursts for the three radars are present,

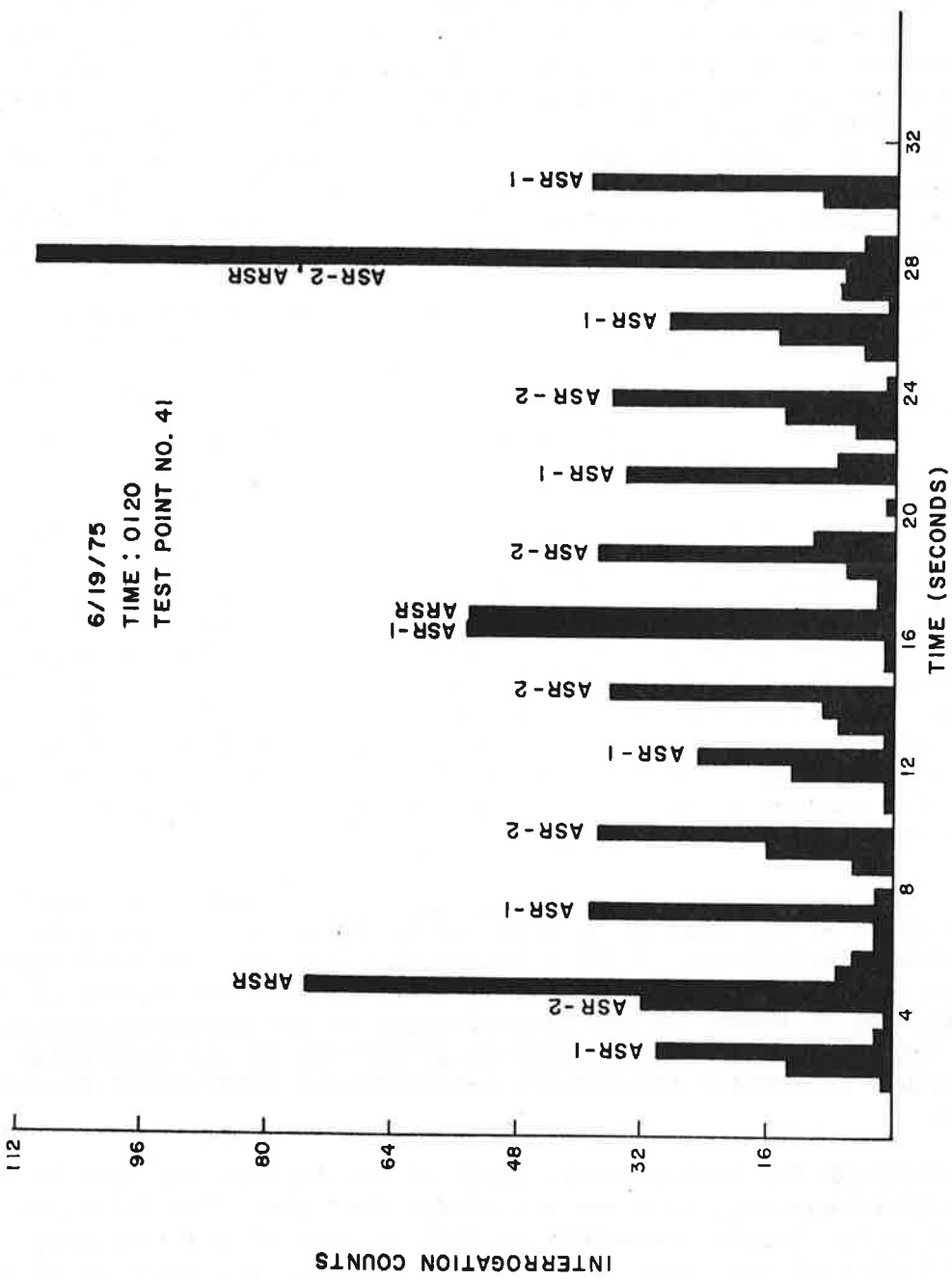

Figure 3-5 TYPICAL INTERROGATION HISTOGRAM FOR LOS ANGELES INTERNATIONAL AIRPORT

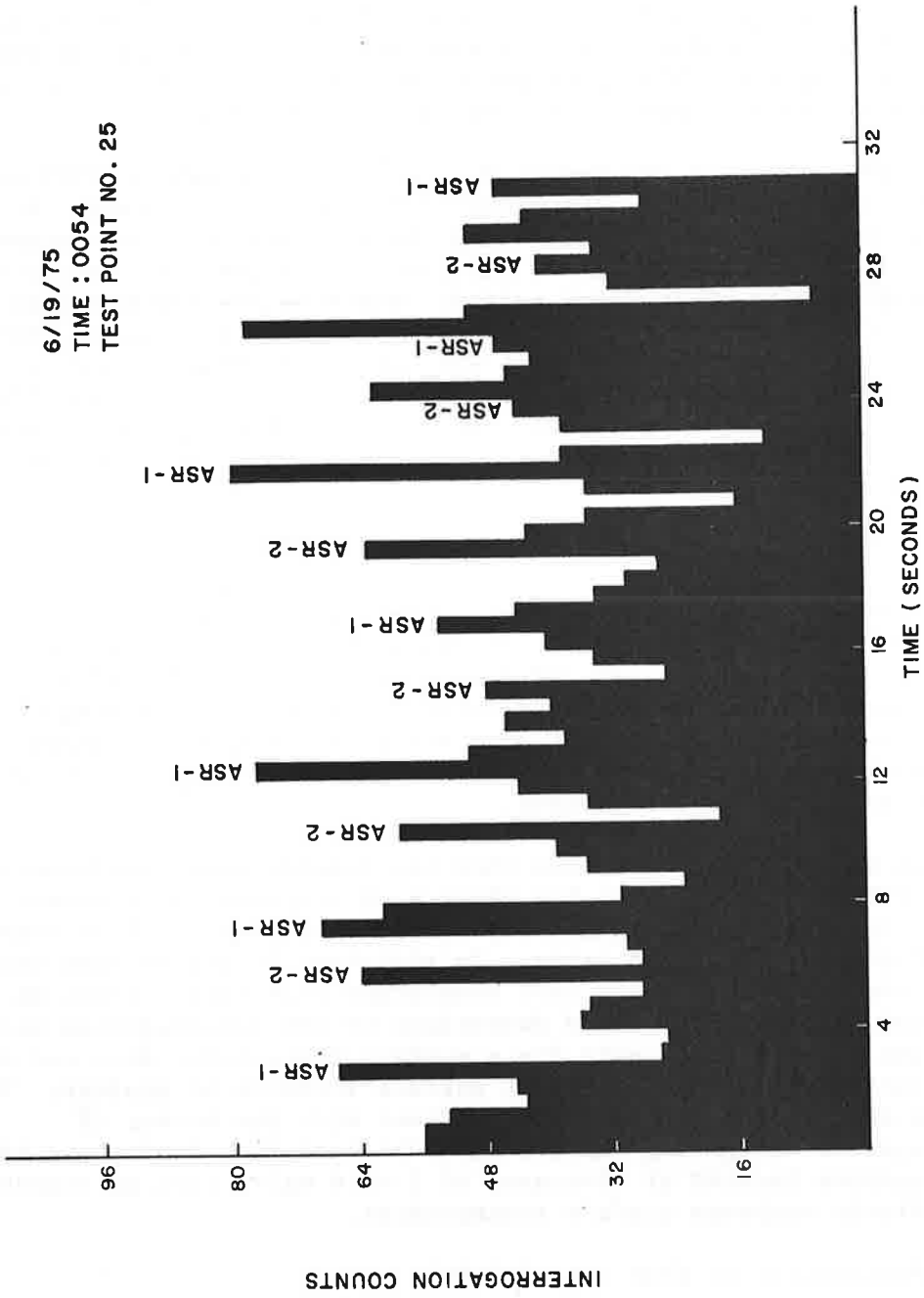

Figure 3-6 INTERROGATION HISTOGRAM FOR LOS ANGELES INTERNATIONAL AIRPORT SHOWING PHANTOM INTERROGATIONS

however, the clean environment between the bursts is now filled in by additional interrogations. Moreover, the replies per scan now appear to be larger than those indicated by Figure 3-5. Thus, it appears that the entire data is biased by 20 to 30 additional interrogations per second. This phenomenon could be caused by some form of omni interrogation signal operating at this low PRF.

At the outset of the second test period from 0020 to 0300 on June 19, the same omni interrogation effect was encountered. At 0100, however, the environment immediately changed; the omni interrogations disappeared and data similar to that shown in Figure 3-5 were obtained for the remainder of the test period. These values are shown in Appendix C. The dramatic change in the environment suggests that precisely at 0100 an interrogator was turned off thereby reducing the average reply rate from 80 per second to 24 per second. Time did not permit identification or location of the omni interrogator, however, it did remain off during the third and final test period on the morning of June 19.

3.3 COMPOSITE DATA SUMMARY

Table 3-1 provides a summary of the interrogation and SLS rates measured for the Logan, NAFEC, O'Hare, and Los Angeles airports. In each case the number of ASR and ARSR interrogators triggering surface transponder replies has been indicated. The average interrogation and SLS rates for each airport are listed with their respective standard deviations. These data were obtained using values measured at each airport's test locations.

The data in Table 3-1 show that the interrogation environments even for Los Angeles, which has often been suggested as a severe surface interrogation environment, are in fact very low when compared to airborne interrogation rates. In addition, it can be seen that the interrogation rates are very consistent over each airport as indicated by the low standard deviations of the interrogation rates. Thus, the interrogation rate for a surface transponder does not show large variations from one airport surface location to another. The average SLS rate is seen to be consistent with the number of interrogators triggering replies with the exception that those ARSR interrogators located at distances of 3 or 4 miles from an airport do not actively suppress surface transponders.

3.4 AVAILABILITY OF TIME FOR ASTC USE

To prevent mutual interference between ATCRBS and ASTC systems, the ASTC system is being designed to synchronize ASTC interrogations to occur only in the dead-time of the local ATCRBS equipment. Should

TABLE 3-1

SURFACE INTERROGATION DATA SUMMARY

AIRPORT	DATE	NUMBER OF TEST POINTS	NUMBER OF INTERROGATORS		AVG. INTERR. RATE PER SEC.	STD. DEV. OF INTERR. RATE	AVG. SLS RATE PER SEC.	STD. DEV. OF SLS RATE
			ASR	ARSR				
Logan	Dec. 1973	52	1	1	9.50	2.69	777	35
NAFEC	March 1974	45	2	1	13.18	2.53	753	5
O'Hare	June 1975	25	1	0	13.12	4.87	408	38
Los Angeles	June 1975	16	2	1	24.21	8.83	767	36

synchronization be required with additional sites, the available time for active ASTC use would be reduced resulting in a possible reduction in the ASTC update rate. As can be seen from Table 3-1, only one interrogator illuminates the O'Hare airport surface and as such synchronization would be required only to the local O'Hare ASR beacon interrogator. This synchronization would not affect the ASTC update since the system is being designed with this requirement in mind.

The environment at Los Angeles is somewhat more severe than that at O'Hare since there are 2 ASR interrogators and one ARSR interrogator illuminating the surface. It is unlikely that synchronization will be required with the ARSR since mutual interference with this site should be low due to its relatively remote location. Nevertheless there remains 2 ASR interrogators to which the ASTC system may have to be synchronized. If this is the case, and assuming the 2 ASRs are not synchronized to each other but are running at approximately the same PRF, the available time for ASTC use may be reduced by as much as one-half. This should not severely impact system performance, however, because sufficient margin has been allowed to provide necessary update rates even for this reduced ASTC PRF requirement. For example, the ASTC system is designed to provide a maximum of 14 interrogations per ATCRBS dead-time. If it is required to synchronize to a second ASR, only 7 ASTC interrogations may be available per equivalent ATCRBS dead-time. Initial estimates suggest, however, that only an average of 3 or 4 ASTC interrogations per dead time may actually be necessary to provide the required update rates. It therefore does not appear that the presence of 2 ASR interrogators at Los Angeles will in any way impact on the implementation of an ATCRBS-based ASTC system. Furthermore, it is not certain at this time whether it will even be necessary to synchronize to both radars.

4. CONCLUSIONS

The analysis and data presented in this report support the following specific statements concerning the surface interrogation environment at Chicago O'Hare and Los Angeles airports.

a. Results show only a single ASR interrogator at O'Hare triggering surface transponder replies. The average surface interrogation rate at O'Hare is 12.82 per second which is only slightly higher than the 9.5 per second measured at Logan airport. It is recommended that surface interrogation data be re-measured at Logan using the new portable equipment.

b. Results show that two ASR and one ARSR interrogators trigger surface transponder replies at Los Angeles. The average surface interrogation rate at Los Angeles is 24.21 per second which is considerably higher than Logan and O'Hare but, nevertheless, is much less than either initial expectations or typical airborne interrogation rates.

c. Although the nominal environment at Los Angeles consists of three interrogators as identified by 2 above, additional surface interrogations can occur from an unknown source. Extraneous interrogations were present during a portion of the tests at Los Angeles and appeared to be from an omnidirectional interrogator using a PRF between 30 and 40 per second.

d. Interrogation rates at both Chicago O'Hare and Los Angeles are very uniform for the respective airport surfaces, with little variation among the data collected for various surface locations.

e. Analysis of data indicates that sufficient time will be available for ASTC use at both Chicago O'Hare and Los Angeles airports. The ASTC system will have to be synchronized to only one ASR interrogator at O'Hare and at most two ASR interrogators at Los Angeles.

f. Data obtained from these tests have shown that the use of topographical maps is not a reliable technique for estimating the surface transponder interrogation environment at airports since analytical results can grossly overestimate the interrogation environment. These tests have clearly demonstrated the utility of field test data in making such determinations.

APPENDIX A

SPECIFICATIONS FOR PORTABLE INTERROGATION AND SLS MEASUREMENT EQUIPMENT

COUNTER ELECTRONICS

INPUT

Switch selectable for either interrogation or SLS suppression counts.

OUTPUT

Interrogation or SLS counts (depends on input switch selector setting) occurring during each sample interval. Data are output for each of 61 sample intervals. Total count is output in interval 62 and total SLS or interrogation count is output in interval 63. For example, if interrogation counts are output in each of the 61 intervals, then total interrogation count will appear in interval 62 and total SLS count will appear in interval 63 and vice versa.

OPERATOR FEATURES

Start - Manual by push button action

Stop - Automatic at end of 61 sample intervals

Reset - (a) Automatic at end of 61 sample intervals
(b) Manual by push button action at any time during data collection period

Readout - (a) Light emitting diode (LED) readout
(b) On-line paper tape printout

SAMPLE INTERVAL TIME PERIOD

Switch selectable in increments of 0.1 seconds from 0.1 seconds to 10.0 seconds.

DATA COLLECTION PERIOD

Dependent on sample interval selected. This period can range from a minimum of 6.1 seconds to a maximum of 610 seconds.

MEMORY

63 registers each containing 4 decimal digits used for storing data for LED readout at the completion of each data collection period.

PRINTER DISPLAY

a. On-line printouts of counts measured in each of the 61 sample intervals, plus total count in intervals 62 and 63.

b. Six column printout; four data columns plus two columns for interval number. Each column is one decimal digit.

c. Printer usable with sample interval time periods greater than 0.4 seconds. Printer not usable below 0.4 seconds due to speed limitations.

READOUT DISPLAY

a. Four digit LED readout for data plus two digit LED readout for memory location.

b. Readout of each of the 61 memory locations by sequence using push button.

c. Readout of memory location 62 by single push button action.

POWER REQUIREMENTS

12 volt supply with connection to either the vehicle cigarette lighter or directly to the battery.

ANTENNA

Stub type mounted on aluminum ground plane. Antenna assembly fastens to the roof of vehicle by two straps which are clipped over the rain gutter.

PACKAGING

Case measuring 18 inches by 12 inches by 8 inches.

TRANSPONDER

TYPE

KING KT-76

SENSITIVITY

-72 dbm

POWER OUTPUT

200 watts

POWER REQUIREMENTS

14 VDC, 1.3 Amps.

OUTPUTS

Interrogation - Single pulse output whenever a mode A or mode C interrogation is successfully decoded.

Sidelobe - Single pulse output whenever P_1 and P_2 pulses meeting suppression requirements are successfully decoded.

Transmitter - Switch selectable for either standby or operative. This function is independent of interrogation or SLS outputs.

Receiver - Output of transponder video available for viewing on an oscilloscope.

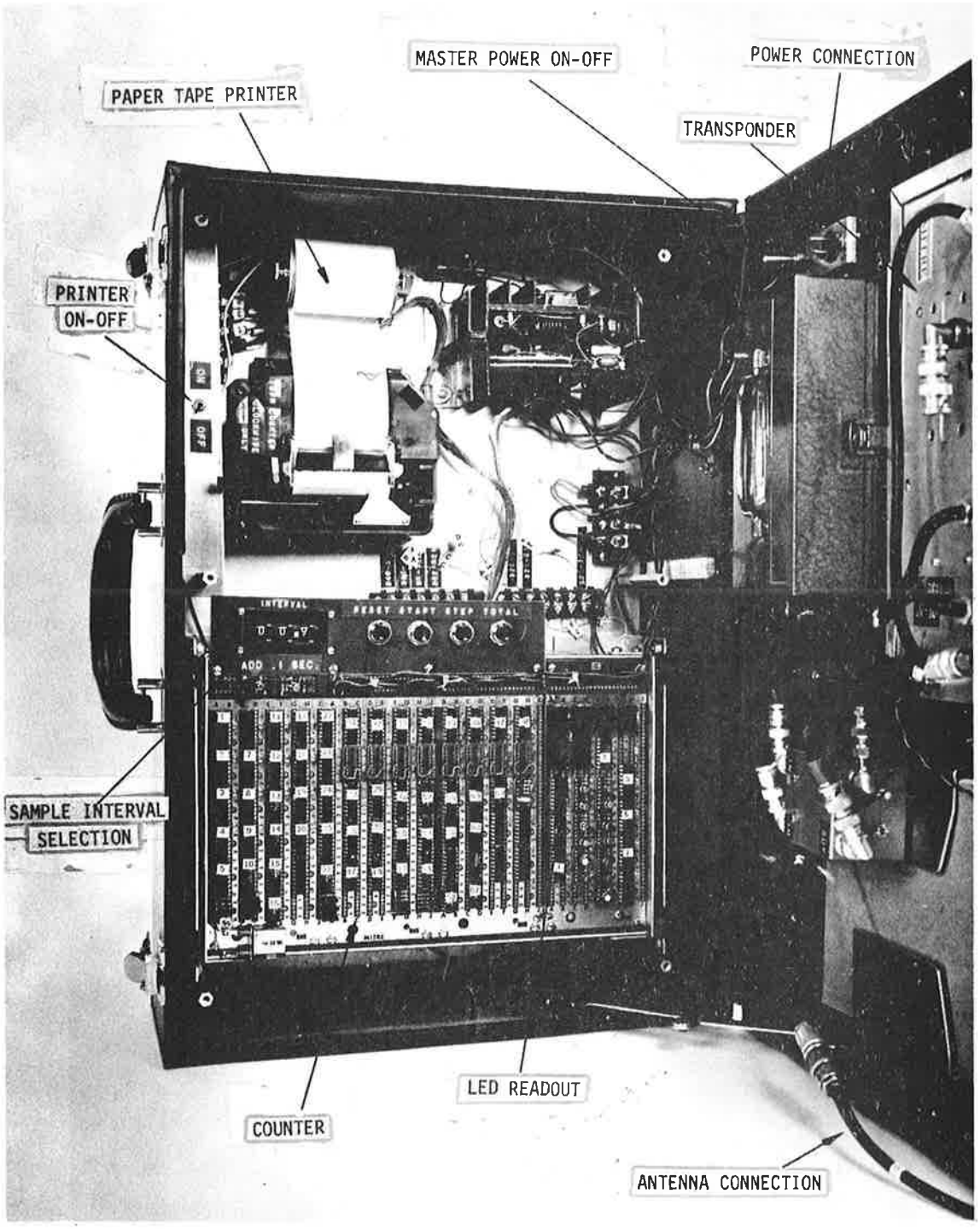

Figure A-1. Portable Interrogation and SLS Measuring Equipment

APPENDIX B

CHICAGO O'HARE DATA

TEST PERIOD I, JUNE 16

Test Point	Time-of-Day	Average Interr Rate per Second	Average SLS Rate per Second
1	1650	12.06	408
3	1703	13.33	405
4	1712	11.87	359
6	1721	11.29	411
8	1727	5.97	417
7	1740	16.39	406
9	1805	9.15	414
11	1816	10.78	412
13	1827	25.13	359
14	1857	15.93	375
15	1910	7.59	416
18	1920	15.35	416
16	1938	9.37	561
22	1958	9.45	413
21	2009	6.35	416
25	2020	14.07	406
24	2028	16.34	406
23	2033	14.99	335
4A	2045	11.64	485

TEST PERIOD II, JUNE 17

1	0106	13.30	406
3	0115	10.61	412
4	0121	9.71	392
6	0128	11.68	407
7	0136	9.26	413

APPENDIX B (Concluded)

TEST PERIOD II, JUNE 17 (Concluded)

Test Point	Time-of-Day	Average Interr Rate per Second	Average SLS Rate per Second
8	0145	9.50	413
9	0150	12.03	411
11	0157	10.10	412
13	0203	14.73	349
14	0210	30.18	483
15	0217	7.08	415
18	0223	11.34	405
16	0225	10.45	378
21	0230	6.77	415
		TEST PERIOD III, JUNE 17	
10	1141	6.00	417
2	1145	12.00	411
4	1149	10.79	381
5	1156	12.00	532
7	1203	8.49	419
11	1215	9.48	413
12	1223	17.80	406
14	1228	44.62	402
17	1236	7.46	415
19	1243	24.61	386
20	1253	17.40	328
22	1307	12.47	427

APPENDIX C

LOS ANGELES DATA

TEST PERIOD I, JUNE 18

Test Point	Time-of-Day	Average Interr Rate per Second	Average SLS Rate per Second
3	1600	20.43	751
2	1610	35.98	976
1	1620	56.33	928
6	1625	94.20	758
7	1636	98.85	746
10	1646	27.61	746
11	1654	81.84	861
12	1702	88.36	726
13	1711	103.60	772
14	1720	89.13	655
5	1732	83.33	690
4	1740	105.92	729

TEST PERIOD II, JUNE 18

3	1836	21.67	739
2	1843	52.61	747
1	1848	73.16	756
6	1942	90.72	713
16	1947	88.28	738
7	1950	91.74	781
8	1954	101.34	778
10	1958	20.07	754
11	2003	79.72	759
12	2007	78.62	791

APPENDIX C (Continued)

TEST PERIOD II, JUNE 18 (Continued)

Test Point	Time-of-Day	Average Interr Rate per Second	Average SLS Rate per Second
13	2013	84.10	754
14	2019	97.11	756
9	2024	24.54	780
15	2038	108.70	739
5	2043	98.11	747
4	2051	82.54	718
		TEST PERIOD III, JUNE 19	
3	0020	37.31	704
2	0028	21.48	727
1	0037	86.57	786
6	0050	83.18	834
7	0054	83.25	776
8	0058	94.33	782
8A	0106	25.70	813
10	0109	26.39	962
11	0115	28.90	841
12	0120	27.27	862
13	0135	25.08	748
14	0140	21.57	755
9	0145	20.57	750
5	0152	26.12	748
15	0158	21.77	886
4	0205	25.67	677
3	0215	25.80	759
2	0218	8.90	762
1	0225	18.82	754

APPENDIX C (Concluded)

TEST PERIOD III, JUNE 19 (Concluded)

Test Point	Time-of-Day	Average Interr Rate per Second	Average SLS Rate per Second
6	0233	20.12	868
16	0236	22.52	710
7	0245	20.89	763

TEST PERIOD IV, JUNE 19

3	1041	20.34	757
2	1047	19.85	750
1	1052	36.47	704
6	1056	20.58	764
16	1101	29.36	705
7	1106	23.50	754
8	1110	54.48	725
10	1116	24.62	660
11	1119	33.91	735
12	1123	29.02	693
13	1130	22.35	762
14	1135	29.13	746
9	1140	26.21	801
15	1149	19.38	767
5	1157	24.68	752
4	1205	23.51	746

REFERENCES

1. Test Plan for Measuring Interrogation Rates for a Surface Operated Transponder at JFK, ORD and LAX Airport, The MITRE Corporation Report, MTR-2993, March 1975.

2. J. D. Vinatieri and H. Glynn, ATCRBS Surface Interrogation and Interference Measurement Program, The MITRE Corporation Report, MTR-2736, Volume I, 12 December 1973.

3. J. D. Vinatieri, ATCRBS Surface Interrogation and Interference Measurement Program, The MITRE Corporation Report, MTR-2736, Volume II, 28 March 1974.

4. J. D. Vinatieri, Measurements of ATCRBS Interference Due to the Use of Transponders on an Airport Surface, The MITRE Corporation Report, MTR-2917, 30 October 1974.

5. J. W. O'Grady, M. J. Moroney, R. E. Hagerott, ATCRBS Trilateration - The Advanced Airport Surface Traffic Control Sensor, 20th Guidance and Control Panel Symposium, North Atlantic Treaty Organization, May 20-23, 1975.